1.0

1.1

1.25

2.8

3.2

3.6

4.0

1.4

4.5

2.2

2.0

1.8

MICROCOPY RESOLUTION TEST CHART

OPTICAL STUDY OF GERMANIUM, GERMANIUM
PLUS ARSENIC, AND GERMANIUM PLUS
GALLIUM IMPLANTS IN GALLIUM ARSENIDE

THESIS

Thomas G. Alley
First Lieutenant, USAF

AFIT/GEP/ENP/87D-1

DEPARTMENT OF THE AIR FORCE

AIR UNIVERSITY

AIR FORCE INSTITUTE OF TECHNOLOGY

Wright-Patterson Air Force Base, Ohio

OPTICAL STUDY OF GERMANIUM, GERMANIUM
PLUS ARSENIC, AND GERMANIUM PLUS
GALLIUM IMPLANTS IN GALLIUM ARSENIDE

THESIS

Thomas G. Alley
First Lieutenant, USAF

DTIC
SELECTE
MAR 0 3 1988
E

AFIT/GEP/ENP/87D-1

OPTICAL STUDY OF GERMANIUM,

GERMANIUM PLUS ARSENIC, AND GERMANIUM PLUS GALLIUM

IMPLANTS IN GALLIUM ARSENIDE

THESIS

Presented to the Faculty of the School of Engineering

of the Air Force Institue of Technology

Air University

In Partial Fulfillment of the

Requirements for the Degree of

Master of Science in Engineering Physics

Accession For		
NTIS GRA&I		☒
DTIC TAB		
Unannounced		☐
Justification		
By		
Distribution/		
Availability Codes		
Dist	Avail and/or Special	
A-1		

Thomas G. Alley, B.A.

First Lieutenant, USAF

December 1987

Approved for public release; distribution unlimited

Table of Contents

Acknowledgements

I am very grateful for the help of all those that provided assistance in tackling this thesis project. I'd like to thank my advisors, Dr. R. L. Hengehold and Dr. Y. K. Yeo for their advice and guidance. Many thanks go to Kevin Keefer for his constant interest in this project and for the amount of time he spent in helium transfers and guiding me through the experimental setup. Additional thanks go to Walt, Bill and Rick for their technical assistance.

Finally, I want to express my deepest gratitude to my wife Valerie for her patience and support when our time together was complicated by school, thesis, and a new son.

Thomas G. Alley

iii

Abstract

The low temperature photoluminescence (PL) properties of single implants of Ge and dual implants of Ge+As or Ge+Ga into semi-insulating Cr-doped GaAs have been analyzed. Room temperature implantation was performed at 120 keV. When dual implantation was used, samples were implanted at the same dose and energy. Ion doses ranged from 1×10^{13} to 1×10^{15}/cm^2. Samples were encapsulated with Si$_3$N$_4$ and then annealed at temperatures ranging from 700 to 950°C. Si$_3$N$_4$ was removed prior to PL measurements.

A PL peak due to Ge-acceptors was identified. A bound exciton peak related to Ge-donors was also observed. An acceptor peak due to residual Si was found in all samples. The heights of the Ge-acceptor peak and exciton peak were compared to the height of the intrinsic Si-acceptor peak. The height comparison was used in an effort to find trends of Ge-acceptor and Ge-donor transitions as a function of anneal temperature and ion dose.

The PL data for GaAs:Ge+As showed a relative decrease of the Ge-acceptor related peak and an increase in the exciton peak with increasing dose. This is generally consistent with electrical measurements in previous work.

The PL data for GaAs:Ge at an anneal temperature of 950°C also showed a relative decrease in the Ge-acceptor related peak and an increase in the exciton peak with

increasing dose. This is also consistent with electrical data. However, trends of dose dependence at other anneal temperatures were more complicated.

The anneal temperature dependence of the Ge related peaks for both GaAs:Ge and GaAs:Ge+As showed complicated behavior. At an anneal temperature of 800°C, the Ge-acceptor related peak becomes obscured in a large Si-acceptor related peak.

For GaAs:Ge+Ga, the addition of Ga to the implantation process generally enhances an observed Ga in As vacancy antisite defect transition.

List of Figures

vii

List of Tables

OPTICAL STUDY OF GERMANIUM,
GERMANIUM PLUS ARSENIC, AND GERMANIUM PLUS GALLIUM
IMPLANTS IN GALLIUM ARSENIDE

I. Introduction

A. Gallium Arsenide

In the world of semiconductors, the demand for ever
faster devices continues. Although the fastest devices in
existing computers can switch on and off in a billionth of a
second (1:80), still faster devices are needed in areas such
as supercomputers and microwave frequency communication
systems. With faster devices, new kinds of radars and
communication satellites could operate in the microwave band
and higher still.

Part of the process of developing better and faster
devices is the characterization of different semiconductor
materials. In the past, much of the emphasis has been focused
on silicon (Si) and germanium (Ge) for application in
integrated circuit technology. One way to make semiconductor
devices operate faster is to use traditional materials such as
Si and make devices smaller, causing a reduction in the
distance an electron has to travel in a circuit. This has
been the traditional approach.

A different approach is to increase the velocity of the
electrons that flow through the semiconductor. To do this,

1

different material other than the traditional Si needs to be employed. Gallium Arsenide (GaAs) is rapidly becoming the semiconductor compound of choice for this new role.

GaAs offers some advantages over Si. GaAs is "fast". The electrons in GaAs behave as if they have a smaller mass than those in a Si crystal. Thus, when an electric field is applied to GaAs, The electrons will be accelerated faster than in Si. At its conduction band minimum, the GaAs electron has a small effective mass (m_e^*) equal to 0.07 times the mass of a free electron (m_e) outside the crystal. On the other hand, for Si, $m_e^* = (0.2) m_e$ at its lowest value.

Other inherent characteristics of GaAs that make it attractive include its electron mobility (up to 6 times that of Si), and its energy band structure. The conduction band and valance bands in GaAs are separated by a band gap of 1.52 eV at 0 K. In Si the band gap minimum is 1.1 eV. GaAs devices are thus able to operate at higher temperatures than Si, due to the reduction of noise caused by electrons that are thermally excited into the conduction band. Because the conduction band minimum in GaAs is found at the zero value of momentum of an energy-momentum Brillioun zone curve, GaAs is known as a "direct-gap" semiconductor. Electrons do not need any momentum from the lattice to make the lowest energy transitions. On the other hand, Si is "indirect-gap" because the lowest energy state in the conduction band is found at nonzero values of momentum. The fact that GaAs is direct-gap

2

and that it is "fast", allows it to sustain electrical oscillations in the microwave band which extends to 30 gigahertz. If someday GaAs device technology allows reduction in gate lengths to a quarter of a micrometer or less, GaAs devices will be able to operate in the millimeter-wave band which extends from 30 to 300 gigahertz, and is now largely unexploited. (1:87) The direct-gap structure of GaAs also allows it to emit photons efficiently and as a result has made GaAs important in the fabrication of laser diodes and light-emitting diodes.

B. Germanium Implanted Gallium Arsenide

By doping GaAs with different types of impurity atoms, different characteristics of the material are achieved. Using Ge as a dopant in GaAs is interesting because as a Group IV element, it is an amphoteric dopant, i.e., it can occupy substitutionally a Ga or an As lattice site. Ge has often been used to produce n-type GaAs in a vapor-phase epitaxy growth method and p-type samples in liquid-phase epitaxy. Ge is used as a dopant in epitaxial layers due to its low diffusion coefficient. GaAs doped with Ge has been used to fabricate p/n junctions and p/n multilayers (2,3).

Recently, ion implantation of impurity dopants into semi-insulating GaAs substrates has been widely used in the fabrication of various electronic and opto-electronic devices. Ge ion implantation has been used to produce reliable and reproducible ohmic contacts to n-type GaAs (4). As a method

3

of doping, ion implantation offers good prospects due to the control one has over various implantation parameters. Control is achievable over the impurity concentration and its depth profile allowing for good reproducibility and uniformity. However, processing after implantation is made more difficult because samples that are ion implanted must be thermally annealed to remove the damage to the crystal caused by ion bombardment.

In Ge implanted GaAs, n-type or p-type electrical activity depends on impurity dose concentration and anneal temperature (5). The electrical properties may be further altered by dually implanting Ga or As with Ge. Electrical investigation has shown that dual implantion of Ge and As enhances n-type behavior, while dual implantion of Ge and Ga enhances p-type behavior (6,7).

C. Objective and Scope

Preliminary photoluminescence studies of Ge implanted GaAs (GaAs:Ge) have been made by Yu (8). The objective of this thesis is to examine a wide assortment of GaAs:Ge, GaAs:Ge+As, and GaAs:Ge+Ga samples through photoluminescence. The amphoteric behavior of Ge implanted into GaAs and its relation to observed photoluminescence peaks is of particular interest. GaAs samples implanted singly with Ge, dually implanted with Ge and As, and dually implanted with Ge and Ga are all investigated and compared with previous electrical and photoluminescence studies.

4

The substrate material used is <100> oriented Cr-doped semi-insulating GaAs obtained from Crystal Specialties, Inc. All ion implantation occured at room temperature at an ion energy of 120 keV. Impurity dose concentrations ranged from 1×10^{13} to $1\times10^{15}/cm^2$. Dually implanted samples were implanted sequentually in equal doses and at the same energy with Ge being implanted first. The samples were annealed at varying temperatures from 700 to 950°C.

II. Theory

A. Intrinsic Semiconductor Energy States

Individual atoms have characteristic discrete energy
levels of electrons surrounding the atom's nucleus. When a
number of atoms are brought together to form a semiconductor
crystal, the discrete energy levels of the electrons broaden
into regions of allowed electronic states or energy bands. An
intrinsic semiconductor is characterized by these energy
bands. McKelvey (10:Ch 8) derives the band structure of an
intrinsic semiconductor using a tight-binding approximation
and a nearly free electron approximation. Other approximation
techniques exist, and the use of one over the other depends on
the type of semiconductor involved.

The outermost, or valence electrons of individual atoms
become the valence band of the semiconductor. The valence
band, which consists of almost completely filled energy states
is used in chemical bonding and essentially provides the
structure to hold the crystal together. Higher allowed energy
states occur in the semiconductor band structure, and these
are known as the conduction band. The conduction band is
almost completely empty. The valence and conduction bands are
separated by a region of forbidden energy states called the
band gap.

An ideal intrinsic semiconductor does not contain
impurities or defects within its lattice structure. The band

6

gap is completely empty of allowed electronic energy states. If enough energy is provided through thermal energy, applied voltage, or photons, such that the amount of energy is equal to or greater than the band gap, an electron from the valence band can transit to the conduction band. In such a transition, a free electron is created in the conduction band, while a positively charged free hole is created in the valance band. Because electrons in the conduction band and holes in the valance band do not take part in the binding of the crystal lattice, they are free to move through the crystal and constitute electrically active carriers.

GaAs is known to have spherically symmetric, parabolic bands near the bottom of the conduction band and the top of the valence band. The minimum band gap corresponds to conduction and valence band extrema located at the same point in momentum space, i.e. k=0, making it a direct gap semiconductor. The band gap has an energy value of 1.52 eV at 0°K.

B. Extrinsic Semiconductors

Semiconductors can contain impurities, whether introduced intentionally or not. If the impurities lead to overall negative or positive electrical activity of a semiconductor, these are known as extrinsic semiconductors. Doping with impurity atoms allows one to control the number of active carriers in a semiconductor. An impurity atom can occupy substitutionally the lattice site of a substrate atom.

When the number of electrons in the valence shell of the dopant is less than that of the substrate atom that it replaces, the dopant atom is known as an "acceptor". An acceptor introduces an extra hole due to its lack of one electron. Acceptors can therefore attract and accept a free electrons from the lattice. If acceptors dominate in semi-conductors, it is known as p-type (or positive type) material.

When the number of electrons in the valence shell of the dopant is greater than that of the substrate atom it replaces, a dopant atom is known as a "donor". Donors introduce extra electrons into the lattice. If donors dominate in a semicon-ductor, the material is known as n-type (or negative type).

Unlike the intrinsic semiconductor, extrinsic semiconduc-tors have energy levels that exist in the band gap due to donor and acceptor impurities. Because a donor has an extra electron, it takes much less energy to ionize that electron and free it to the conduction band than it does for a transition to occur from the valence band to the conduction band. It also takes less energy for an electron to transit from the valance band to an acceptor than it does from the valance band to the conduction band. An energy level struc-ture for an extrinsic semiconductor is shown in Fig. 1.

8

```
 _ _ _ _ _ _ _ Conduction Band _ _ _ _ _ _ _
 _ _ _ _ _ _ _ _ _ _ _ _ _ _ _ _ _ _ _ _
_____
 + + + + + + + + + +              Donor level
                          E_G
 - - - - - - - - - -              Acceptor level
_____
 + + + + + + + + + + + + + + + + + + + +
 + + + + + + + Valence Band+ + + + + + + +
```
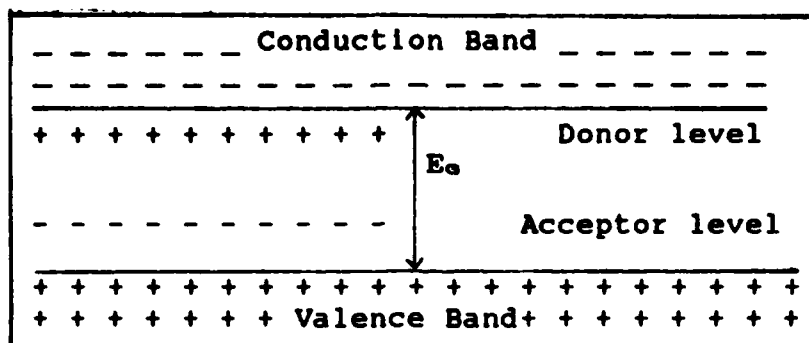
Fig. 1   Donor/Acceptor states located within the band gap.

The electron or hole ionization energy can be
approximated by a hydrogen-like approximation for both donors
and acceptors.   Their ionization energies (E_I), are given by:

$$E_I = (e^4 m^*/2K^2 \hbar^2) \qquad (1)$$

where e is the electronic charge, m^* is the effective mass of
the electron or hole, K is the dielectric constant, and $\hbar$ is
Planck's constant divided by 2π.

The energy required to activate holes or electrons will
vary, depending on the type of impurities present in the
substrate and the type of semiconductor substrate used.   For
GaAs, a hydrogen-like approximation yields a donor ionization
energy of 5.2 meV and an acceptor ionization energy of 34 meV
for simple centers (11:327).   A simple center is defined as an
impurity that sits on the Ga or As lattice site and
contributes only one additional carrier to the binding.

C. Amphoteric Behavior

Common semiconductor materials of interest include those
made of an element from Group IIIA of the periodic table
combined with those of Group VA, which are called III-V

9

compounds. In their p-shells, Group III atoms contain one valence electron, while Group V atoms contain three. When these atoms bond together, the three Group V electrons are shared with the one Group III electron to form two covalent bonds.

If an element from Group IV of the periodic table is doped into a semiconductor made of III-V material, it can substitutionally occupy either a lattice site of the Group III element or that of the Group V element. This is known as amphoteric behavior. A Group IV atom contains two valence p-shell electrons. If it occupies a Group III lattice site, an extra electron is present, making it a donor. If it occupies a Group V lattice site, an electron is lacking, making it an acceptor. Thus the Group IV dopant can behave as either an acceptor or a donor. Whether or not the Group IV atom replaces the Group III or Group V element depends on implantation parameters such as dopant dose, the temperature at which the semiconductor is annealed, and the combination of dopants used.

Ge is known to be an amphoteric dopant in GaAs. Using photoluminescence as a diagnostic tool, the amphoteric behavior of Ge in GaAs is the main theme of this thesis.

D. Other Impurities and Defects

Besides those intentionally implanted or doped, other impurities are found to exist within the substrate. These can result from contaminants introduced in the process in which

the substrate is grown or from other processing techniques such as capping and annealing that take place after crystal growth. These inherent impurities can cause respective donor and acceptor energy levels within the band gap.

Several other types of defects can also be introduced into the substrate as a result of fabrication and processing. An impurity atom that lodges in a non-lattice site is an interstitial defect, while the abscence of a substrate atom in its respective lattice site is known as a vacancy defect. If, for example, a Ga atom occupies an As site or vice versa, it is known as an anti-site defect. These defects are also known as point defects. Defects can cause energy levels within the band gap, and because they are usually too broad and too deep in the band gap to be approximated by the hydrogenic approximation, they are known as "complex centers"(11:359), whereas shallow impurity levels are often simple centers and are approximated by the hydrogenic approximation.

E. Ion Implantation

In semiconductor fabrication, it is desirable to control various parameters associated with the doping of impurity atoms. In the growth of GaAs, introducing the dopant during the growth process as in liquid phase epitaxial (LPE) growth, vapor phase epitaxial (VPE) growth, etc., have had limited success in the control of the doping parameters. A method such as diffusing the impurity into a heated substrate (thermal diffusion) that is used with silicon substrates has

11

not been developed for GaAs.

Ion implantation, on the other hand, offers advantages such as control over impurity concentration, uniformity, reproducibility, various depth profiles of the implanted impurity, selective area implantation through masking, lower annealing temperatures, only slight lateral spreading, application in planar type devices, and the prospect of high yields at low cost. The objective of ion implantation is to develop a reliable, reproducible, and precisely predictable doping result. Ion implantation is used in several types of GaAs devices such as microwave devices, optoelectronic devices and solar cells.

Ions are implanted into the near surface region of a substrate by accelerating the ions to a high velocity and then directing them in a beam to the surface of the semiconductor. The ions' mass, velocity and particle flux are used to control the impurity concentration and its depth profile (12:109).

As a result of implantation, damage occurs in the substrate and defects are introduced. Crystalline defects such as point defects, clusters of point defects, dislocations and dislocation loops, and stacking faults are produced in the substrate. To reduce this problem, thermal annealing is required and this results in a reduction in the number of defects. In this experiment annealing was done at temperatures of 700 to 950°C. Because of the tendency of substrate elements such as As in GaAs to out-diffuse during

12

annealing and cause surface decomposition, encapsulation is required during the annealing process. Silicon nitride (Si_3N_4) is the common encapsulant used.

F. Dual Implantation

When a dopant is implanted in a III-V compound and it occupies substitutionally a normal substrate lattice site, it replaces an original Group III or Group V atom. If, for instance, a Ge atom replaces an As atom in GaAs, the As atom is displaced somewhere else within the lattice, and after annealing, creates a vacancy for a Ga atom. To maintain equal pairs of Ga and As for bonding it is advantageous to implant Ga atoms to fill the Ga vacancies. For instance, when Ge atoms replace Ga atoms, then dually implanting As atoms should help to maintain the stoichiometry of GaAs. Heckingbottom and Ambridge (13:31) argued on the basis of solid state theory that by implanting dual-ion combinations one can maintain the stoichiometry of GaAs and enhance electrical activity of the dual-implanted sample over that of the single-implanted one.

By dually implanting As with Ge into GaAs, one expects increased probability of Ge occupancy of Ga sites and therefore enhanced n-type electrical activity (Fig. 2). By implanting both Ga and Ge, one expects increased probability of As sites being occupied by Ge atoms and therefore enhanced p-type activity (Fig. 3).

G. Photoluminescence

Photoluminescence (PL) has become a sensitive method of

13

ENHANCEMENT OF N-TYPE ACTIVITY BY DUAL IMPLANTATION

CO-IMPLANTING ARSENIC:

1. MAINTAINS STOICHIOMETRY OF LATTICE

2. IMPROVES PROBABILITY OF Ge OCCUPANCY OF Ga SITES

Fig. 2 Dual Implantation of Ge and As

ENHANCEMENT OF P-TYPE ACTIVITY BY DUAL IMPLANTATION

CO-IMPLANTING GALLIUM:

1. MAINTAINS STOICHIOMETRY OF LATTICE
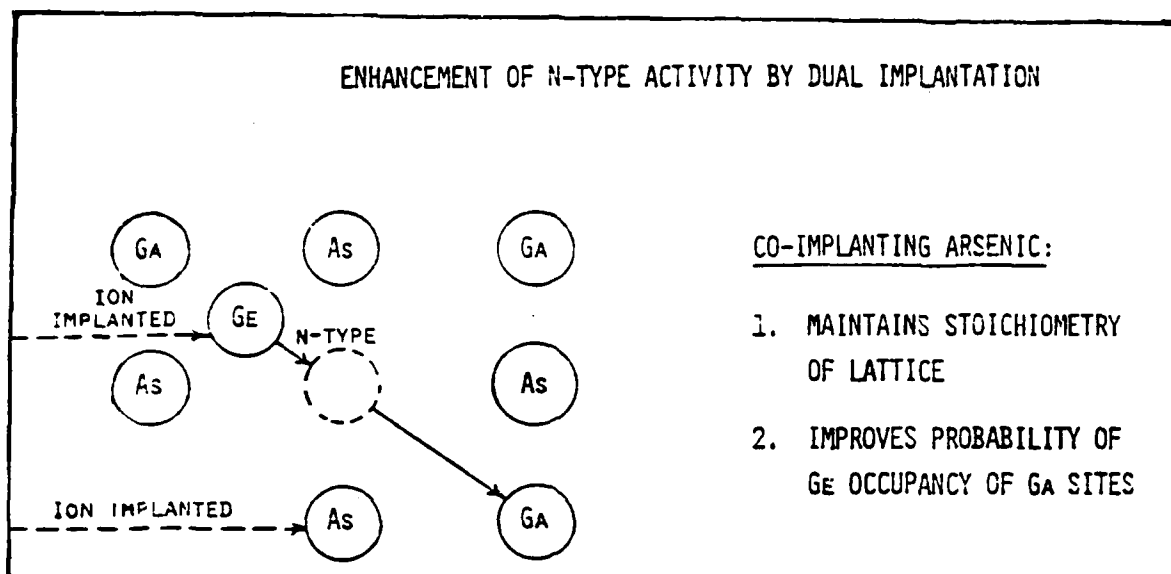
2. IMPROVES PROBABILITY OF Ge OCCUPANCY OF As SITES
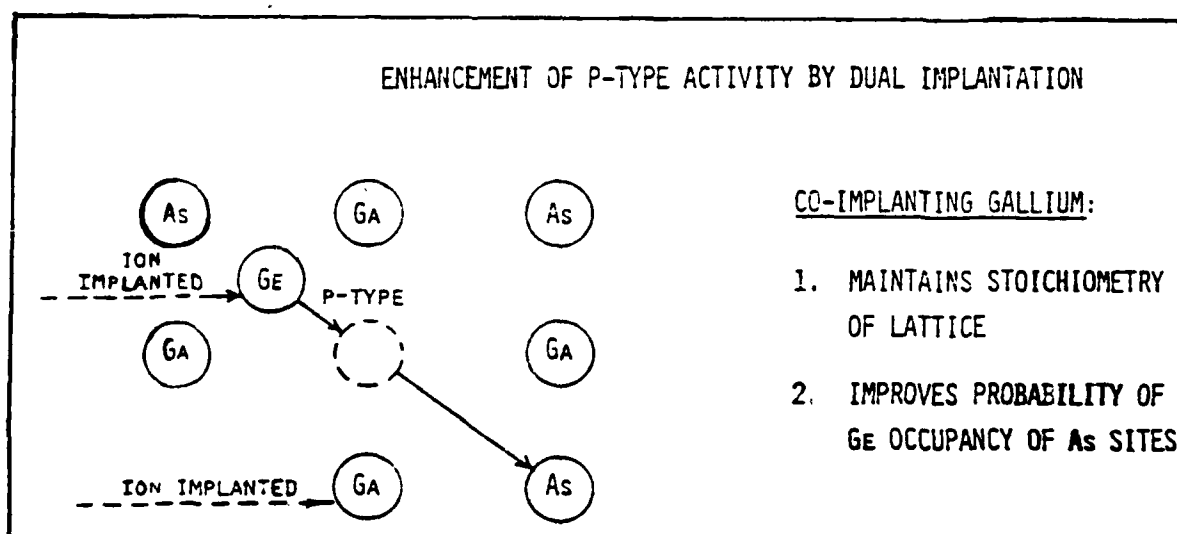
Fig. 3 Dual Implantation of Ge and Ga

14

semiconductor analysis. It offers the advantage of being a non-destructive and contact-less technique. Through PL, bulk impurities as well as point defects within a sample can be detected.

PL is the optical excitation of a sample to cause electrons to move from low energy states to higher energy states; the optical source usually being a laser. If the laser has a wavelength and associated energy greater than the band gap, electrons can be excited to the conduction band from the valance band. These excited electrons eventually decay back to their unexcited states either radiatively or non-radiatively. The radiative decay will result in photons with energies equal to the difference of the energies of the states from which the decay took place. These photons can then be detected with a sensitive spectrometer and photomultiplier tube. By scanning photon energies below the band gap, a plot of relative photon flux can be made. Peaks at certain energies will occur and correspond to different radiative transitions. Many PL studies have dealt with the identifica-tion of these transitions and the impurities and defects which cause them.

PL studies are usually made at temperatures held at 4.2 K (liquid helium temperature) through 10 K. At these extremely low temperatures, almost all electrical carriers are in their ground state, which eliminates problems with complicated analysis of interactions between the ground state and excited

states. Low temperatures also reduce non-radiative transitions due to thermal processes, and reduce thermal line broadening making discrimination between different peaks more apparent.

Lasers are usually used as the source of optical excitation due to their localized spatial resolution and ability to select one coherent wavelength line from a variety available. Because laser lines of different wavelengths have different penetration depths into the sample, one can select an appropriate sampling depth to probe by just choosing a corresponding laser line. A Krypton-Ion laser with a wavelength of 647.1 nm has a penetration depth of about 3000 Å in GaAs (8:7167). For ion implanted GaAs, it is important that the laser penetrate the ion implanted layer to identify the extrinsic PL peaks. The peak projected range of Ge implants in GaAs is 464 Å with a standard deviation of 173 Å at 120 keV. The Ge distribution is from 0 to 2400 Å (8:7165,7167). So a laser with λ=647.1 nm will more than penetrate the implanted layer.

H. Radiative Transitions

A radiative transition occurs when an electrons in an excited energy state decays to a lower energy state and emits energy in the form of photons. The fundamental and most commonly observed PL transitions are illustrated in Fig. 4. They are band-to-band recombination, excitonic (free exciton recombination), free electron to acceptor (free-to-bound), and

16
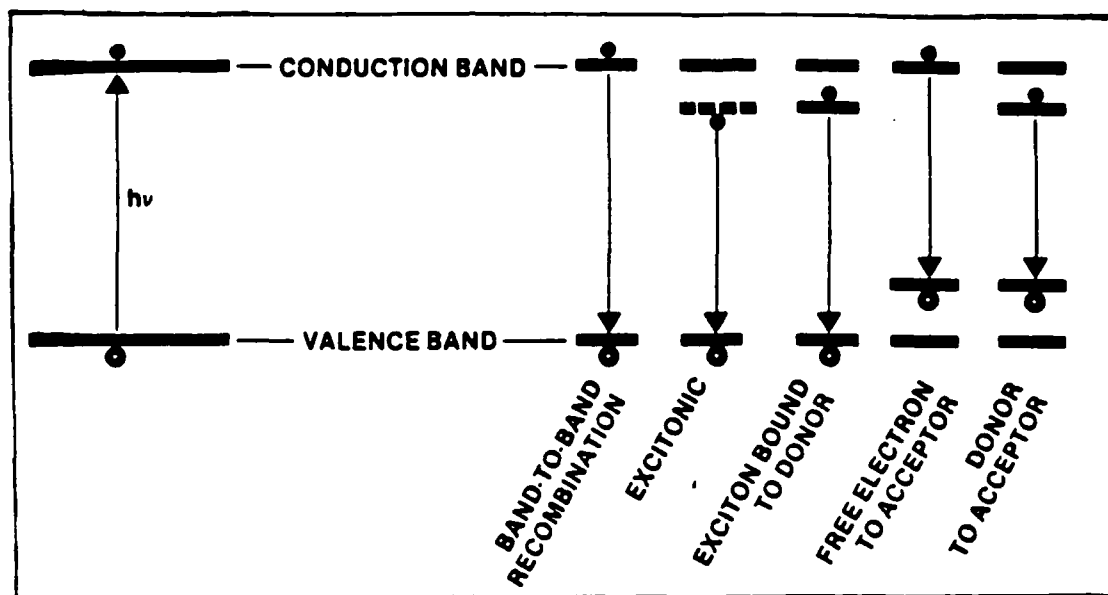
Fig. 4 Commonly observed PL transitions. Photon absorption occurs on the extreme left. Radiative recombination occurs through any of the transitions on the left.

17

donor-to-acceptor.

1. Band-to-Band Recombination

An electron in the conduction band that directly recombines with a hole in the valence band makes a band-to-band transition. The photon energy emitted in the process is equal to E_o, the band gap energy. This transition is rarely seen in materials with small effective masses such as GaAs (14:173).

2. Excitons

An electron and a hole can combine in such a way that they will orbit around each other due to coulombic attraction. This electron-hole pair is called an exiton. Because the exciton has such a small ionization energy, it is observed only at low temperatures. The Schrödinger equation for the exciton is analogous to that of the hydrogen atom, and gives solutions of the form:

$$E_x = (-\mu e^4 / 2\hbar^2 K^2 n^2) \qquad (2)$$

where μ is the reduced mass of the respective effective masses of the electron-hole pair, e is the electronic charge, $\hbar$ is Planck's constant divided by 2π, K is the dielectric constant, and n is the quantum number describing the exciton state. For an unbound exciton that is free to move through the lattice, the expected value for the electron-orbital radius is:

$$\langle r \rangle_n = (n^2 a_o K m_e / m_e^*) \qquad (3)$$

where a_o is the Bohr radius (0.53 Å) and m_e^* is the effective mass of the electron.

In GaAs, $K = 12.5$ and $m_e^*/m_e = 0.0065$. The expected value of

18

the orbital radius for n=1 is then $\langle r \rangle_1 = 1040$ Å. This radius is extremely large due to the small m_e^* and extends over thousands of Bohr radii! (14:173)

a. Free Exciton Transitions

An electron-hole pair that is free to move through the lattice is known as a free exciton. When the electron and hole recombine, a transition occurs where a photon is emitted. The photon energy is given by:

$$h\nu = E_\sigma - E_x \qquad (4)$$

where E_σ is the band gap energy value, and E_x is the excitonic energy as given in eqn. (2). Therefore a free exciton can have recombination energy up to $(\mu e^4/2\hbar^2 K^2)$ less than E_σ.

In GaAs, the higher free exciton states are not always distinguishable. The ground state free exciton, however, can sometimes be distinguished as a narrow peak at 1.515 to 1.5153 eV (15:464).

b. Bound Exciton Transitions

The presence of an impurity can sometimes increase the binding energy of an exciton, making it more energetically favorable to remain in the vicinity of the impurity. This situation is called a "bound" exciton. When the electron and hole of a bound exciton recombine, the photon energy is given by the modified equation (4):

$$h\nu = E_\sigma - E_x - E_\flat \qquad (5)$$

where $E_\flat$ is the additional binding energy which depends on the impurity to which the exciton is bound.

19

All exciton peaks disappear rapidly with increasing temperature. Bound excitons will first free themselves of the impurity and then dissociate into individual electrons and holes due to thermal ionization.

3. Free-to-Bound Transitions

Free-to-bound (FB) transitions, also known as band impurity transitions, can either be a transition from the donor level to the valence band or a transition from the conduction band to the acceptor level. The photon energy from such a transition is simply:

$$h\nu = E_g - E_i \qquad (6)$$

where E_i is the same as in eqn. (1) and can be written as E_D for conduction band to donor level and E_A for acceptor level to valence band. Typically E_D ranges from 5 to 7 meV for shallow donors (14:177). Because the donor levels are so close to the band edge, it is difficult to identify them unambiguously. Usually free-to-bound PL studies are necessarily limited to free electron to acceptor transitions.

As impurity concentrations are increased, donor or acceptor levels tend to broaden into a band of states (16:135-136) due to overlapping of the wave functions of electrons. This can make identification of different impurity peaks more difficult.

4. Donor-Acceptor Pair Transitions

When donors and acceptors are simultaneously present in the material, the impurities often form a pair known as a donor-acceptor pair (DAP). The normal ionization energy is

20

reduced by the coulombic interaction between the electron of the donor and the hole of the acceptor. The recombination photon energy is then:

$$h\nu = E_G - E_A - E_D + (e^2/Kr) \qquad (7)$$

where E_G, E_A, and E_D are as defined previously, K is the dielectric constant, and r is the separation between impurities. Note that the last term represents the coulombic interaction.

If it is assumed that most of the impurities are substitutional and located at lattice sites, the separation r will take on discrete values depending on the statistical distribution of the impurities. As a result, a series of sharp DAP lines can often be observed corresponding to the discrete values of r. Contributions from distant pairs will be unresolvable and merge into a broader peak.

If the activation energies E_A and E_D are quite small, only recombinations at relatively distant DAP give bound states according to eqn. (7), and the discrete series of lines are not observed, leaving only the broader peak of the distant pairs (17:119). Discrete DAP lines are not observable in GaAs because E_A is modest and E_D very small.

Williams and Bebb (11:336) list several characteristics that give evidence for DAP emission:

    a) A shift to higher energies as the excitation
    intensity increases (about 1 meV per decade of
    excitation intensity in GaAs).
    b) Narrowing of the emission band with increasing
    intensity.
    c) A shift to higher energies as the donor

21

concentration increases.
d) A rapid decrease in intensity as the temperature
increases from 25 to 35 K.
e) A shift to higher energies with increasing
temperature (line broadening occurs also).

It is also interesting to note that with high doping

levels or increases in temperature that the near band gap

luminescence will usually show larger FB peaks than DAP peaks

in GaAs.(17:145-6)

5. Phonon Assited Transitions

All optical transitions must conserve both energy and

momentum. In an indirect gap semiconductor, this means that

phonon coupling with the lattice is required for minimum

energy transitions. In GaAs, which is direct gap, no phonon

assistance is required to conserve momentum. However, phonon

coupling can occur and resulting radiative transitions at

lower energies can be found in GaAs. As the binding energy of

an electron or hole bound to an impurity gets stronger, its

interaction with lattice vibration increases. This non-

radiative process then reduces the energy released in the

radiative transition. In GaAs, the longitudinal optical (LO)

phonon coupling is by far the strongest, and can reduce

radiative transitions by integer multiples of $36(\pm 2)$ meV

(11:387-8). Any number of lower energy replicas of near band

gap peaks may be observed in a given GaAs PL spectrum.

III. Previous Work

A. Photoluminescence

A previous PL study has been made on Ge implanted GaAs. Yu (8) studied Ge implanted GaAs as a function of exciting wavelength, excitation intensity, temperature, and depth of the implanted layers. Yu used Cr-doped semi-insulating GaAs substrates that were implanted at room temperature at an energy of 120 keV.

The study by Yu included first of all a control substrate with PL peaks which were assigned as follows:

1.514 eV -- Due to unresolved excitons and a donor
to valence band transition
1.488 eV -- Due to Si acceptor in the substrate

For Ge implanted samples the following peaks were observed as the dose was varied from 5×10^{12} to $3 \times 10^{15}/cm^2$ and were assigned as follows:

A) 1.468-1.480 eV -- Donor-Ge acceptor pair transition
B) 1.43-1.46 eV   -- Donor-Ge acceptor pair modified by
a random impurity potential
C) 1.435 eV   -- As vacancy-Ge acceptor complex
D) 1.38 eV   -- Ga vacancy-deep acceptor transition
E) 1.18 eV   -- Ga vacancy-Ge donor complex

In addition, Yu made the following conclusions:

1) The As vacancy-Ge acceptor complex emission was dominant in the near surface region (0-300 Å), the donor-Ge acceptor pair emission was dominant in the region 300-1000 Å, and the Si acceptor related emission was dominant in the region 1000-3000 Å.

2) Emissions due to the donor-Ge acceptor pair are

23

present in all Ge-implanted layers.

    3) The binding energy associated with the Ge acceptor is 40±3 meV.

B. Electrical Measurements

Yeo *et.al.* studied the electrical properties of Ge implanted GaAs which was reported in a series of papers (5,6,7,18). Cr-doped semi-insulating GaAs samples were implanted with Ge, Ge+As, and Ge+Ga. Annealing temperatures were varied between 700-1000°C and the dose concentration was varied between $5x10^{12}$ to $3x10^{15}/cm^2$ for different samples. Tables 1 through 3 show a summary of the type of electrical activity manifested in each sample. In the tables, P represents p-type behavior, N represents n-type, and T_A represent the anneal temperature.

Table 1
Electrical Activity: Ge Implanted GaAs

Ion Dose\T_A	700	750	800	850	900	950	1000
$1x10^{13}/cm^2$	P	P	P	P	P	P	
$3x10^{13}$	P	P	P	P	P	P	
$1x10^{14}$	P	P	P	P	P	P	
$3x10^{14}$	P	P	P	P	P	N	N
$1x10^{15}$	N	N	N	N	N	N	N
$3x10^{15}$	N	N	N	N	N	N	N

Table 2
Electrical Activity: Ge+Ga Implanted GaAs

Ion Dose\T_A	700	750	800	850	900	950	1000
$1x10^{13}/cm^2$	P	P	P	P	P	P	P
$3x10^{13}$	P	P	P	P	P	P	P
$1x10^{14}$	P	P	P	P	P	P	P
$3x10^{14}$	P	P	P	P	P	P	P
$1x10^{15}$	P	P	P	P	P	N	N
$3x10^{15}$	P	P	P	P	P	N	N

Table 3
Electrical Activity: Ge+As Implanted GaAs

Ion Dose\T_A	700	750	800	850	900	950	1000
$1 \times 10^{13}/cm^2$	P	P	P	P	P	P	P
3×10^{13}	P	P	P	P	P	P	P
1×10^{14}	N	N	N	N	N	N	N
3×10^{14}	N	N	N	N	N	N	N
1×10^{15}	N	N	N	N	N	N	N
3×10^{15}	N	N	N	N	N	N	N

The following conclusions were reached:

a) P-type and n-type layers were produced, depending on ion dose and anneal temperature.

b) For Ge singly implanted, samples had p-type electrical activation efficiency of up to 38% at an ion dose of $1 \times 10^{13}/cm^2$ and an anneal temperature of 950°C. N-type samples had low activation efficiencies with the highest at 5% at a dose of $1 \times 10^{15}/cm^2$ and an anneal temperature of 950°C.

c) At lower dose and anneal temperature, Ge atoms apparently prefer to locate in As sites. As the Ge-ion dose and anneal temperature increase, an increasing number of Ge atoms tend to go into Ga sites, raising the degree to which p-type behavior is compensated by n-type. At higher dose and anneal temperatures, it seems more Ge atoms tend to replace Ga atoms than As atoms, but the electrical activity remains highly compensated.

d) The dual implantation of As with Ge enhances the n-type activity for ion doses $\geq 1 \times 10^{15}/cm^2$, a type conversion occurs for intermediate doses, and has little effect on p-type activity for ion doses $\leq 3 \times 10^{13}/cm^2$. The maximum electrical activation efficiency was 50% at a dose of $1 \times 10^{13}/cm^2$ and an

25

anneal temperature of 950°C for p-type samples, while it was 24% at a dose of $3x10^{14}/cm^2$ and an anneal temperature of 1000°C for n-type samples.

e) The dual implantation of Ga with Ge enhances the p-type activity for ion doses $\leq 3x10^{14}/cm^2$, while the original n-type activity of Ge singly implanted changed to p-type for doses $\geq 1x10^{15}/cm^2$, except for anneal temperatures > 900°C. The maximum p-type activation efficiency was 68% at a dose of $1x10^{13}/cm^2$ and an anneal temperature of 950°C.

IV. Description of Experiment

A. Sample Preparation

The substrate material used was <100> oriented semi-insulating (SI) Cr-doped GaAs obtained from Crystal Specialties, Inc. The substrate was grown by the Horizontal Bridgman method. The sample size ranged from 1/4 to 3/16 inch square wafers. Before ion implantation, the samples were carefully cleaned with acquasol, deionized water, trichloroethylene, acetone, and methanol and dried with nitrogen gas. Next, the samples were free-etched with an $H_2SO_4 : 30\%H_2O_2 : H_2O$ solution in a 3:1:1 ratio by volume for 90 sec. Free-etching removes unwanted surface damage caused by crystal cutting and polishing.

Ion implantation was performed at an ion energy of 120 keV at room temperature. The incident ion beam was directed from a hot cathode source at 7° off the <100> crystal axis to minimize ion-channeling effects. Ion implantation took place using a Varian/Extrion model 400-10AR ion implanter (Fig. 5). When dual implantation was accomplished, the doses and energy were made equal and implanted sequentually. Implantation was carried out at dose concentrations ranging from $1x10^{13}$ to $1x10^{15}/cm^2$.

After implantation, the samples were once again cleaned and subsequently encapsulated with an approximately 1000 Å layer of silicon nitride (Si_3N_4) in a cold-wall pyrolitic
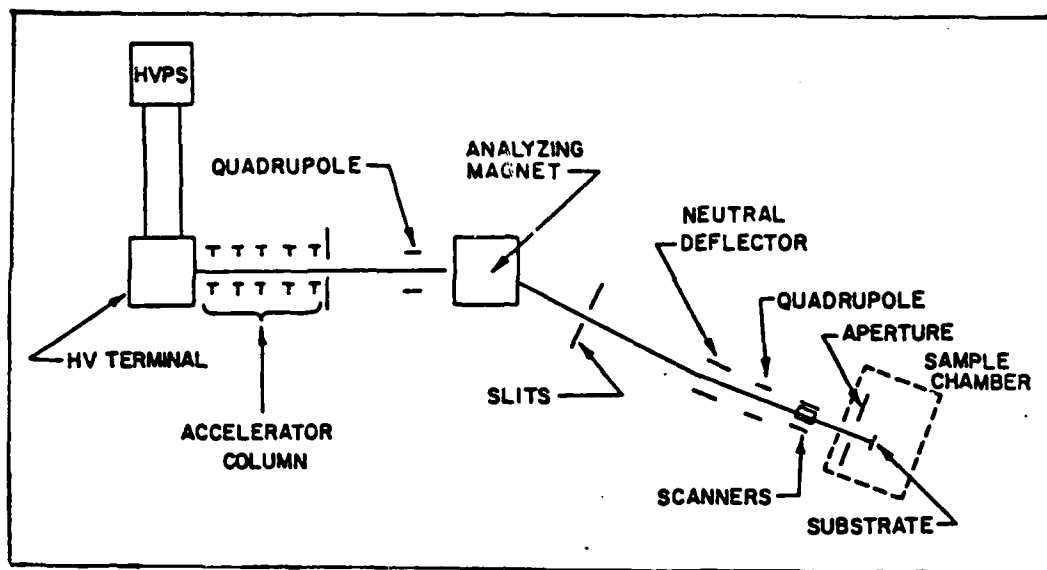
Fig. 5 Schematic diagram of Ion Implantation Machine

28

reactor. The Si_3N_4 deposition took place in 35 sec. at 700°C, the samples reaching 700°C within 9 sec. (18:618). Encapsulation was preparatory to thermal annealing and prevented the tendency of As to outdiffuse, thereby protecting the surface from decomposition via the encapsulant.

The samples were then annealed at various temperatures in flowing hydrogen gas for 15 min. Anneal temperatures ranged from 700 to 950°C. The samples were placed cap-side down on a GaAs substrate to improve the performance of the encapsulant at high anneal temperatures. No sign of surface degradation could be observed by visual inspection (6:5786). Dissolution of the encapsulant took place in 48% hydroflouric acid for 3 min. The samples were then given one final careful cleaning using trichloroethylene, acetone, methanol and deionized water; being blown dry with dichlorodiflouromethane gas.

B. Photoluminescence Experimental Setup

Photoluminescence measurements were taken using the experimental setup as shown in Fig. 6.

1. Excitation Source and Setup

The optical excitation source used was a Spectra-Physics series 2000 Krypton-ion laser. A single red line set at 6741 Å was used.

Most measurements were taken at a low laser power of 8 to 9 milliwatts (mW). However, certain data was taken at up to 80 mW. To achieve this, the laser was set in its constant power mode at 200 mW with the plasma tube current running at
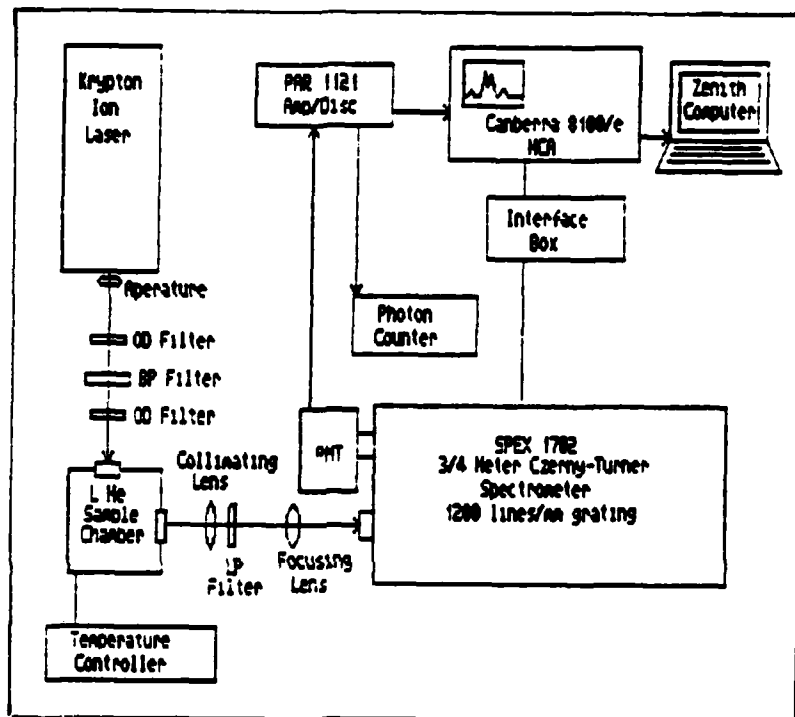
Fig. 6 Photoluminescence experimental setup

30 amps and the magnet current running at about 5 amps. After
the beam exited the laser aperture it was desired that stray
ultraviolet light be removed from the laser beam, so a 6500 Å
narrow band-pass filter was placed in the beam's path. This
reduced the beam power to near 80 mW. To reduce the beam even
more, two 0.5 optical density filters were placed in the beam
path, reducing the laser power to approximately 8.5 mW. The
beam then passed through a mirrored optical periscope and was
directed through quartz windows into the cooled sample chamber
and onto the sample. The beam waist was approximately 2 mm in
diameter. As a result, the approximate power density for a
laser power of 8.5 mW was 0.27 W/cm^2. This was the usual
setting. At a power of 80 mW the maximum power density was
2.55 W/cm^2.

2. Optical Detection System

After the sample is optically excited by the laser,
photoluminescence is emitted and travels through the sample
chamber window. The PL is approximately collimated outside
the sample chamber by a lens (focal length= 70mm). The PL
then passes through a long-pass filter (passes $\lambda > 6650$ Å) and
then is focused through a second lens (f#=5) onto the
spectrometer entrance slit.

The PL emission was then dispersed with a SPEX 1702 3/4
meter Czerny-Turner Spectrometer. The grating used was blazed
for 5000 Å at 17° 27' and had 1200 lines/mm. The grating was
used for first order diffraction. The spectrometer had linear
reciprocal dispersions of 10.24 to 9.70 respectively, for the

31

end values of the range from 8100 to 9320 Å (19:19). The entrance and exit slit widths were 75 and 150 μm, respectively. For maximum throughput, the exit slit should be at least twice the entrance slit (19:20). The resulting average resolution was approximately 0.75 Å or 0.125 meV in the wavelength range mentioned.

At the beginning of each experimental run, the entrance and exit slits were set to 10 and 20 μm each, so that an argon lamp could be used to calibrate the spectrum. The 8115.31 Å argon line was used as the calibration point. Immediately after scanning this line the slits were set to 75 and 150 μm to complete the run.

An EMI GENCOM #9808B Photomultiplier Tube (PMT) was connected to the exit slit of the spectrometer to collect the dispersed PL. The PMT was liquid nitrogen cooled and employed an S-1 type photocathode. The PMT's spectral response curve is shown in Fig. 7.

The PMT electrical signals were next sent to a Princeton Applied Research (PAR) Model 1121A Amplifier/Discriminator (AD) with a built in high voltage supply to run the PMT. In order to achieve the best signal to noise ratio, threshold controls on the AD were optimized for the desired wavelength region.

At this point, a PAR Model 1112 Photon Counter/Processor was used to get a real time look at photon counts. The initial photoluminescence alignment into the spectometer was
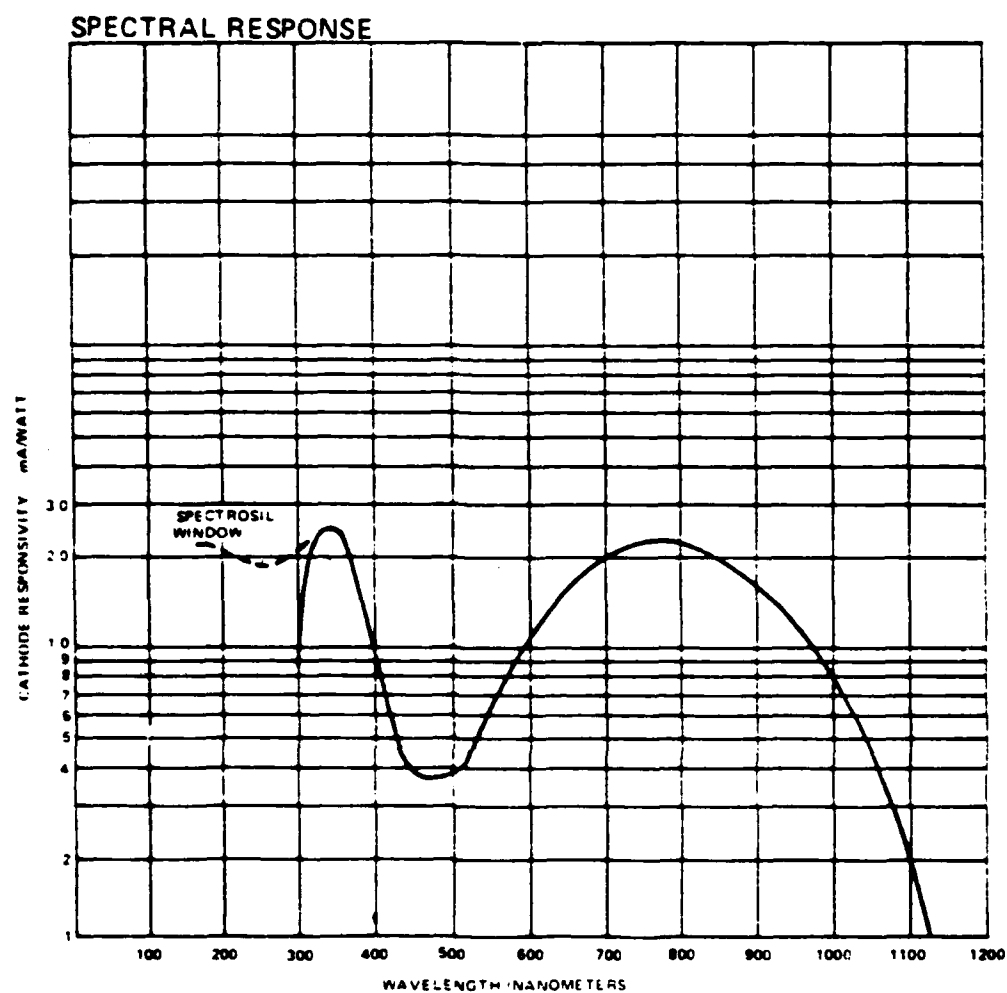
32

SPECTRAL RESPONSE

Fig. 7   Response curve of EMI GENCOM #9808B PMT

33

made much easier by watching and optimizing the photon count number.

The signal from the AD was next sent to a Canberra 8100/e Multi-Channel Analyzer (MCA). In order to make the MCA channel advance rate synchronous with the spectrometer scan rate, an interface consisting of an external step motor driver was used. The scan rate was set to scan at 0.434 Å/channel for all experimental runs.

It is important for the resolution obtained from the electrical components of the optical detection system to be at least as good as the resolution obtained from the spectrometer (4:38). In this experiment the electronic component resolution (0.434 Å) was better than the spectrometer slit resolution (0.75 Å).

3. Sample Cryogenics

Photoluminescence is highly dependent on temperature. At temperatures as high as room temperature a great deal of the optical transitions cannot take place due to excessive thermal excitation. A cryogenic system is used to remedy this situtation and cool samples to near liquid helium temperatures. An Andonian Cryogenics, Inc. cryostat was used to cool the sample. A schematic of this cryostat and its support vacuum pumps is shown in Fig. 8.

The cryostat consisted of an outer 4-liter liquid nitrogen (LN$_2$) reservoir and an inner 3-liter liquid helium (LHe) reservoir. Each reservoir is surrounded by a vacuum chamber to insulate from external temperatures and keep heat
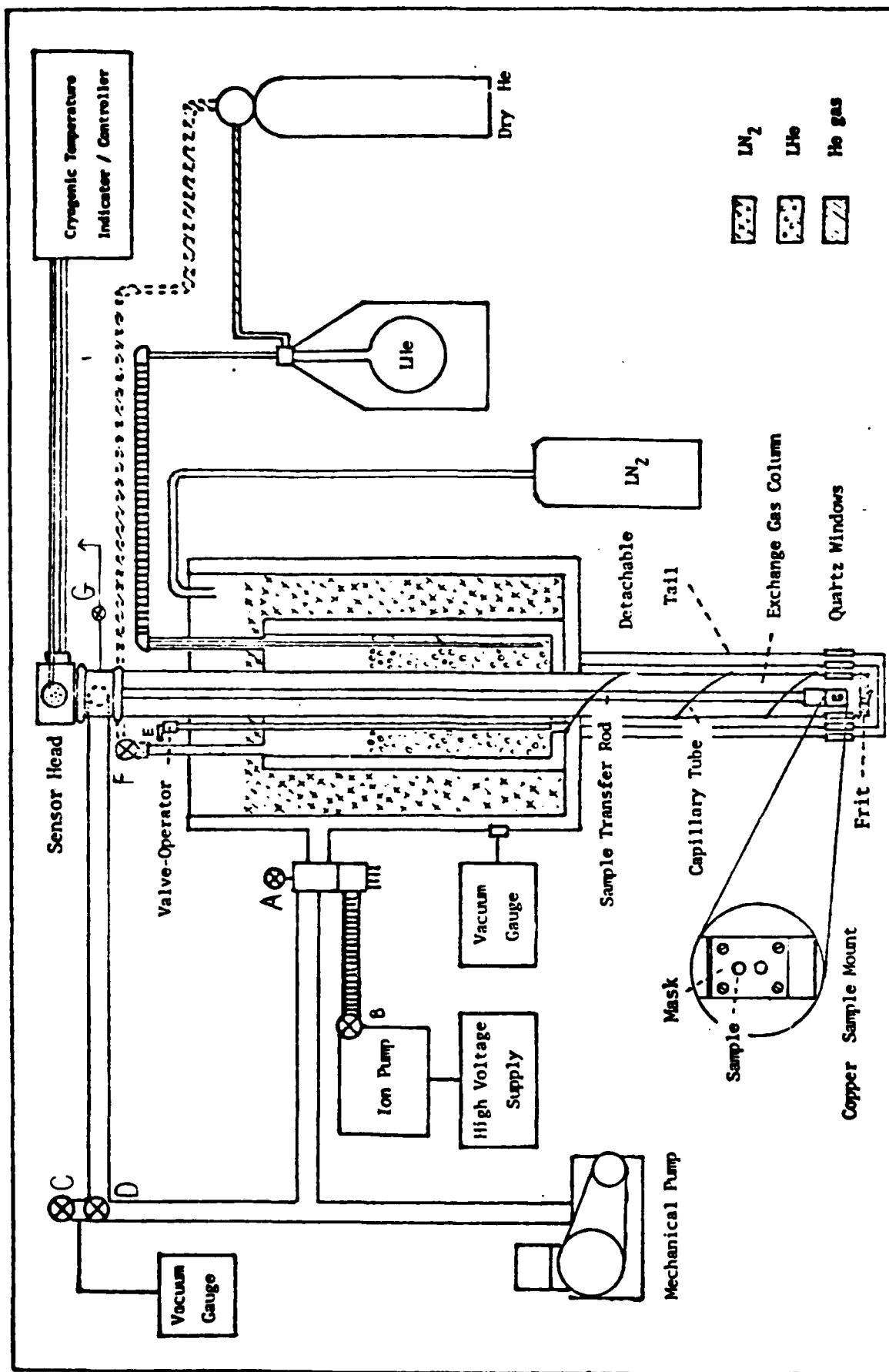
34

Figure 8 Cryogenic and Evacuation System

35

transport to a minimum. The LN$_2$ reservoir acted as a cold buffer between the room temperature environment and the LHe reservoir. As the LHe slowly boils off in its reservoir, the cold liquid helium passes through a capillary tube into the sample chamber located in the tail of the cryostat. The sample is cooled by the evaporated helium. Care had to be taken to control the needle valve to the capillary tube to avoid flooding the sample chamber with LHe and avoid the resulting interference due to turbulent boiling.

The following procedure was used in evacuating and cooling the cryostat:

a) A mechanical roughing pump was used to evacuated the vacuum chamber to about 10^{-3} torr by opening valve A.

b) Next, a forepump followed by a diffusion ion pump evacuated the chamber to about 10^{-6} torr by opening valve B and closing valve A.

c) The LHe reservoir is next flushed out with helium gas through fill hole F, through the capillary tube into the sample chamber, and out through the flowmeter (G). This is to ensure that air and moisture are removed to prevent freezing and blockage of the capillary tube and needle valve. A valve at fill hole F is closed with a back pressure of helium gas.

d) LN$_2$ was poured into its reservoir through a funnel placed in the LN$_2$ fill hole. A vent hole is opened during the filling process. After filling completely, the reservoir is allowed to settle and both holes are plugged with rubber

stoppers.

e) LHe was transferred through a transfer line into the LHe fill hole. A vent hole was open during the process. Care was taken to transfer slowly to avoid a volatile transfer. There was indication that the transfer was complete when a strong opaque plume caused by helium vapor was observed at the vent hole.

f) Throughout an experimental run, the needle valve E was adjusted to maintain a stable temperature.

Samples were inserted into the cryostat by first being mounted on a sample finger. At the end of the sample finger was a copper block. On opposing sides, cut into the copper block, were square depressions to place the samples. Samples were mounted with a small sticky film of GE varnish applied to their backsides to prevent them from dislocating within the sample chamber. Thin copper sheets containing circular apertures 4 mm in diameter were placed over the samples in the block and secured into place with two screws. The circular apertures overlayed the center of each sample. The sample finger with the mounted samples was then placed into the center of the cryostat.

The temperature of the samples was monitored via a temperature sensing diode that was attached to the sample copper block. This in turn was connected to a Lakeshore Cryotronics Temperature Controller. The temperature was maintained at 4.5 to 5 K for most experimental runs.

37

V. Results and Discussion

The photoluminescence spectra of semi-insulating GaAs
can be difficult to evaluate. Crystals grown by the
horizontal Bridgman method produce PL emission peaks that
are broad and the luminescent efficiencies tend to be low
(14:177). Peaks that are broad often hide information. In
the measurements taken in this experiment, with the exception
of one run, peaks due to exciton transitions were always
unresolved. Also, peaks due to several different impurity
acceptor transitions could merge into one or two peaks,
leaving one with less ability to identify the peaks' origin.
However, more often than not, there was enough resolution in
the measurements presented here to distinguish and compare
important acceptor related peaks.

A. Control Substrate

An unimplanted, uncapped, unannealed sample of Cr-doped
semi-insulating GaAs was used as the control substrate. Its
photoluminescence spectrum is shown in Fig. 9. The
identified peaks and their assignment are as follows:

        1.514 eV -- Unresolved excitons bound to neutral
                    donors
        1.490 eV -- Neutral donor - C acceptor transition
        1.470 eV -- Possibly due to an As vacancy transition

In a study by Heim and Hiesinger (15:464), a series of
exciton emission lines occur in GaAs between 1.5133 and 1.515
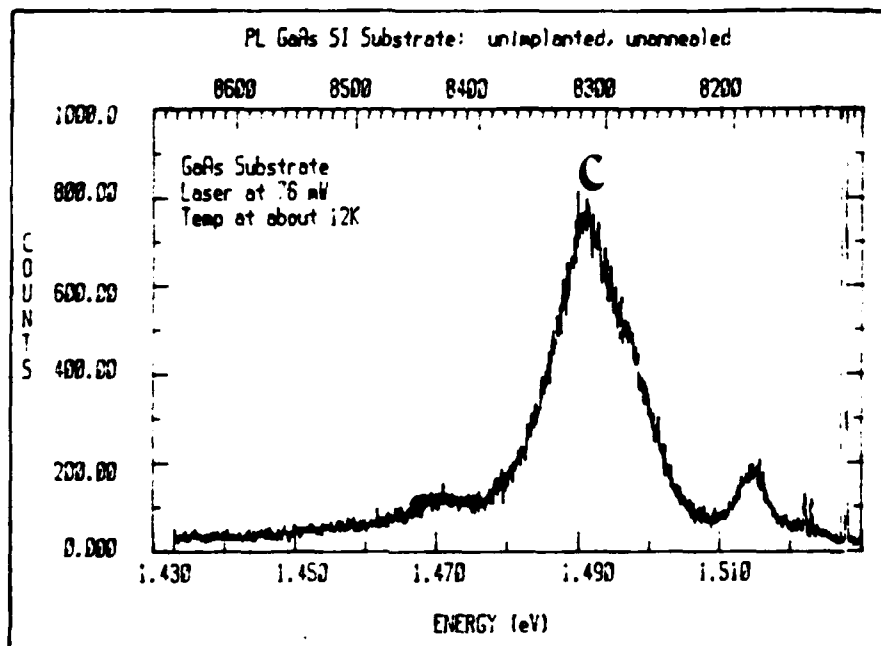eV which all involve excitons bound to neutral or ionized

Fig. 9   PL spectrum of GaAs substrate.   Source
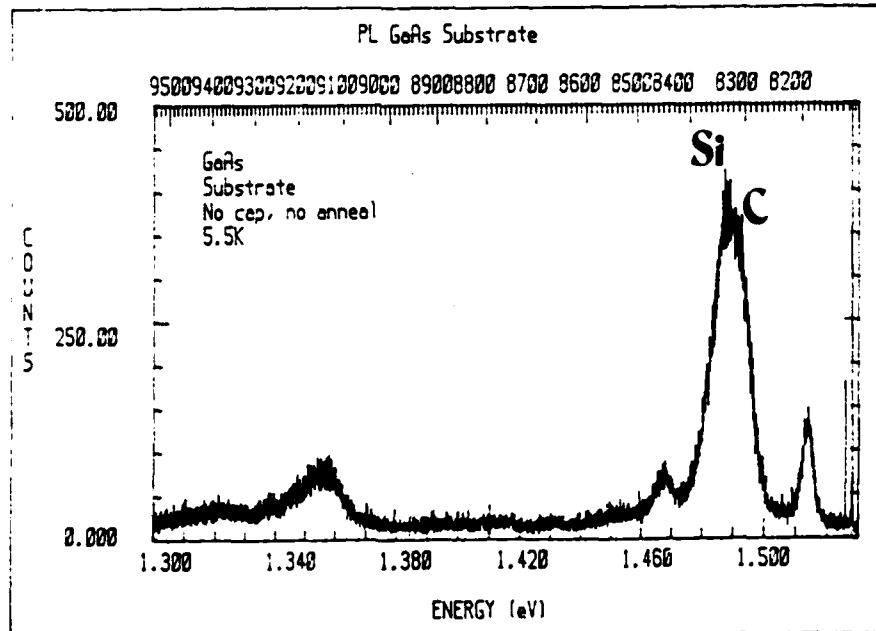   intensity: 2.4 W/cm².

Fig. 10   PL spectrum of control substrate contributed by
          K. Keefer.   Source intensity: 1.4 W/cm².

donors. The exciton line observed in this control substrate
is unresolved with a peak in the range ascribed to donor
bound excitons. Yu observed a similar peak and assigned it
as several unresolved excitons and a donor to valence band
transition (8:7165).

The next peak, 1.490 eV, is assigned as a neutral donor
to C acceptor peak. It is generally known that carbon is a
common residual impurity in GaAs grown in many different
methods. A donor-C acceptor peak is often observed at about
1.49 eV. In Cr-doped semi-insulating GaAs this peak was seen
at 1.490 eV by Swaminathan et. al. (20:159). Keefer also
observed this peak at 1.491 eV in LEC grown GaAs (21).

It is probable that because of its broadness, the 1.490
eV peak is an unresolved combination of the C-related peak and
a conduction band to Si acceptor transition. In the contol
substrate in Yu's study, a large emission band assigned as a
Si acceptor related peak was observed at 1.488 eV. The
samples used by Yu were similar to those used in this study.
Measurements taken by Keefer with a similar control substrate,
using the identical experimental equipment used in this study,
resulted in the spectrum shown in Fig. 10. A peak due to Si
at 1.487 eV is evident and merges in such a way that a
shoulder due to C is present at 1.491 eV. As will be seen
later, the Si related peak was always observed in implanted
samples used in this study, and usually dominated the C
related peak. In implanted samples, the Si related peak was
probably enhanced due to the fact that a Si_3N_4 encapsulant was

used during the annealing process. Yu, in another study (22:5046), reported that in n-type GaAs substrates that had been heat treated and encapsulated with Si_3N_4, "acceptors in the heat-treated layers are mainly Si diffused from the Si-rich film under an As-vacancy-rich atmosphere with the Si_3N_4 film."

The origin of the peak at 1.470 eV is unclear. However, it is possible it is due to an As vacancy related transition. Adegboya and Tuck (23) observed such a peak at 1.4736 eV in Cr-diffused GaAs. Chatterjee et. al. (24) observed a 1.47 eV peak in annealed GaAs and assigned it to an As vacancy or related defects. With the exception of one sample, a 1.470 eV peak was not observed in implanted samples in this study.

B. Main Indicators of Activity

Before examining the spectra in this study, it should be noted that there are peaks that are especially important to consider. First, the peaks that relate to Ge acceptors are important because these are indicators of Ge atoms occupying As sites and contributing to the p-type behavior of the sample. Second, the exciton peaks are important because the excitons in this study are bound to donors. An increase in relative exciton intensity is an indicator of an increase in the number of donors which contribute n-type activity. Third, the Si-acceptor (Si_{As}) related peak is important because it provides a reference to make a first order comparison of the relative strength of germanium acceptor (Ge_{As}) peaks and

41

exciton peaks. Since Si is "intrinsic" to all samples, it is used for comparison.

This comparison method is adopted in order to draw some correlation between electrical data and PL data. Tajima (25) used the approach in silicon samples to take the ratio of "intrinsic" impurity peaks to extrinsic impurity peaks and found a correlation between higher resistivities and higher intensities of intrinsic peaks relative to extrinsic peaks. This relative intensity approach is only an approximate way to try and identify a trend. The approach assumes that the relative intensity of the Si_{AS} peak doesn't vary much from sample to sample.

Another important point to mention in regard to peak intensity and photoluminescence, is that luminescent efficiency is dependent on surface quality. Surface defects can reduce the overall intensity of a sample's PL spectrum (14:176). A wide assortment of samples was used in this study with varying surface quality. Some samples had much stronger PL than others due to variables in the experiment such as surface quality and also PL alignment into the spectrometer.

C. Ge Implanted GaAs

The PL data of Ge implanted GaAs will be presented first to have a foundation to build upon for further discussion.

1. Peaks Observed

A matrix of different samples of Ge singly implanted into GaAs were measured optically. Three different dose

42

concentrations were used: 1×10^{13}, 3×10^{14}, and $1 \times 10^{15}/cm^2$.
Anneal temperatures that were used were 700, 750, 800, 900,
and 950°C. The peaks observed are listed below along with
their assignments.

Peak (eV)	Assignment
1.5274	-- 8115.31 Å argon lamp calibration line
1.513-1.514	-- Unresolved excitons bound to neutral or ionized donors. (BE)
1.493	-- Conduction band - C acceptor. (e, C_{As})
1.491-1.492	-- Donor - C acceptor pair. (D, C_{As})
1.487-1.488	-- Conduction band - Si acceptor. (e, Si_{As})
1.483-1.484	-- Donor - Si acceptor pair. (D, Si_{As})
1.476-1.478	-- Ge acceptor related transition. (Ge_{As})
1.471	-- Unknown.
1.453-1.458	-- LO phonon replicas of Si or C free-to-bound or donor-acceptor pair transitions.
1.448-1.450	-- Ga in As vacancy anti-site defect. (Ga_{As}) or LO phonon replica of 1.484-1.486 eV peak.
1.440-1.442	-- LO phonon of Ge acceptor transition.
1.406-1.408	-- Donor-deep acceptor pair, possibly related to manganese. (Mn_{Ga})
1.391	-- Unknown.
1.370-1.371	-- LO phonon of 1.406-1.408 eV peak.
1.356-1.359	-- Ga vacancy related defect.

In this study the 1.476-1.478 eV peak is important and is
Ge acceptor related. Its energy value is close to that of
1.4790 eV reported for a Ge free to bound (FB) transition

(26:1051). However, in this study, it showed signs of donor-acceptor pair (DAP) behavior by shifting to a higher energy with increasing excitation intensity and increasing sample temperature. Whether or not it is FB, DAP, or a combination of both is uncertain, but it is important to note that it is Ge related.

Among all the implanted samples, the 1.471 eV peak was only observed at a dose of $1 \times 10^{13}/cm^2$ and an anneal temperature of 950°C. It behaved like a donor-acceptor pair by shifting to a higher energy with an increase in excitation intensity, and it also merged with the previously mentioned Ge_{As} peak at a high excitation intensity. Its assignment is uncertain. It is possibly a donor-Ge acceptor modified by a random impurity potential similar to band observed by Yu (8) at 1.43-1.46 eV, or an As vacancy transition as mentioned in the control subsrate section. However, there is not enough information available here to determine its origin.

The peak at 1.448-1.450 is probably associated with the neutral state of the Ga_{As} antisite double acceptor defect. Evidence in the literature for the identification as an antisite defect is circumstantial, but it is based on studies where Ga-rich melts in crystal growth favor the formation of Ga_{As} antisite defects (27:1785). The samples studied here give support for its assignment as a Ga_{As} defect because the peak is enhanced in samples dually implanted with Ge and Ga.

The 1.406-1.408 eV peak is caused by a donor-deep acceptor pair transition. In this study, the peak shifted to

44

higher energy with increasing excitation intensity, suggestive
of a DAP. Hallais et. al. (28) and Zucca (29) have attributed
this peak to an isolated Mn_{Ga} acceptor based on Mn-doped GaAs.
Swaminathan et. al. (20:163-164), report that this peak may
not necessarily be due to Mn and were unable to identify the
peak as that of the donor and acceptor.

The last peak to be discussed is one observed at 1.356-
1.359 eV. Chatterjee et. al. (24) studied defects generated
by outdiffusion of Ga and As during annealing, and assigned
the peak at 1.35 eV as that associated with Ga vacancies
(V_{Ga}). In this study, the V_{Ga} peak disappears with high
anneal temperature.

2. Dose and Anneal Temperature Dependence

The peaks mentioned just previously can be seen in
the comparative spectra in Figs. 11-18. These figures show
Ge dose concentration or anneal temperature dependence, with
each figure representing either one anneal temperature or one
dose concentration.

Figs. 19 and 20 show several graphs summarizing the
relative intensity ratios observed in the comparative
spectra. Each graph shows points of the relative heights of
the Ge_{As} peak to the (e,Si_{As}) peak and connects the points
with a dashed line, and also shows points of the relative
heights of the donor bound exciton peak and the (e,Si_{As}) peak
and connects those points with a solid line.

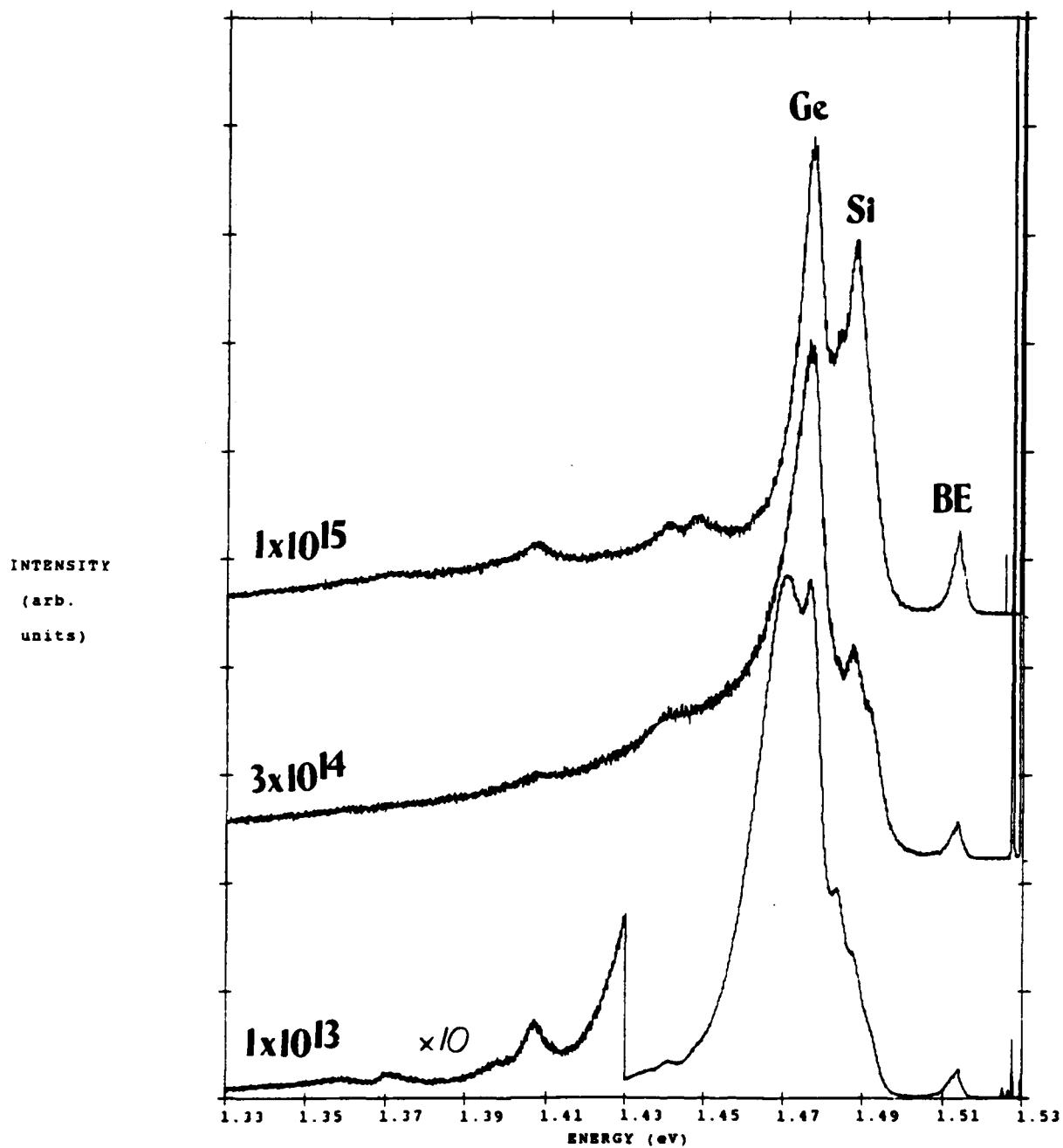For an anneal temperature of 950°C the trend of dose

45

Fig. 11 PL dose dependence comparative spectra of GaAs:Ge
at about 5°K using 6471 Å line. Source intensity: 0.27
W/cm². Anneal temperature T_A=950°C for 15 min.
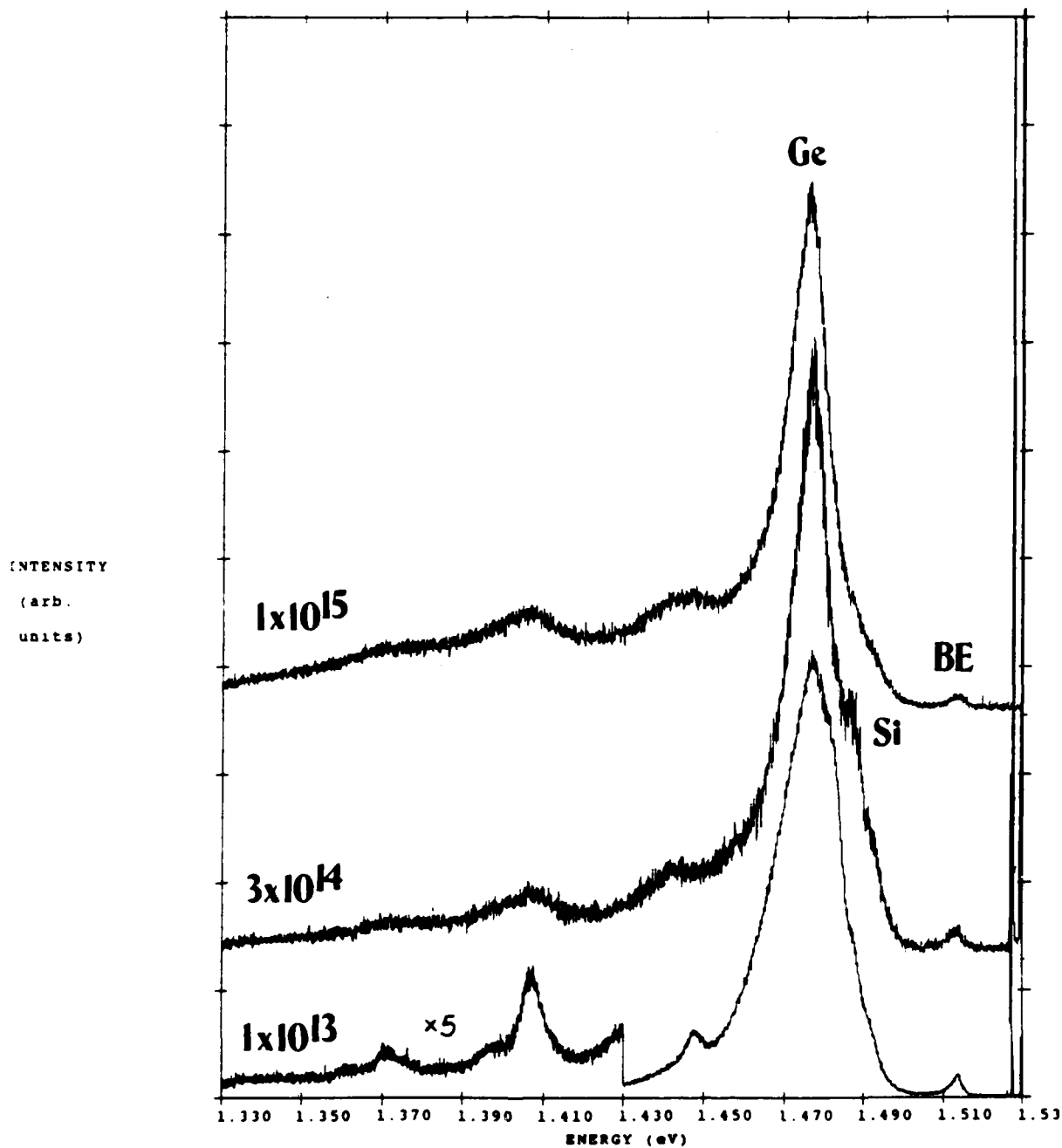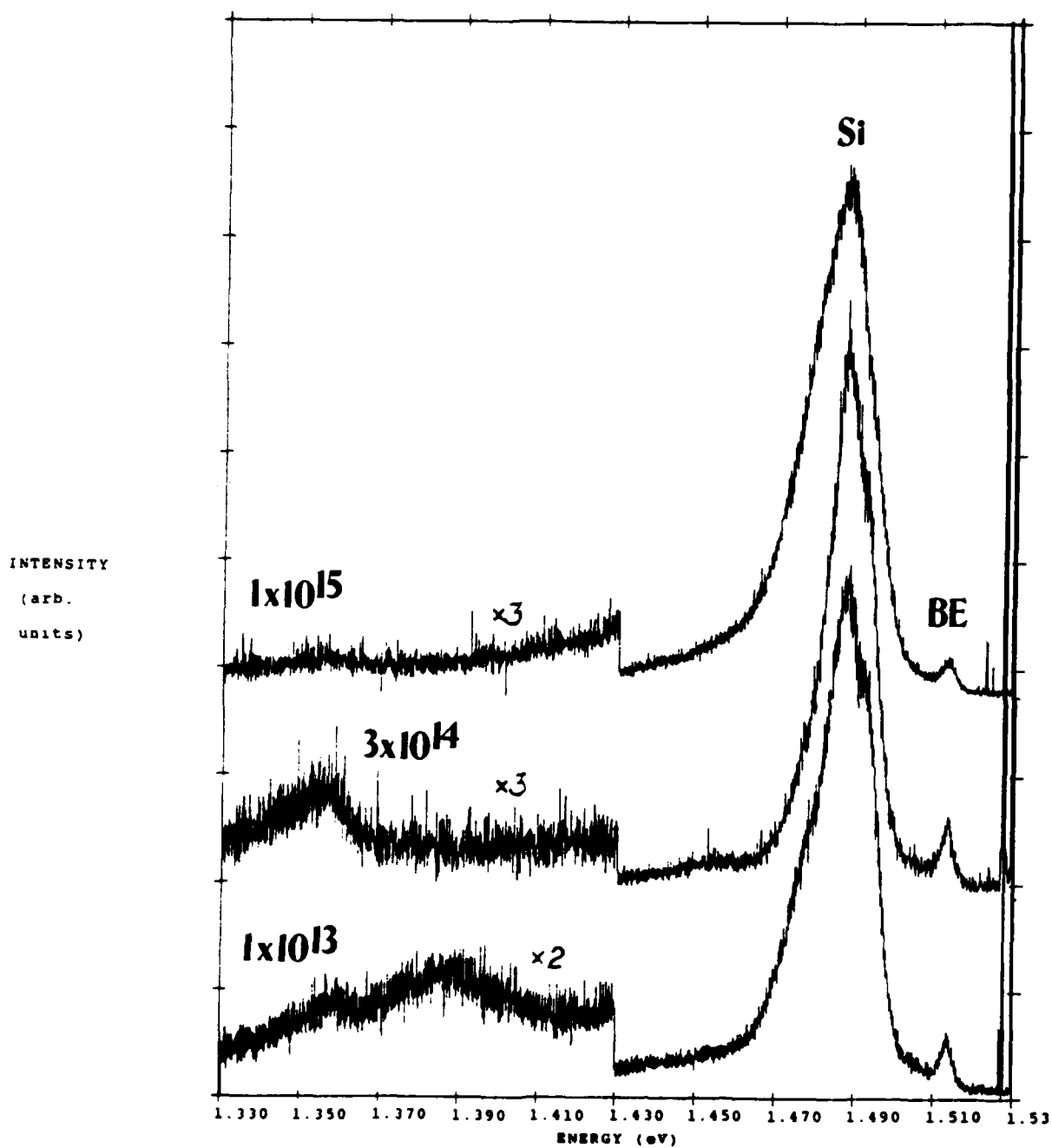
46
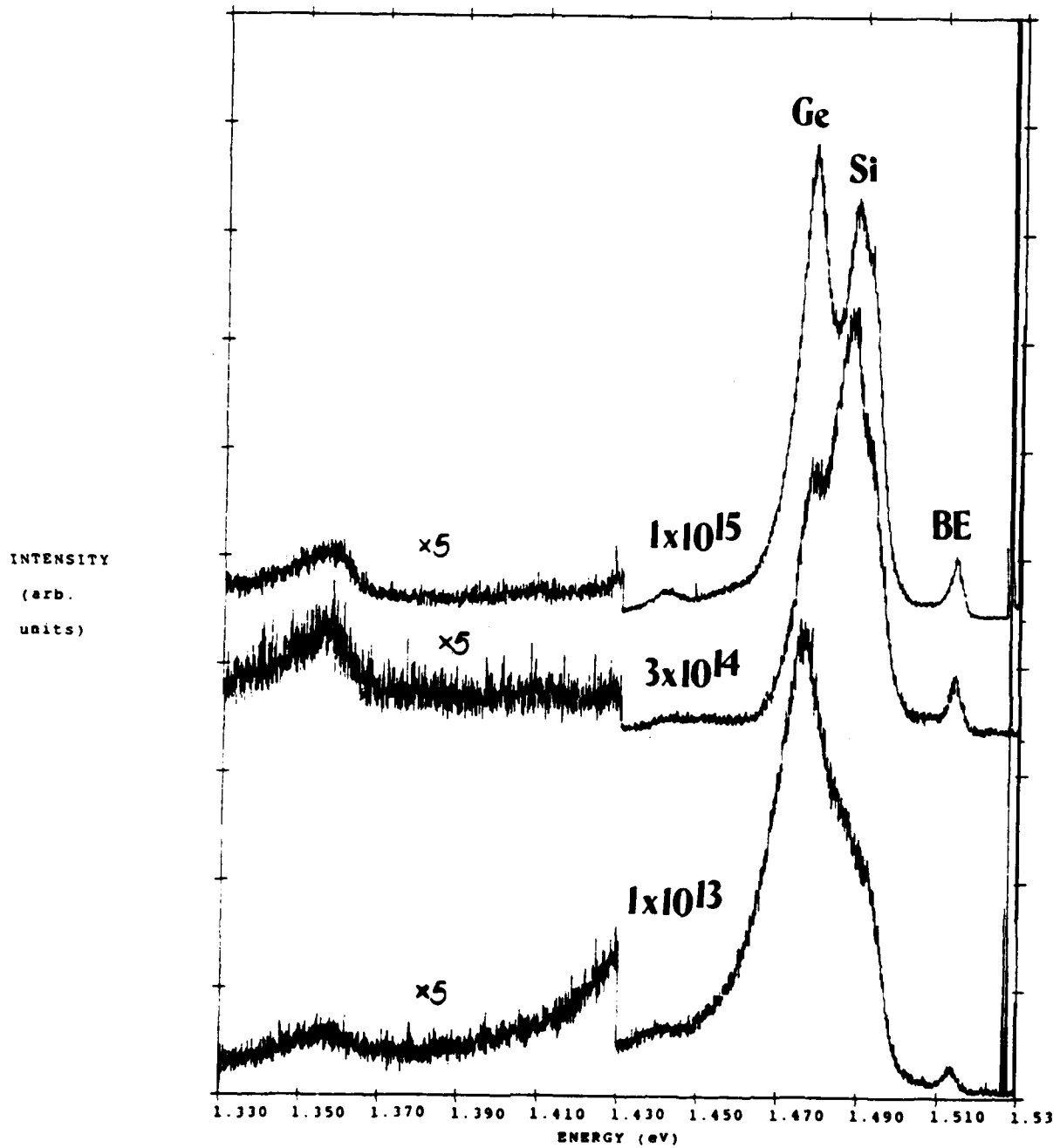
Fig. 12   PL dose dependence comparative spectra of GaAs:Ge at about 5°K using 6471 Å line.   Source intensity: 0.27 W/cm².   Anneal temperature T_A=900°C for 15 min.

47

Fig. 13 PL dose dependence comparative spectra of GaAs:Ge
at about 5°K using 6471 Å line. Source intensity: 0.27
W/cm². Anneal temperature T_A=800°C for 15 min.

48

Fig. 14 PL dose dependence comparative spectra of GaAs:Ge
at about 5°K using 6471 Å line. Source intensity: 0.27
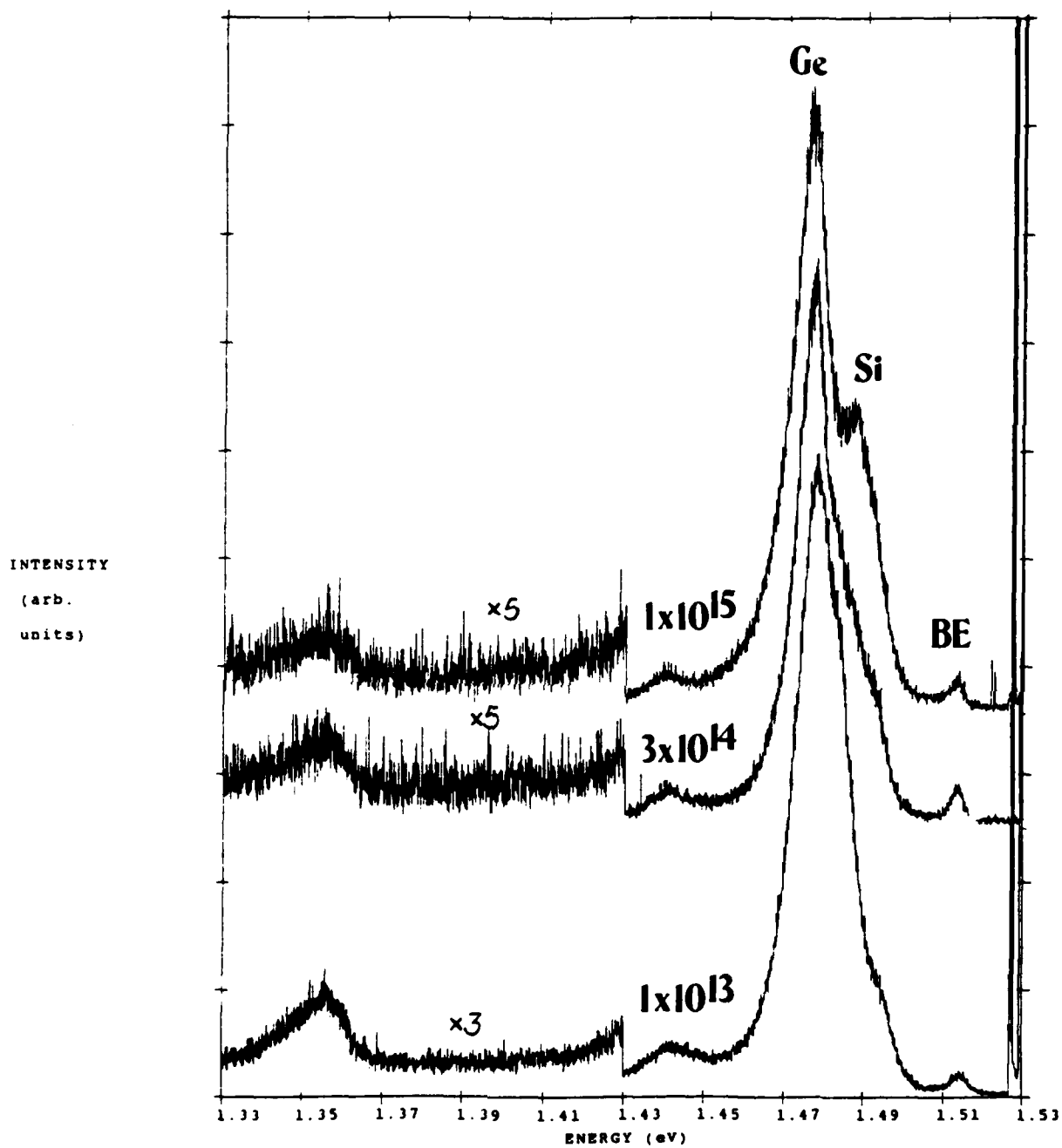W/cm². Anneal temperature T_A=750°C for 15 min.

49

Fig. 15 PL dose dependence comparative spectra of GaAs:Ge at about 5°K using 6471 Å line. Source intensity: 0.27 W/cm². Anneal temperature T_A=700°C for 15 min.
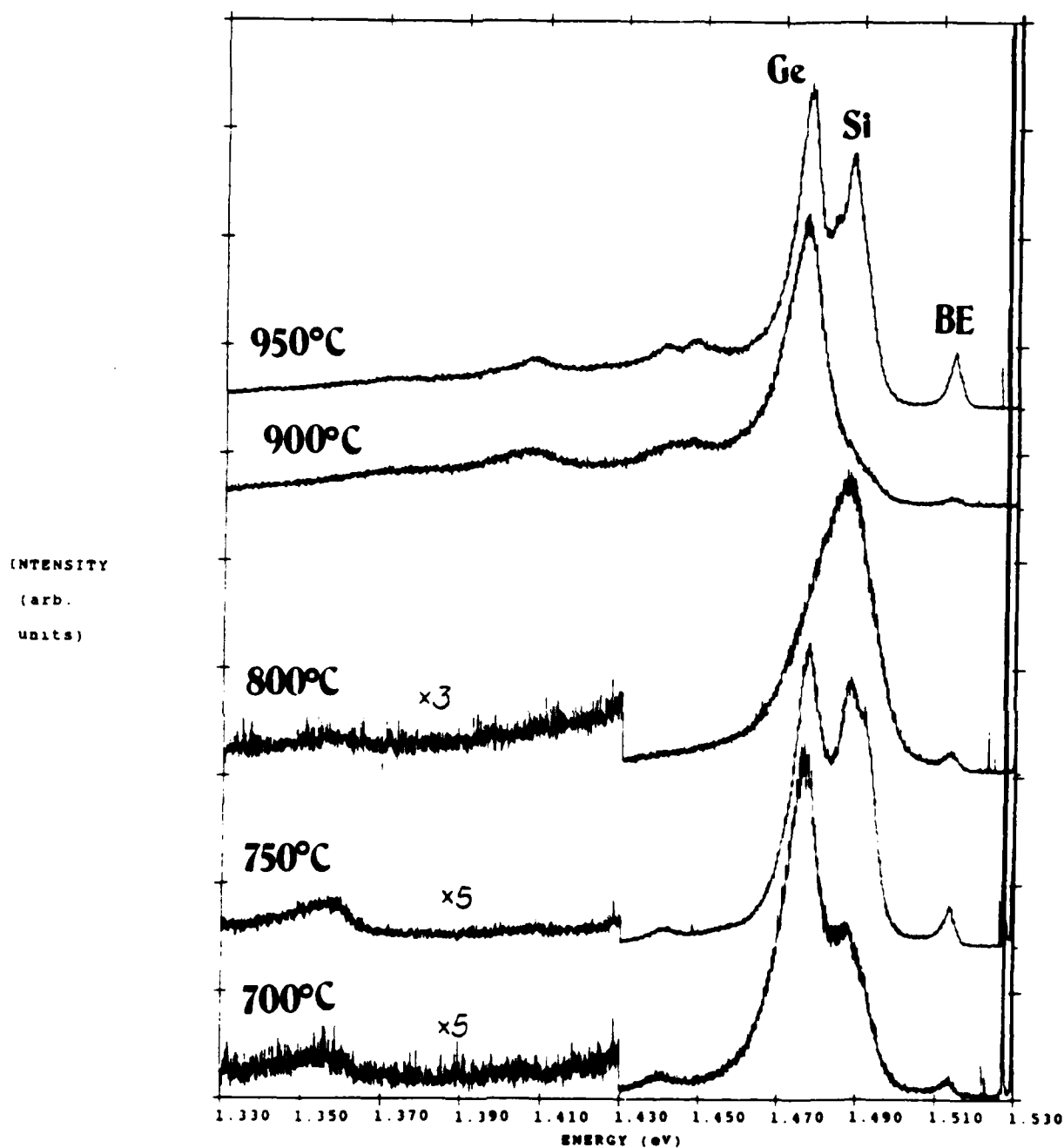
Fig. 16 PL anneal temperature dependence comparative
spectra of GaAs:Ge at about 5ºK using 6471 Å line. Source
intensity: 0.27 W/cm². Dose = 1x10¹⁷ions/cm².

51

Fig. 17 PL anneal temperature dependence comparative
spectra of GaAs:Ge at about 5°K using 6471 A line. Source
intensity: 0.27 W/cm². Dose = 3×10^{14} ions/cm².

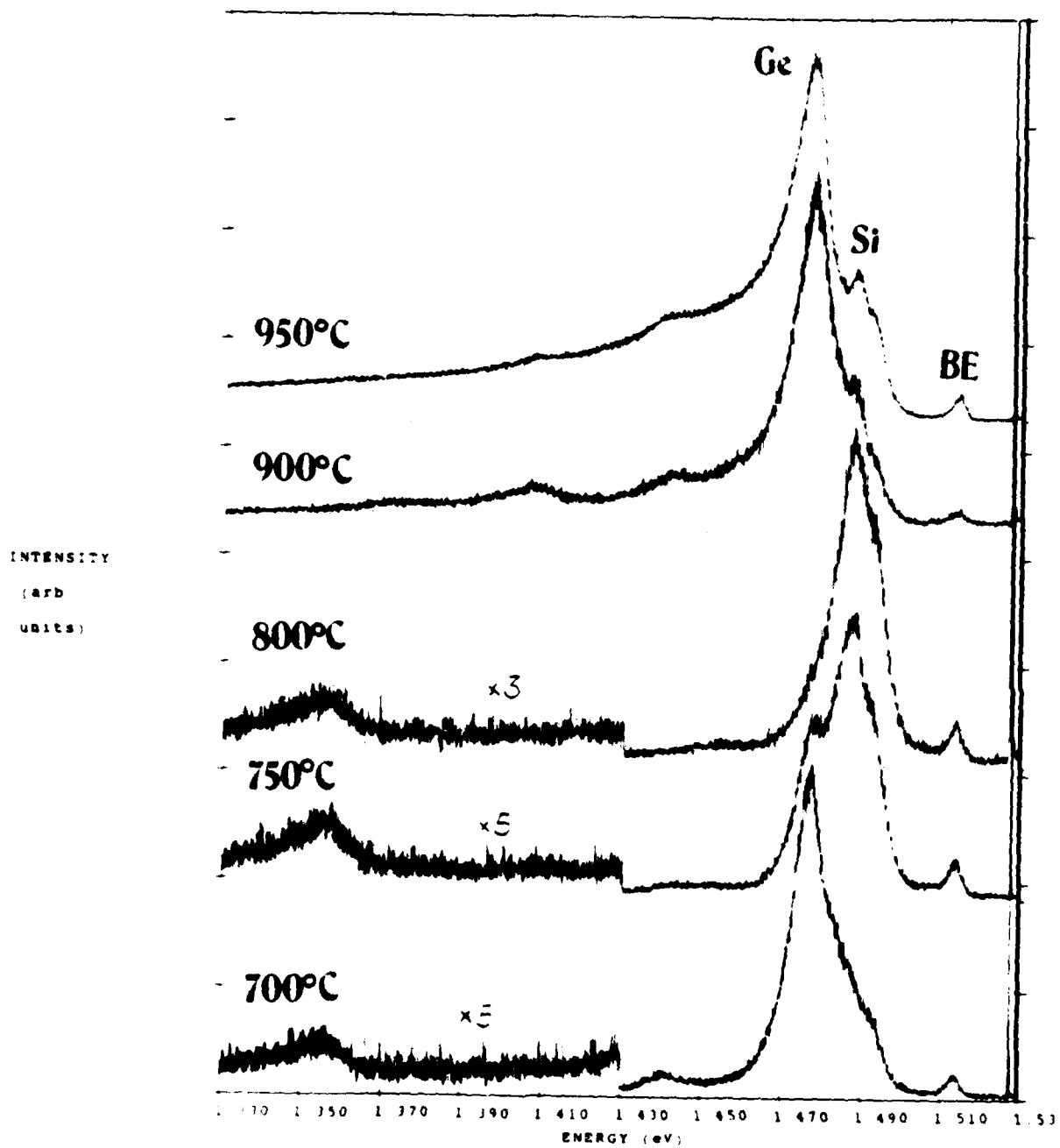52

INTENSITY
(arb.
units)

Fig. 18 PL anneal temperature dependence comparative spectra of GaAs:Ge at about 5°K using 6471 Å line. Source intensity: 0.27 W/cm². Dose = 1x10¹³ions/cm².
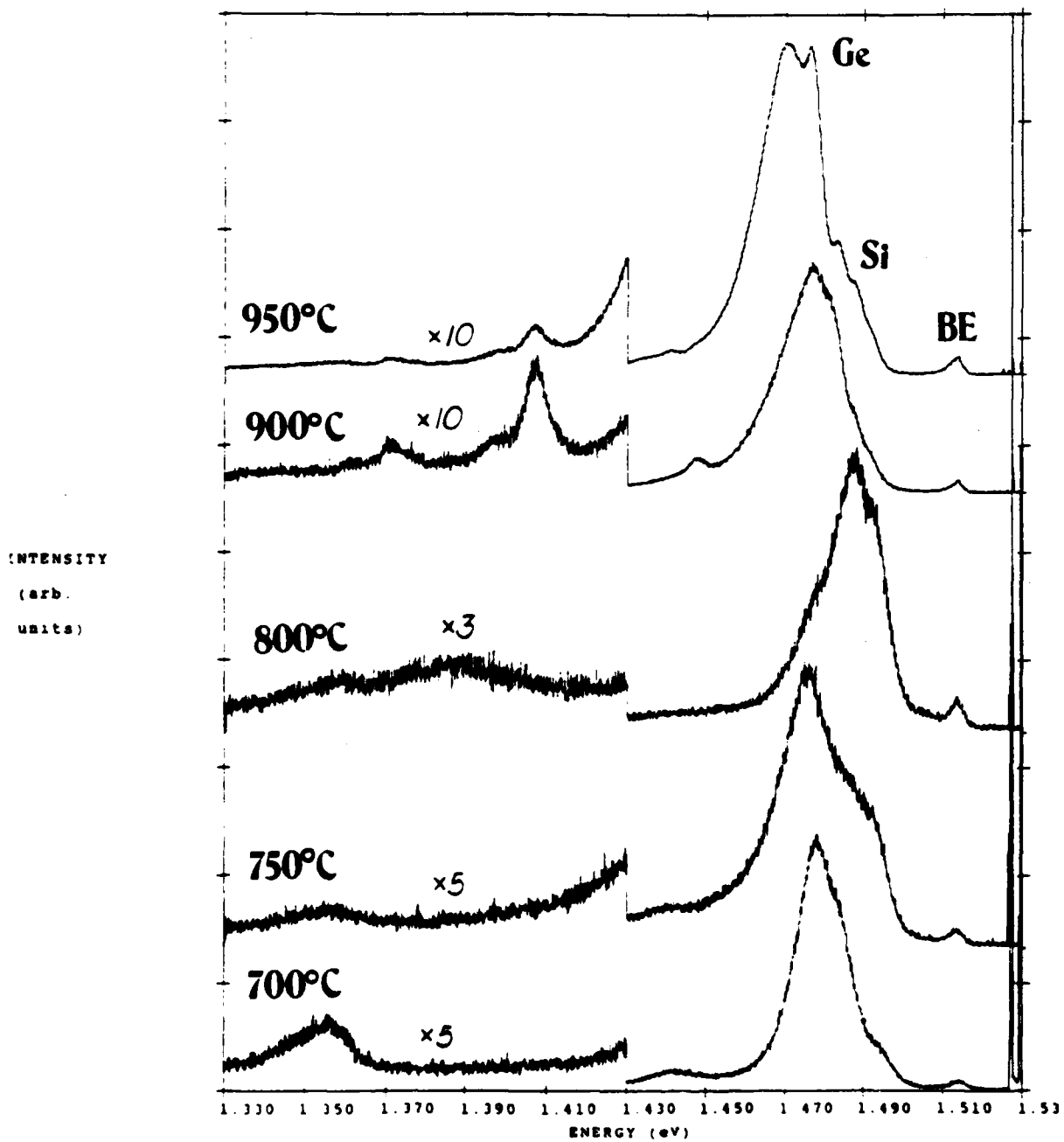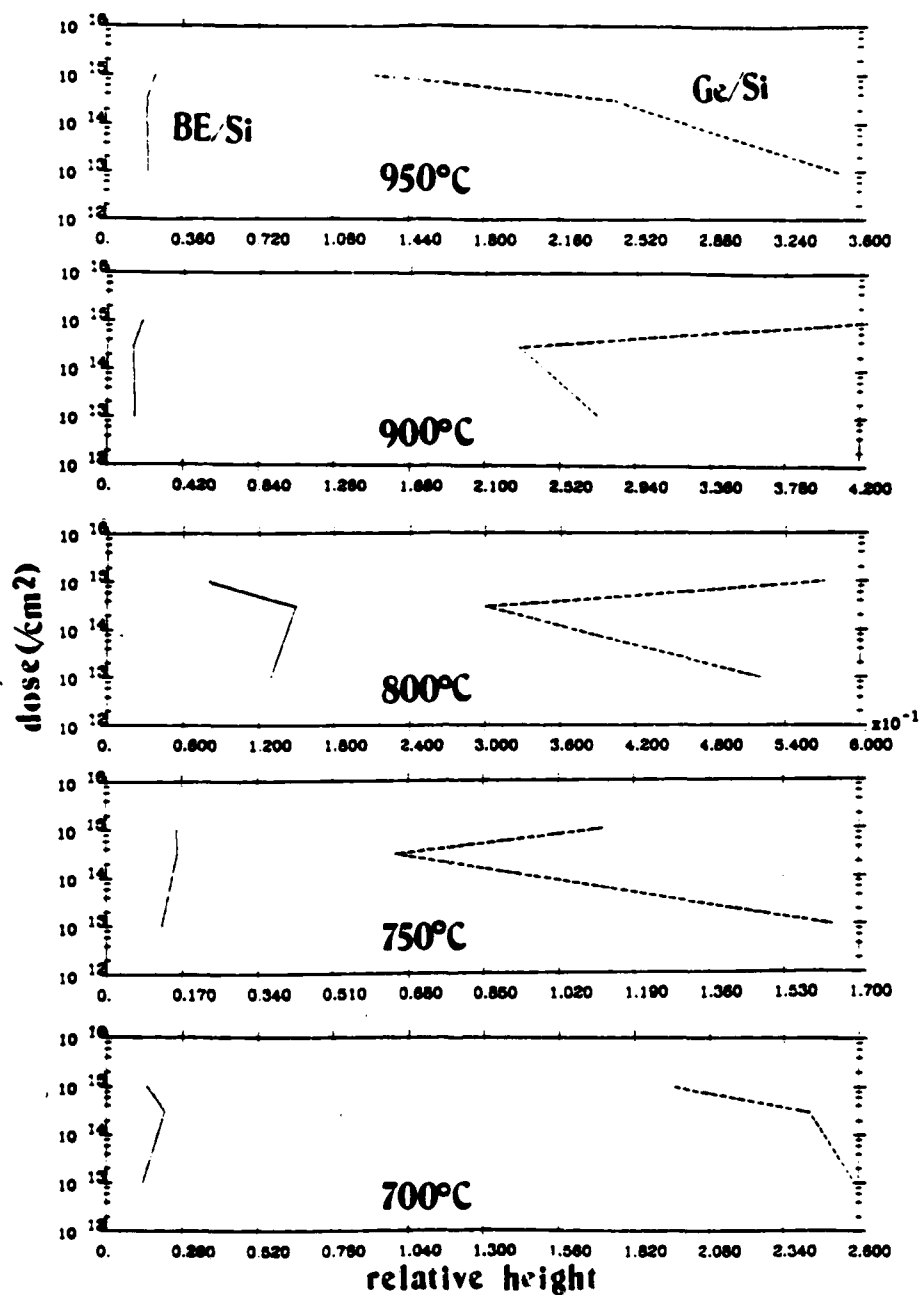
53

Fig. 19 Relative intensity ratios for different anneal temperatures from PL spectra of GaAs:Ge. Dashed line represents Ge_{As}/Si_{As} relative peak height. Solid line represents exciton/Si_{As} relative peak height. The X-axis shows ratio value, Y-axis shows dose concentration (/cm²).
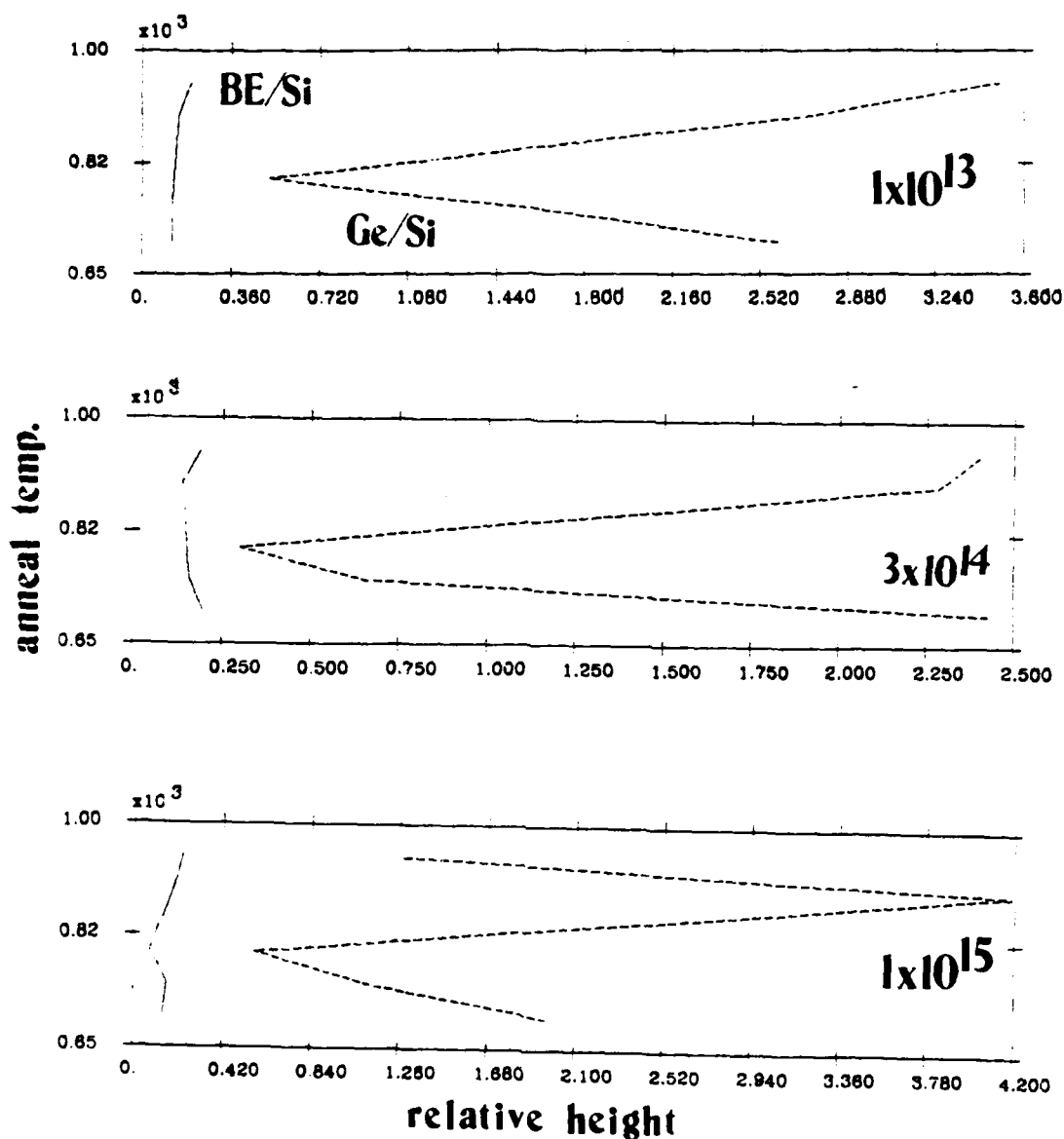
Fig. 20 Relative intensity ratios for three doses from PL
spectra of GaAs:Ge. Dashed line represents Ge$_{As}$/Si$_{As}$
relative peak height. Solid line represents exciton/Si$_{As}$
relative peak height. The X-axis shows the ratio value, the
Y-axis shows anneal temperature (in 100's ºC).

dependence is clearest as shown in Figs. 11 and 19. The
relative height of the Ge_{As} peak decreases while the relative
height of the exciton peak increases as the dose increases.
As mentioned previously, relative height refers to a
comparison ratio with the Si_{As} peak. The PL data seems to
indicate that an increasing number of Ge atoms are being
located on Ga sites with an increasing dose concentration at
this high anneal temperature. Electrically, a type conversion
occured between doses of $1x10^{13}$ and $3x10^{14}/cm^2$ according to
the electrical study mentioned in chapter III (5).

The dose dependence trend for lower anneal temperatures
isn't as clear. At anneal temperatures $\leq 800^oC$ the relative
height of the exciton peak is increasing up to a dose of
$3x10^{14}/cm^2$ and then decreases at $1x10^{15}/cm^2$. At 900^oC the
relative height of the exciton peak seems to increase, but the
conclusion is not obvious because the Si_{As} peak is obscured by
a large Ge_{As} peak. At 800^oC the Ge_{As} peak is obscured by a
large Si_{As} peak. The relative height of the Ge_{As} peak at
anneal temperatures at or between 750 and 900^oC show a
decrease in size at a dose of $3x10^{14}/cm^2$ and then an increase
in size at $1x10^{15}/cm^2$.

In Fig. 20 we can see a complicated behavior in the
anneal temperature dependence of the both the Ge_{As} peak and
the exciton peak. At all dose concentrations, the relative
height of the Ge_{As} peak decreases between 700 and 800^oC, and
then increases again. This increase continues up to 950^oC for
a dose concentration of $1x10^{13}$ and $3x10^{14}/cm^2$, whereas for a

dose of $1 \times 10^{15}/cm^2$, the increase continues to 900°C and then makes a sharp decline at 950°C. The relative height of the exciton peak shows an increase between 900 and 950°C for all doses. An overall increase in the relative height of the exciton peak with increasing anneal temperature is observed for both 1×10^{13} and $1 \times 10^{15}/cm^2$. This suggests a trend of increasing donor activity with increasing anneal temperature.

In the electrical data, the Ge implanted samples showed n-type behavior at all anneal temperatures for a dose of $1 \times 10^{15}/cm^2$, and also at an anneal temperature of 950°C and a dose of $3 \times 10^{14}/cm^2$. The activation efficiencies for these samples were low, apparently due to an electrical compensating effect that occurred between Ge donors and Ge acceptors. The PL trends that correlate best with electrical data are those at high anneal temperatures where p-type activation was the highest for low doses, and n-type activation was highest at the high doses.

It is also noted that for the samples annealed at higher temperatures of 900 and 950°C, and having higher doses of 3×10^{14} and $1 \times 10^{15}/cm^2$, a high luminescent background is detected at energies below the Ge_{As} peak. Also, the Ga_{As} antisite defect is observed, and the 1.406-1.408 eV DAP peak becomes apparant.

At lower anneal temperatures, the Ga vacancy related transition at 1.356-1.359 eV is observed and disappears at higher temperatures.

57

D. <u>Ge+As Implanted GaAs</u>

GaAs substrate was dually implanted with equal doses of Ge and As, Ge being implanted first. Samples were implanted with one of three dose concentrations: 1×10^{13}, 3×10^{14} and $1 \times 10^{15}/cm^2$. Anneal temperatures involved were 700 to 950°C in increments of 50. Figs. 21-29 show comparative PL spectra for the Ge+As samples. The figures show dose dependence or anneal temperature dependence with each figure representing either one dose concentration or one anneal temperature.

The peaks observed in the figures are similar to those observed in Ge singly implanted in GaAs and are listed in section C.

In the electrical data (6), dually implanting Ge and As into the GaAs significantly enhanced the n-type electrical activity for a dose of $1 \times 10^{15}/cm^2$, produced a type conversion at a lower dose ($1 \times 10^{14}/cm^2$), and had little effect on the p-type activity of the lower dose ($1 \times 10^{13}/cm^2$). This n-type enhancement seems to have brought out a clearer trend in the PL measurements too.

Fig. 30 shows the dose dependence of the relative heights of the Ge_{As} peak with the Si acceptor peak and also the relative heights of the exciton peak with the Si acceptor peak. There is a general trend of a relative decrease in the Ge_{As} peak with increasing dose for all the anneal temperatures with sharp decreases occuring between 3×10^{14} and 1×10^{15} for most anneal temperatures. The relative height of the exciton

58

Fig. 21 PL dose dependence comparative spectra of
GaAs:Ge+As at about 5°K using 6471 Å line. Source
intensity: 0.27 W/cm². Anneal temperature T_A=950°C for
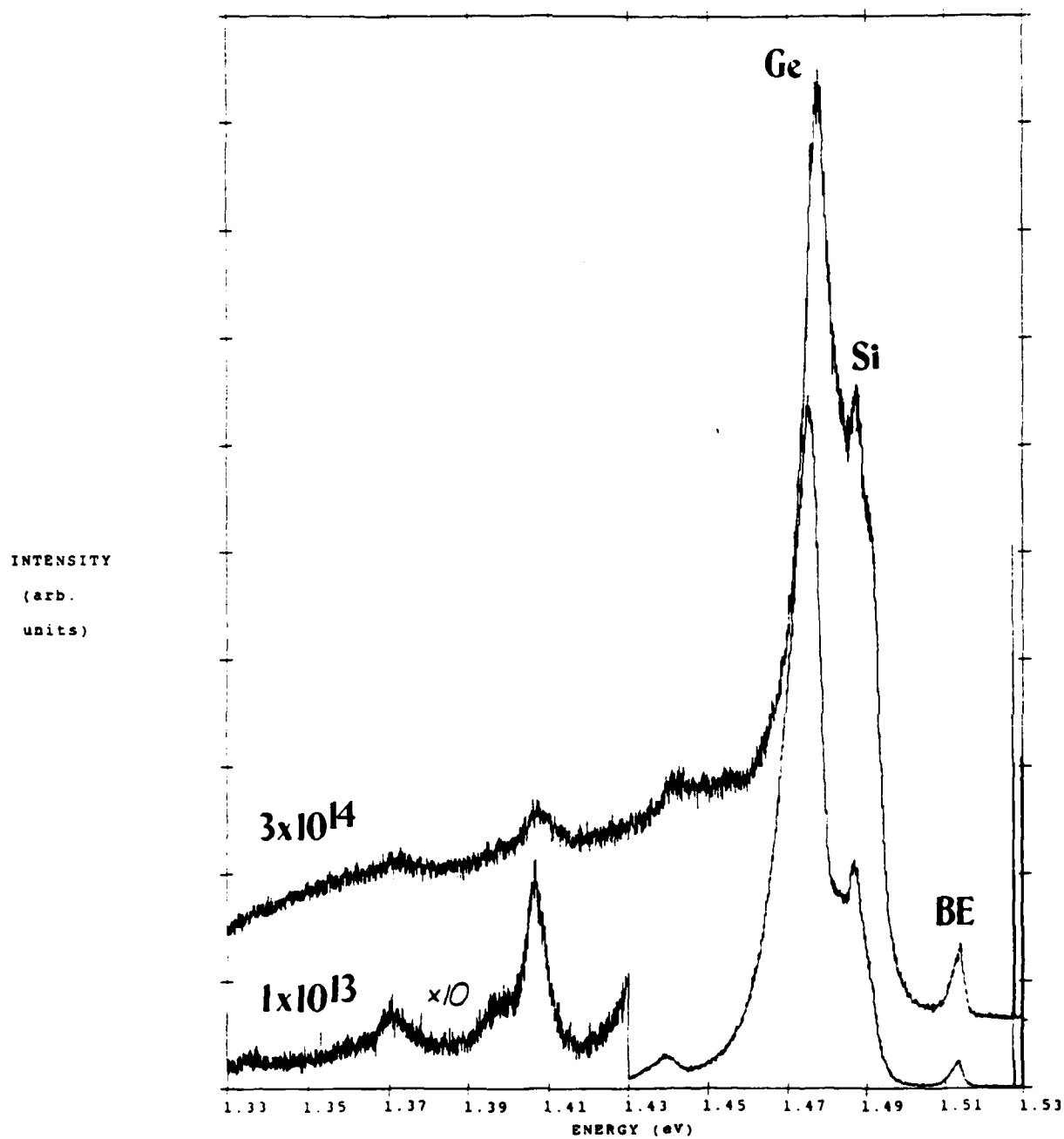15 min.

Fig. 22 PL dose dependence comparative spectra of
GaAs:Ge+As at about 5ºK using 6471 Å line. Source
intensity: 0.27 W/cm². Anneal temperature T_A=900ºC for
15 min.
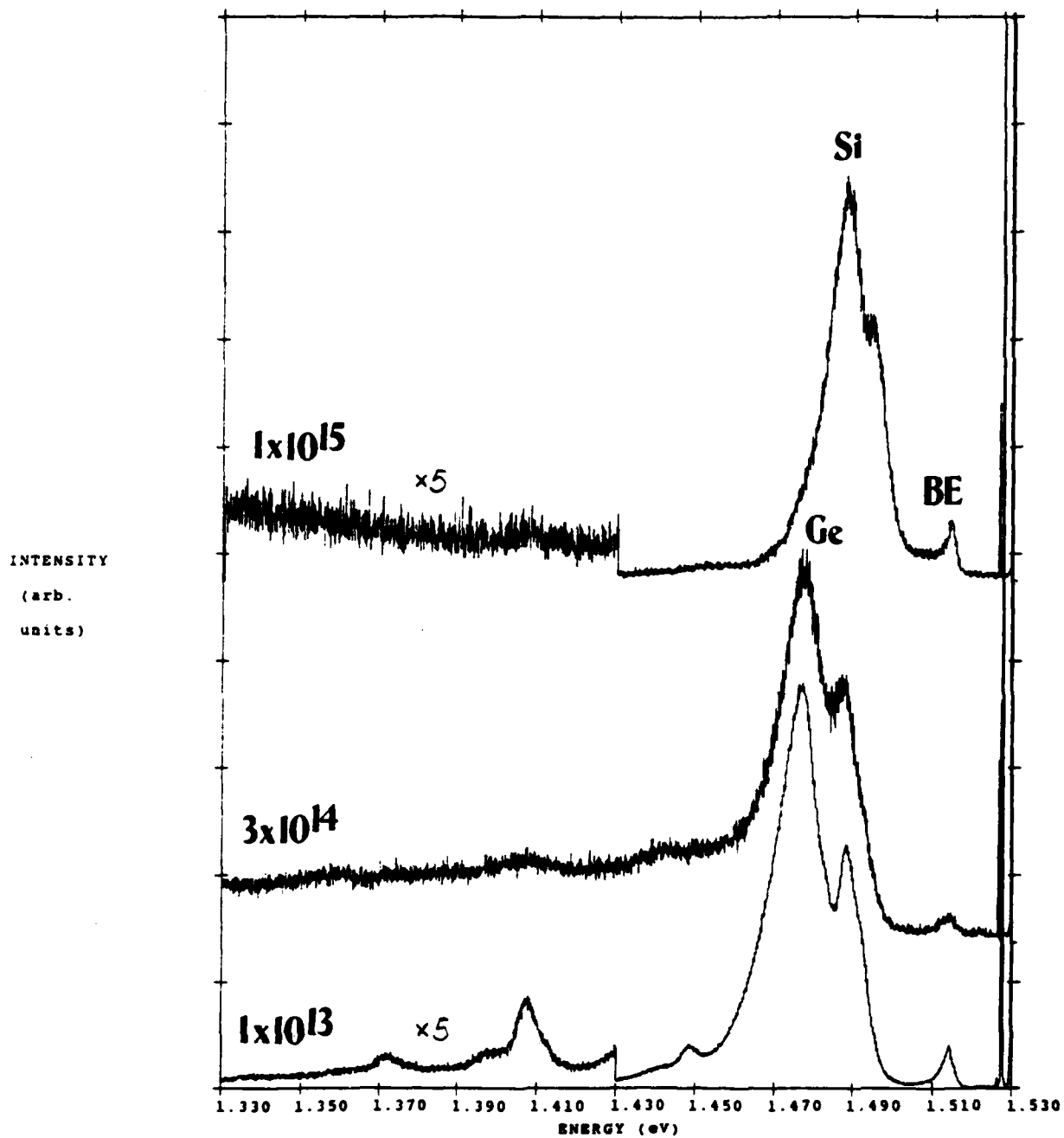
Fig. 23 PL dose dependence comparative spectra of
GaAs:Ge+As at about 5°K using 6471 Å line. Source
intensity: 0.27 W/cm². Anneal temperature $T_A=850°C$ for
15 min.

61

Fig. 24 PL dose dependence comparative spectra of
GaAs:Ge+As at about 5°K using 6471 Å line. Source
intensity: 0.27 W/cm². Anneal temperature T_A=800°C for
15 min.

62

INTENSITY
(arb
units)

Si

Ge   BE

1×10^{15}

$\times 5$

3×10^{14}

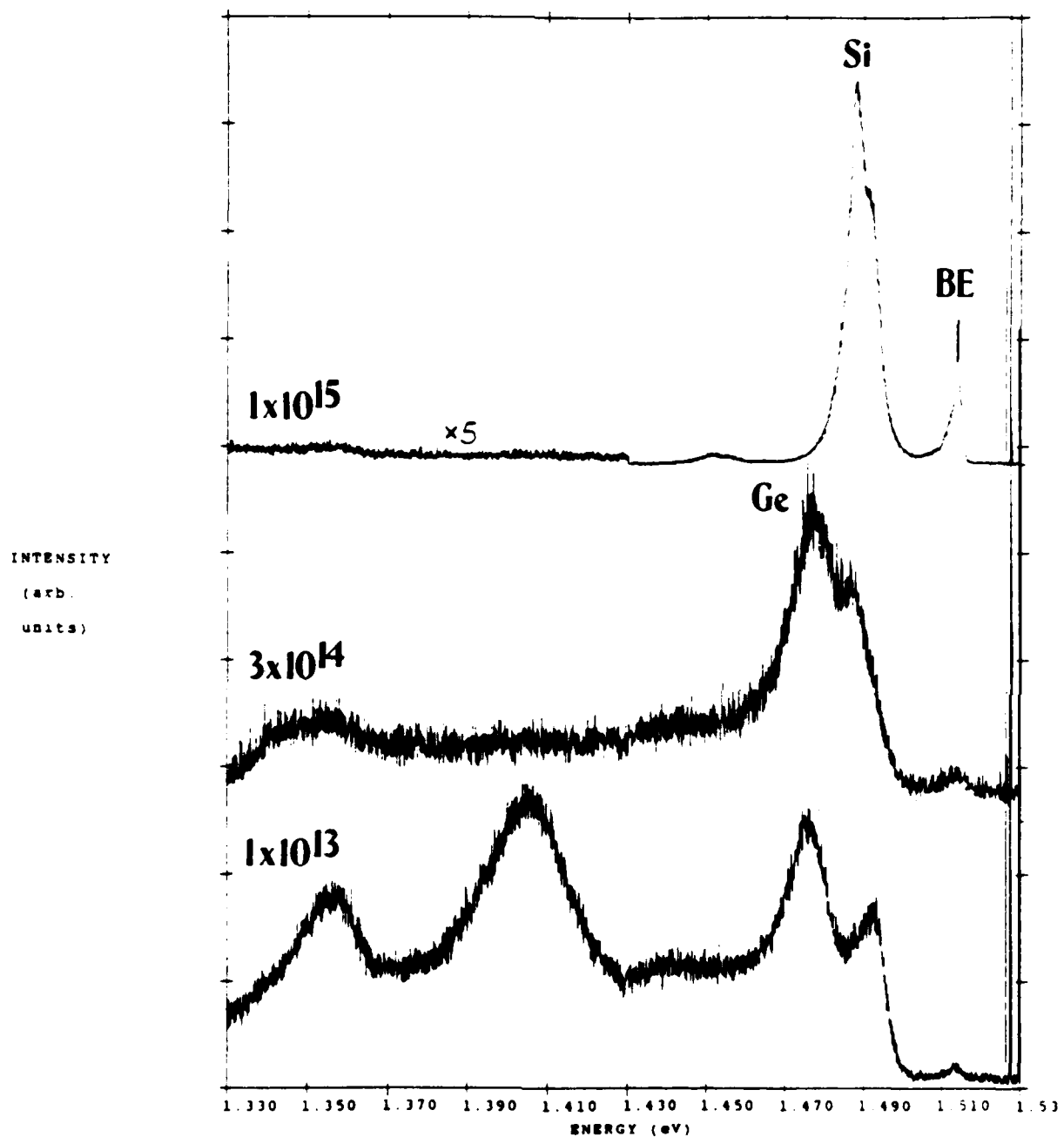1.33 1.35 1.37 1.39 1.41 1.43 1.45 1.47 1.49 1.51 1.53

ENERGY (eV)

Fig. 25 PL dose dependence comparative spectra of GaAs:Ge+As at about 5°K using 6471 Å line. Source intensity: 0.27 W/cm². Anneal temperature $T_A = 750°C$ for 15 min.

63
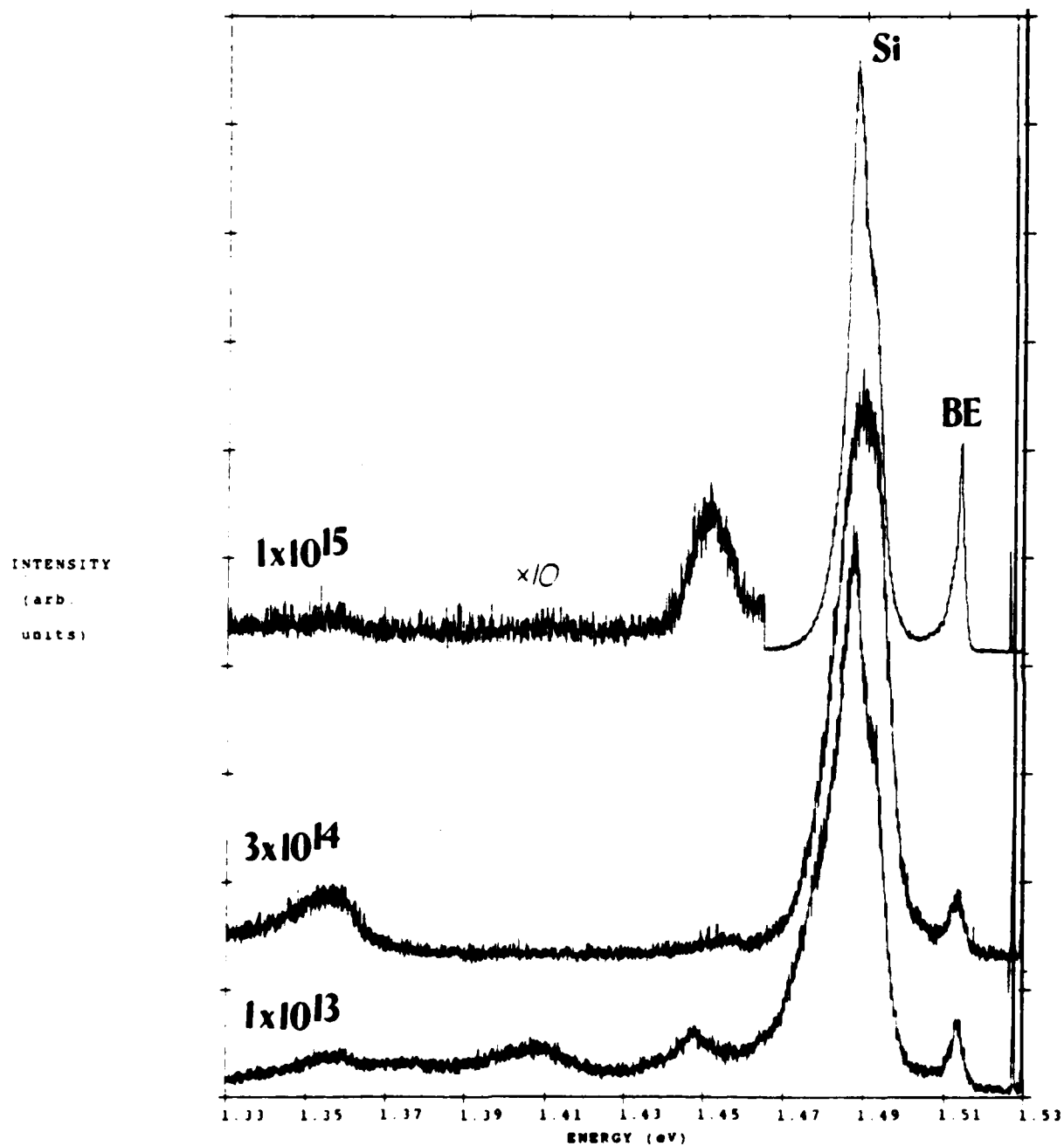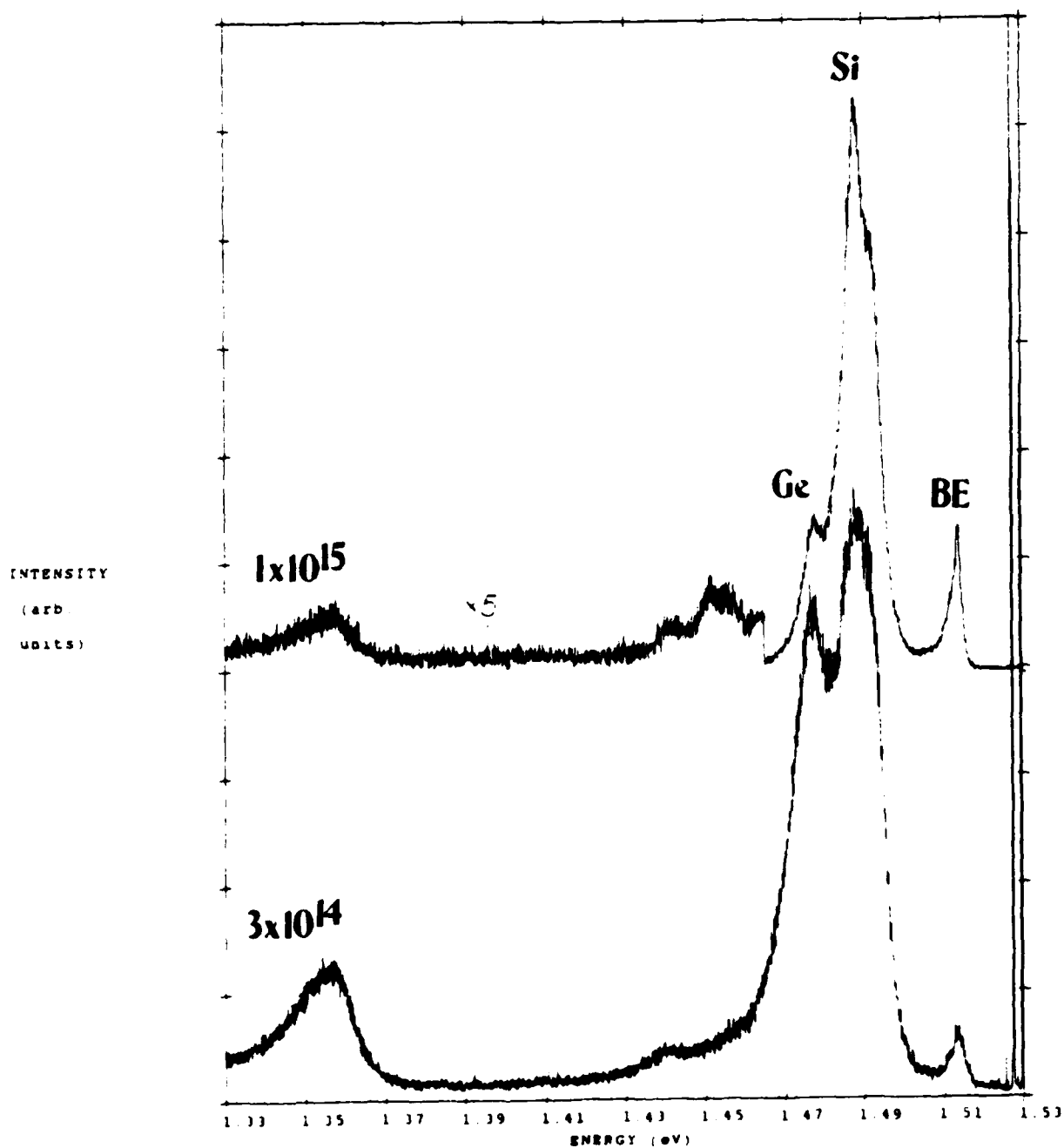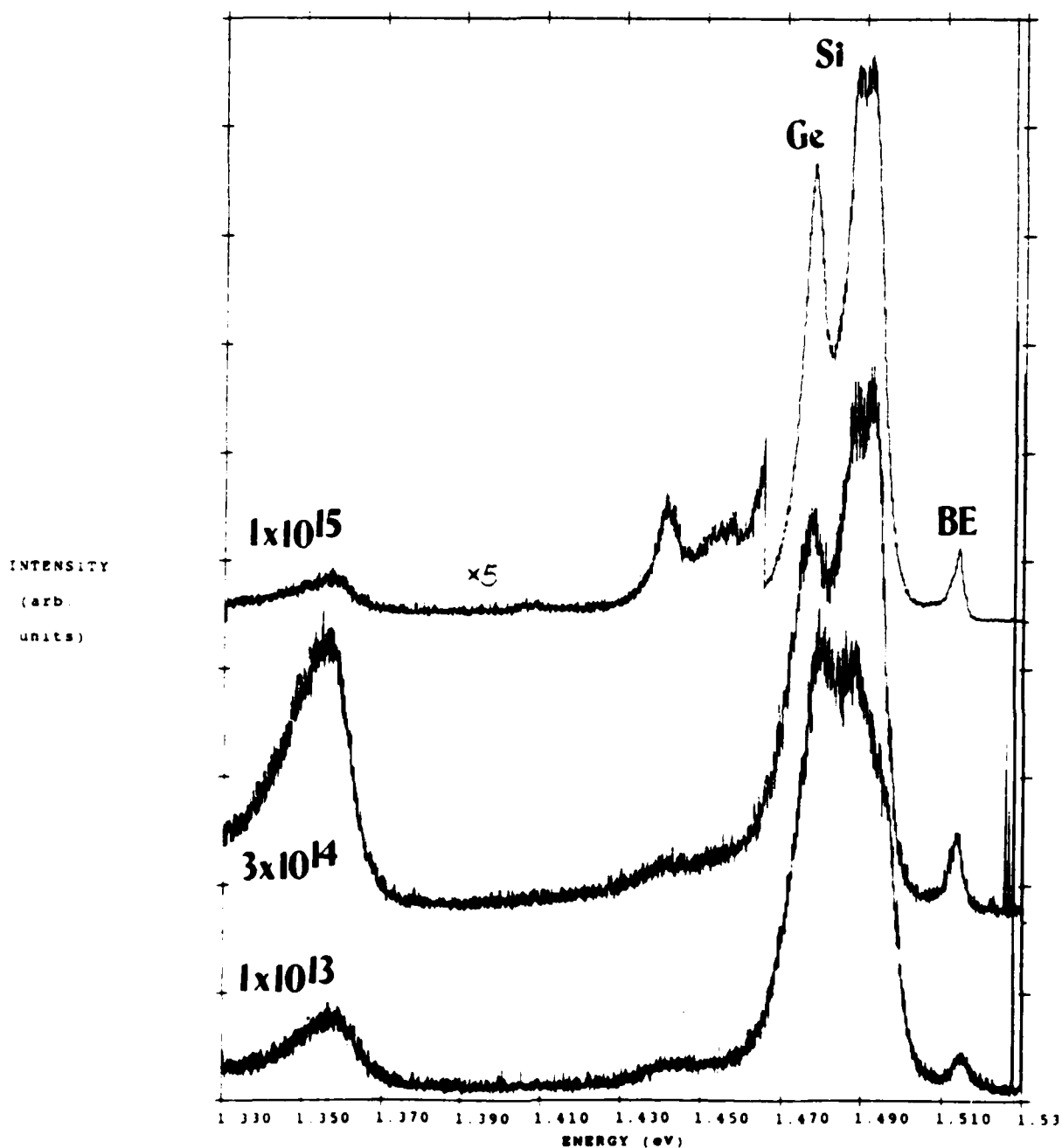
Fig. 26   PL dose dependence comparative spectra of
GaAs:Ge+As at about 5°K using 6471 Å line.   Source
intensity: 0.27 W/cm^2.   Anneal temperature T_A=700°C for
15 min.

Fig. 27 PL anneal temperature dependence comparative
spectra of GaAs:Ge+As at about 5°K using 6471 Å line.
Source intensity: 0.27 W/cm². Dose = 1×10^{13} ions/cm².

65

Ge

Si

950°C

900°C

BE

850°C

INTENSITY

(arb.

units)

800°C

750°C

700°C

1.330   1.350   1.370   1.390   1.410   1.430   1.450   1.470   1.490   1.51   1.53

ENERGY (eV)

Fig. 28 PL anneal temperature dependence comparative
spectra of GaAs:Ge+As at about 5°K using 6471 A line.
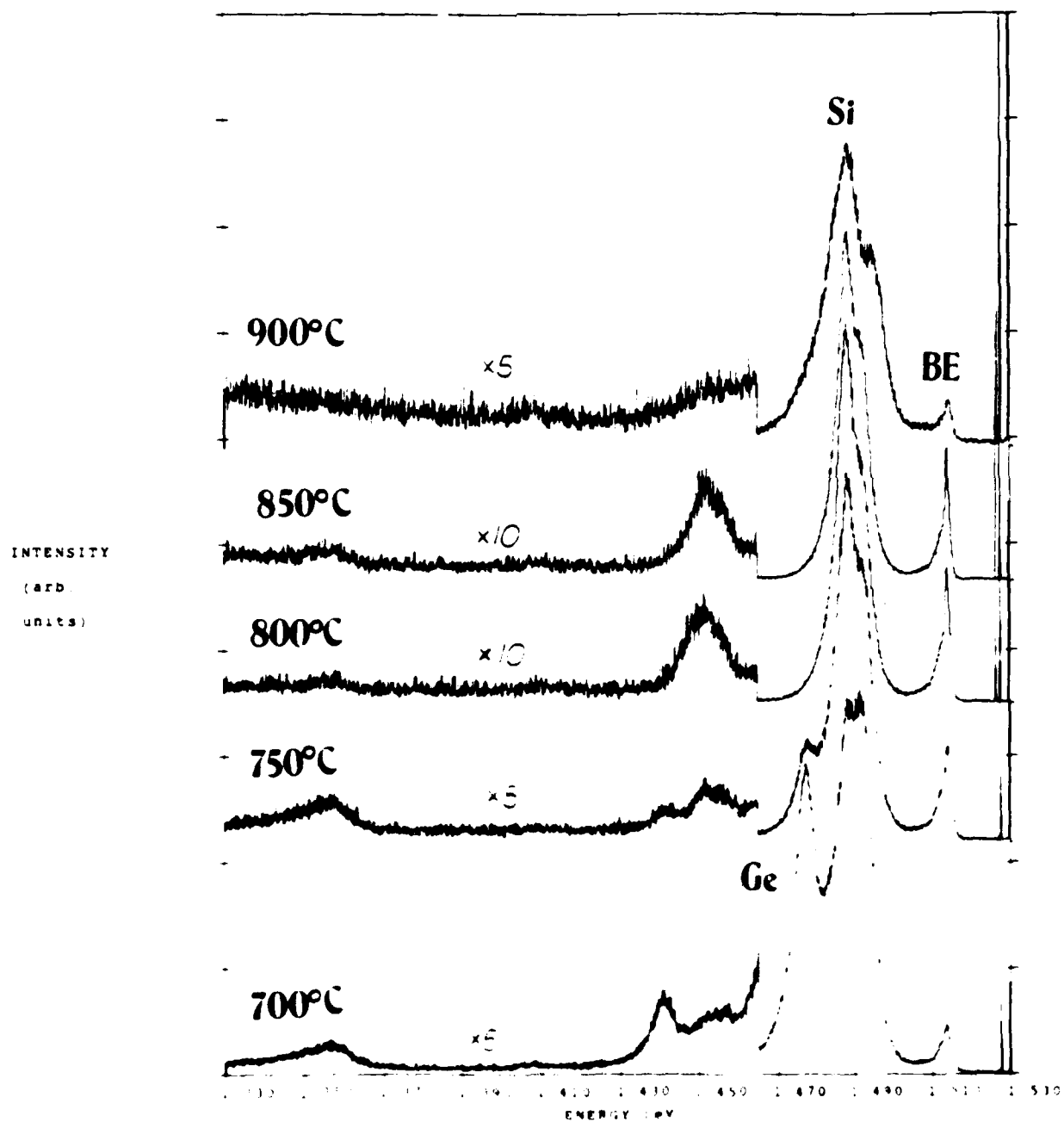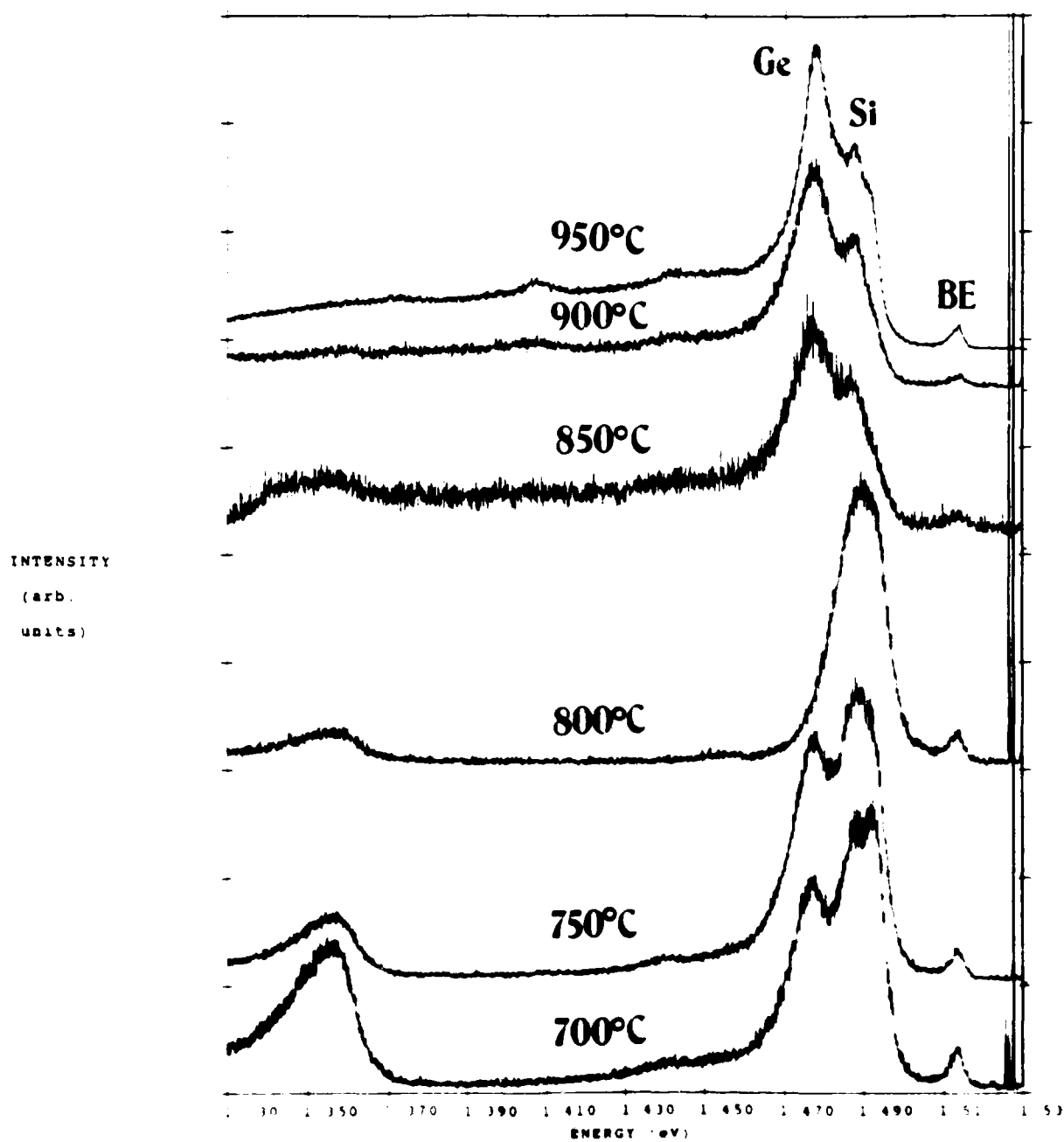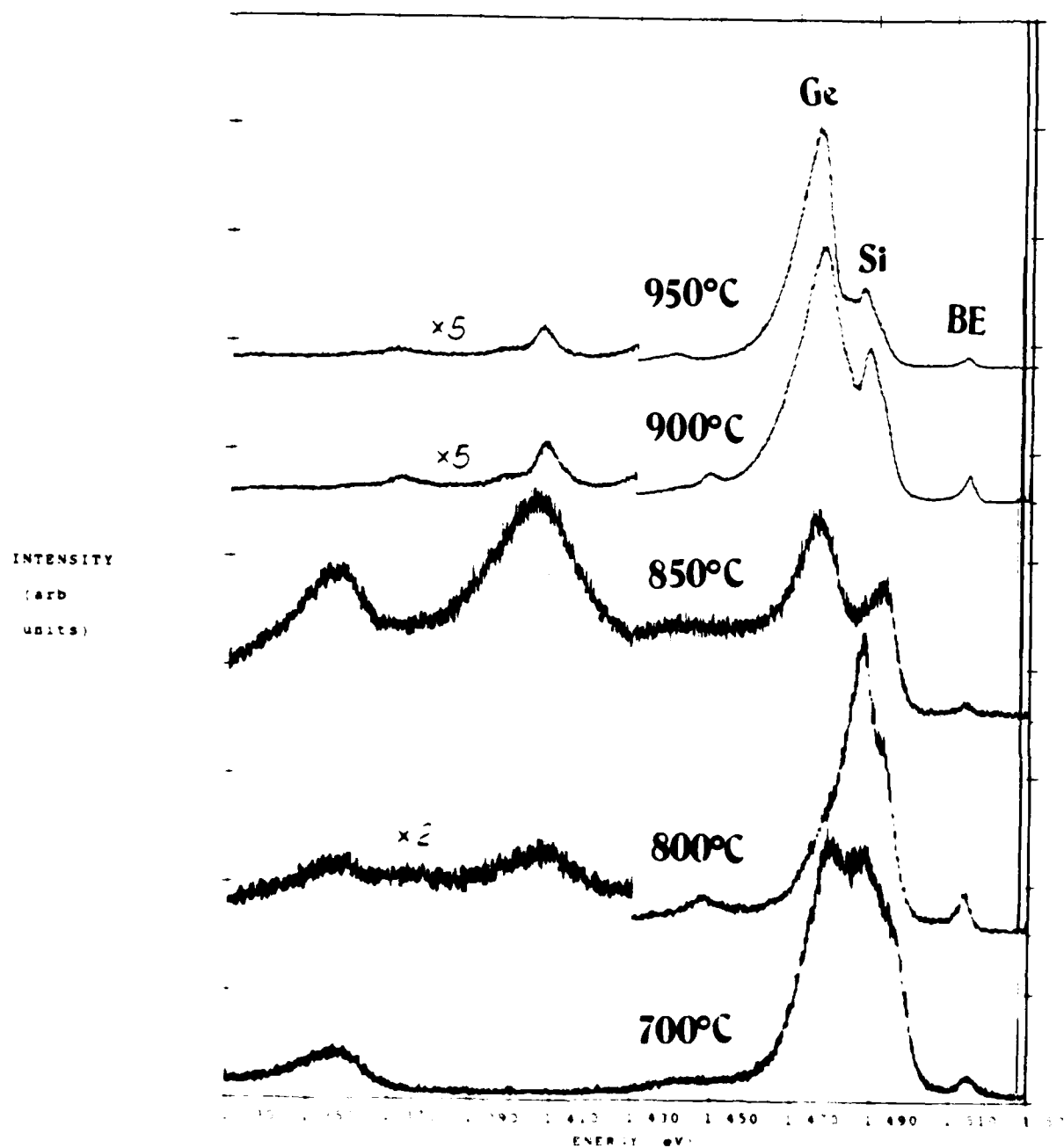Source Intensity: 0.27 W/cm².   Dose = 3×10^{14} ions/cm².

66

Fig. 29 PL anneal temperature dependence comparative
spectra of GaAs:Ge+As at about 5°K using 6471 Å line.
Source Intensity: 0.27 W/cm². Dose = 1x10¹³Ions/cm².

Ge/Si

BE/Si   950°C

10 .0 10 10

| 0.310 | 0.620 | 0.930 | 1.240 | 1.550 | 1.860 | 2.170 | 2.480 | 2.790 | 3.100 |

900°C

| 0.170 | 0.340 | 0.510 | 0.680 | 0.850 | 1.020 | 1.190 | 1.360 | 1.530 | 1.700 |

850°C

| 0.170 | 0.340 | 0.510 | 0.680 | 0.850 | 1.020 | 1.190 | 1.360 | 1.530 | 1.700 |

800°C

x10^{-1}

| 0.500 | 1.000 | 1.500 | 2.000 | 2.500 | 3.000 | 3.500 | 4.000 | 4.500 | 5.000 |

750°C

| 0.100 | 0.200 | 0.300 | 0.400 | 0.500 | 0.600 | 0.700 | 0.800 | 0.900 | 1.000 |

700°C

| 0.110 | 0.220 | 0.330 | 0.440 | 0.550 | 0.660 | 0.770 | 0.880 | 0.990 | 1.00 |

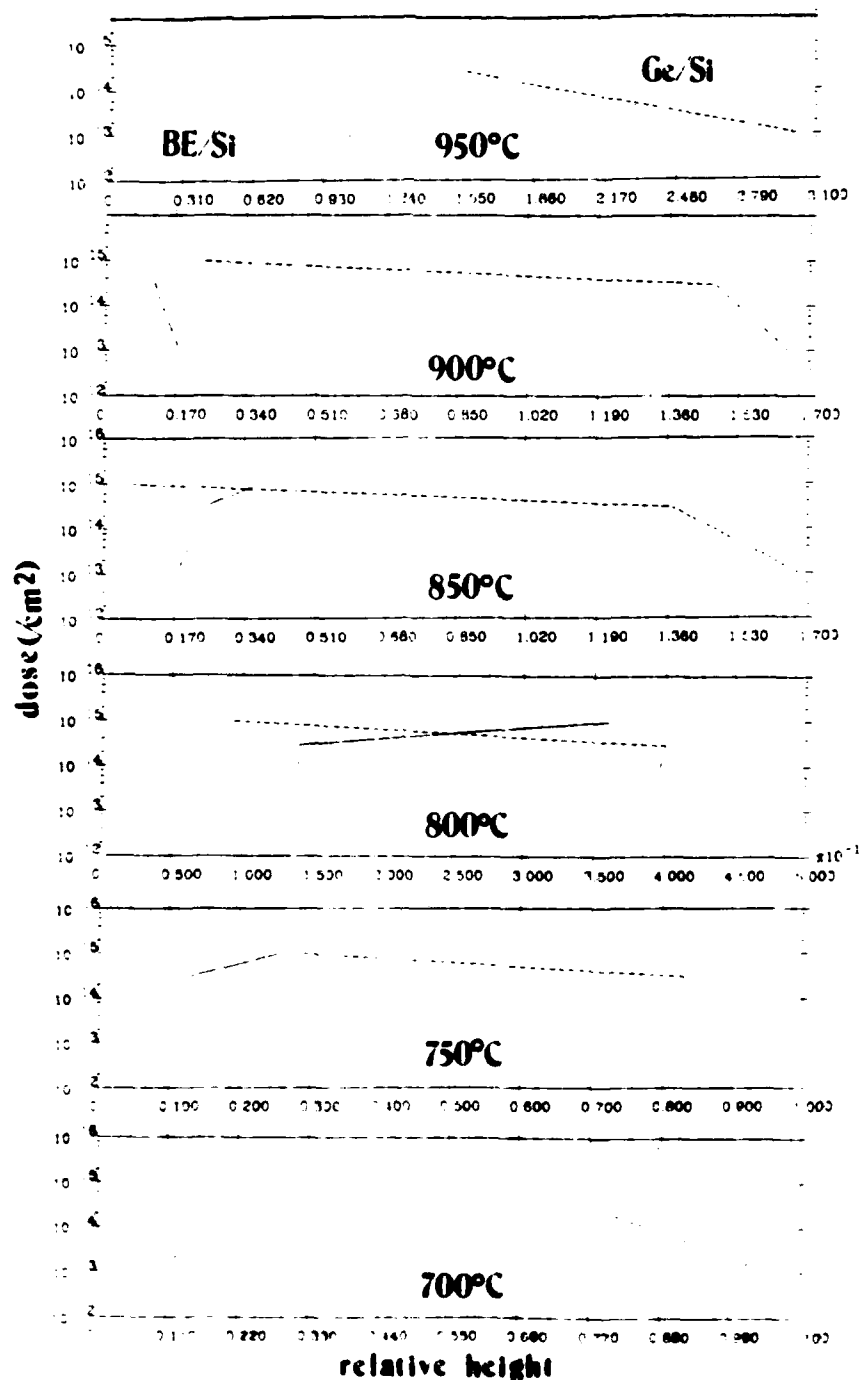dose($/cm^2$)

relative height

Fig. 30 Relative intensity ratios for different anneal
temperatures from PL spectra of GaAs:Ge+As. Dashed line
represents Ge$_{As}$/Si$_{As}$ relative peak height. Solid line
represents exciton/Si$_{As}$ relative peak height. The X-axis
shows ratio value, Y-axis shows dose concentration ($/cm^2$).

68

peak increases between doses of 3×10^{14} and $1 \times 10^{15}/cm^2$ for anneal temperatures 750-900°C. In the electrical data, the sharpest increase in sheet carrier concentration and activation efficiency occured between 3×10^{14} and $1 \times 10^{15}/cm^2$ for anneal temperatures $\geq$ 850°C. The dose dependence suggests a trend of a decreasing percentage of Ge atoms locating on As sites with increasing dose, whereas an increasing number of Ge atoms locating on Ga sites which becomes apparant at the higher doses.

The anneal temperature dependence (Figs. 27-29) shows a similar behavior to that of Ge singly implanted in GaAs, in that the Ge_{As} peak becomes obscured in a large Si_{As} peak at an anneal temperature of 800°C. This gives the trend of relative Ge_{As} intensity a characteristic "V" shape as graphed in Fig. 31. This relative Ge_{As} peak height tends to decrease up to 800°C and then increase again at higher anneal temperatures. At a dose of $1 \times 10^{15}/cm^2$, the Ge_{As} peak decreases up until it has mostly disappeared at an anneal temperature of 850°C, and then slightly beg s to reappear as part of a broad Si_{As} at 900°C. The exciton mirrors this behavior by increasing in relative height up to 850°C and then by decreasing at 900°C. This dose does seem to show an overall trend towards increasing n-type activity with increasing anneal temperature. On the other hand, the other two doses show an overall trend of increasing p-type activity with anneal temperature.
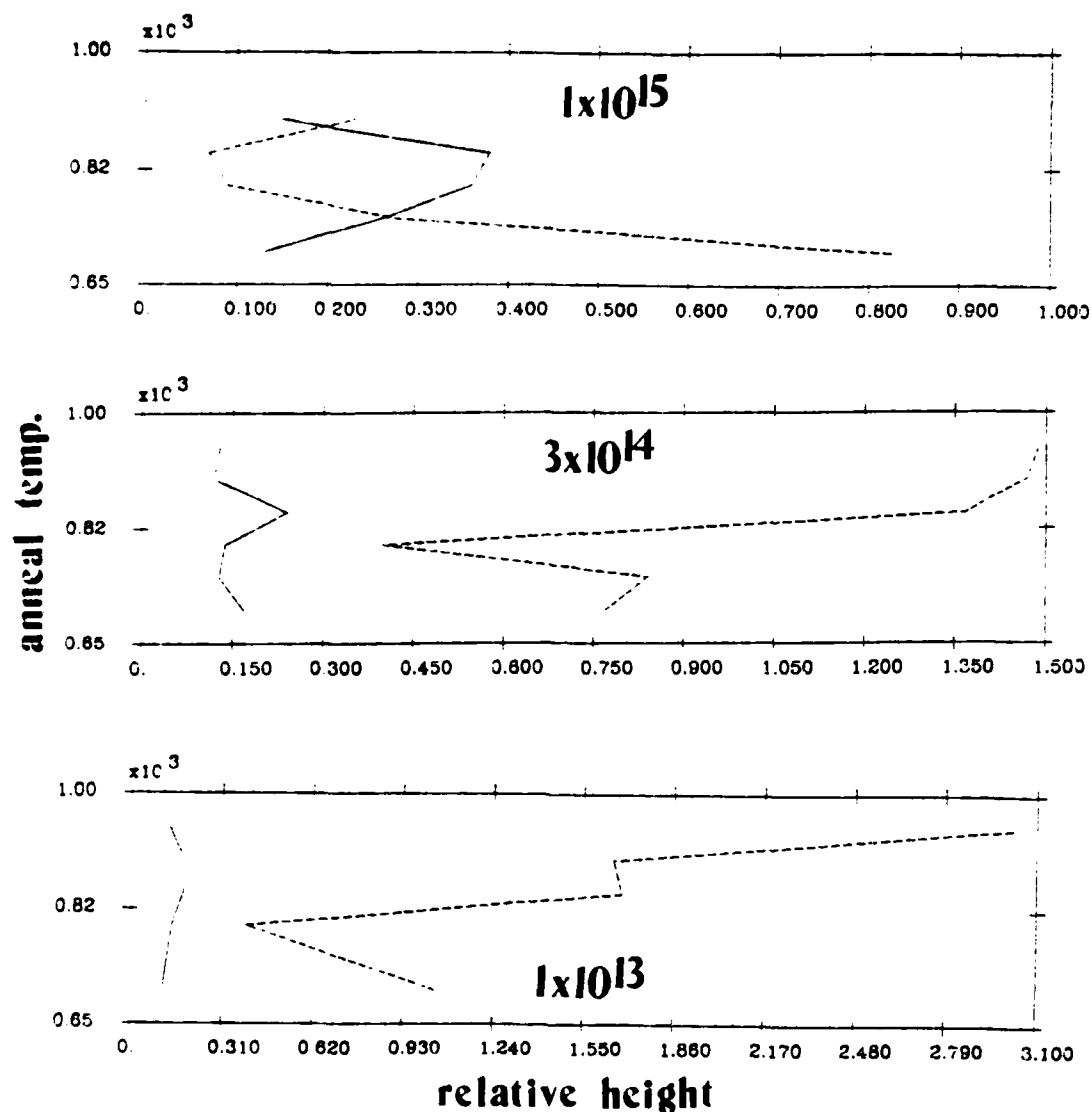
It is interesting to note that like Ge singly implanted

Fig. 31 Relative intensity ratios for three doses from PL spectra of GaAs:Ge+As. Dashed line represents Ge$_{As}$/Si$_{As}$ relative peak height. Solid line represents exciton/Si$_{As}$ relative peak height. The X-axis shows ratio value, Y-axis shows anneal temperature (in 100's °C).

GaAs, the V_{Ga} defect at 1.356-1.359 eV only appears in samples that were annealed at temperatures $\leq$ 850°C. The 1.406-1.408 eV DAP peak appears in samples with anneal temperatures $\geq$ 800°C for a dose of $1\times10^{13}/cm^2$, and at temperatures $\geq$ 900°C for a dose of $3\times10^{14}/cm^2$, and is not observable for a dose of $1\times10^{15}/cm^2$. For an anneal temperature of 850°C and a dose of $1\times10^{13}/cm^2$, the 1.406 eV peak is the most significant peak in the PL spectrum.

Ge+As implanted GaAs, like Ge implanted GaAs, sometimes shows a high relative background emission at energies below the Ge_{As} peak. This occured at 850-950°C for a dose of $3\times10^{14}/cm^2$, and 850°C for a dose of $1\times10^{13}/cm^2$.

E. Ge+Ga Implanted GaAs

For these samples, Ge and Ga were implanted sequentually into GaAs substrate. The dose concentrations were 1×10^{13}, 1×10^{14}, 3×10^{14}, and $1\times10^{15}/cm^2$. Only two anneal temperatures were studied, 900 and 950°C. The peaks observed were again similar to those seen in Ge singly implanted GaAs, with two exceptions: a) A resolved exciton peak at 1.512 eV shows up at an anneal temperature of 950°C and a dose of $1\times10^{13}/cm^2$. According to Heim and Hiesinger (15:464) this peak fits the assignment of an exciton bound to a neutral acceptor. b) A peak at approximately 1.239 eV was observed at a dose of $3\times10^{14}/cm^2$ and an anneal temperature of 950°C (it is not shown in the figure). This seems to be the same peak that has been observed at 1.283 eV by Shanabrook et. al., and they
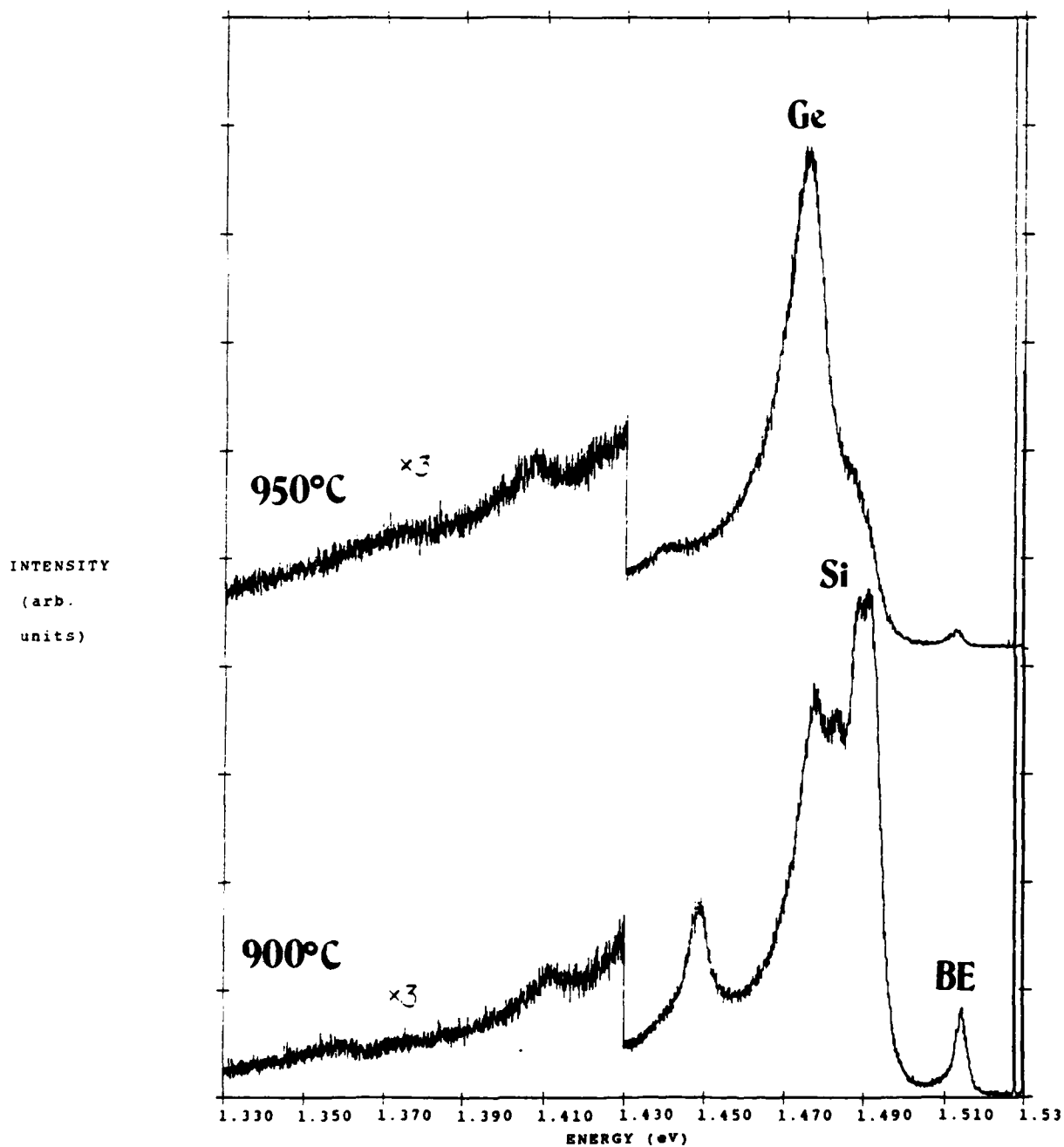
Fig. 32 PL anneal temperature dependence comparative spectra of GaAs:Ge+Ga at about 5°K using 6471 Å line. Source intensity: 0.27 W/cm². Dose = 1x10¹⁵ions/cm².

72

INTENSITY
(arb.
units)

Si

950°C

BE

900°C   ×5

1.330 1.350 1.370 1.390 1.410 1.430 1.450 1.470 1.490 1.510 1.53
ENERGY (eV)

Fig. 33 PL anneal temperature dependence comparative
spectra of GaAs:Ge+Ga at about 5ºK using 6471 Å line.
Source intensity: 0.27 W/cm². Dose = 3×10^{14} ions/cm².

73

Fig. 34   PL anneal temperature dependence comparative
spectra of GaAs:Ge+Ga at about 5°K using 6471 Å line.
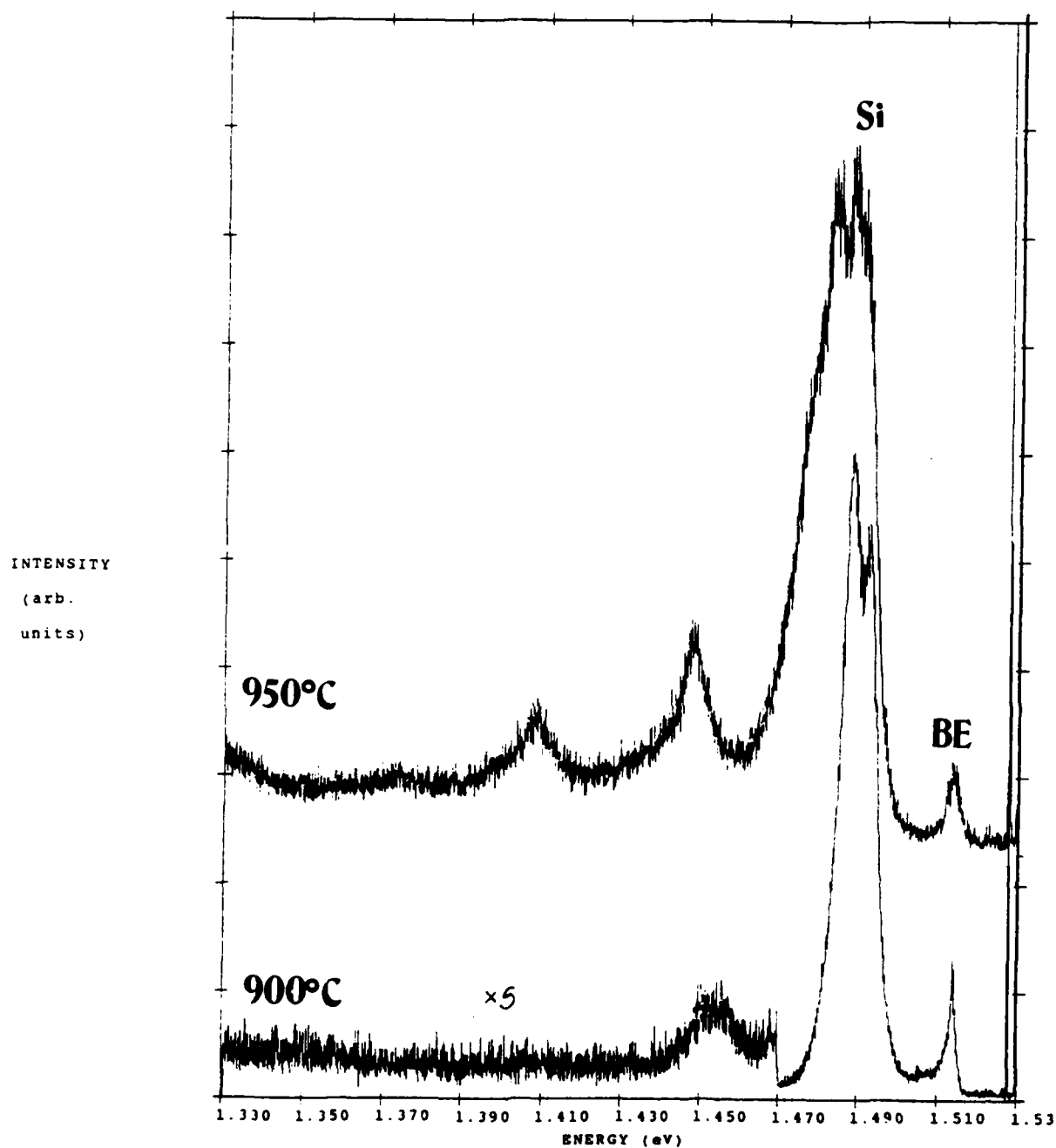Source intensity: 0.27 W/cm². Dose = 1x10¹³ions/cm².

74
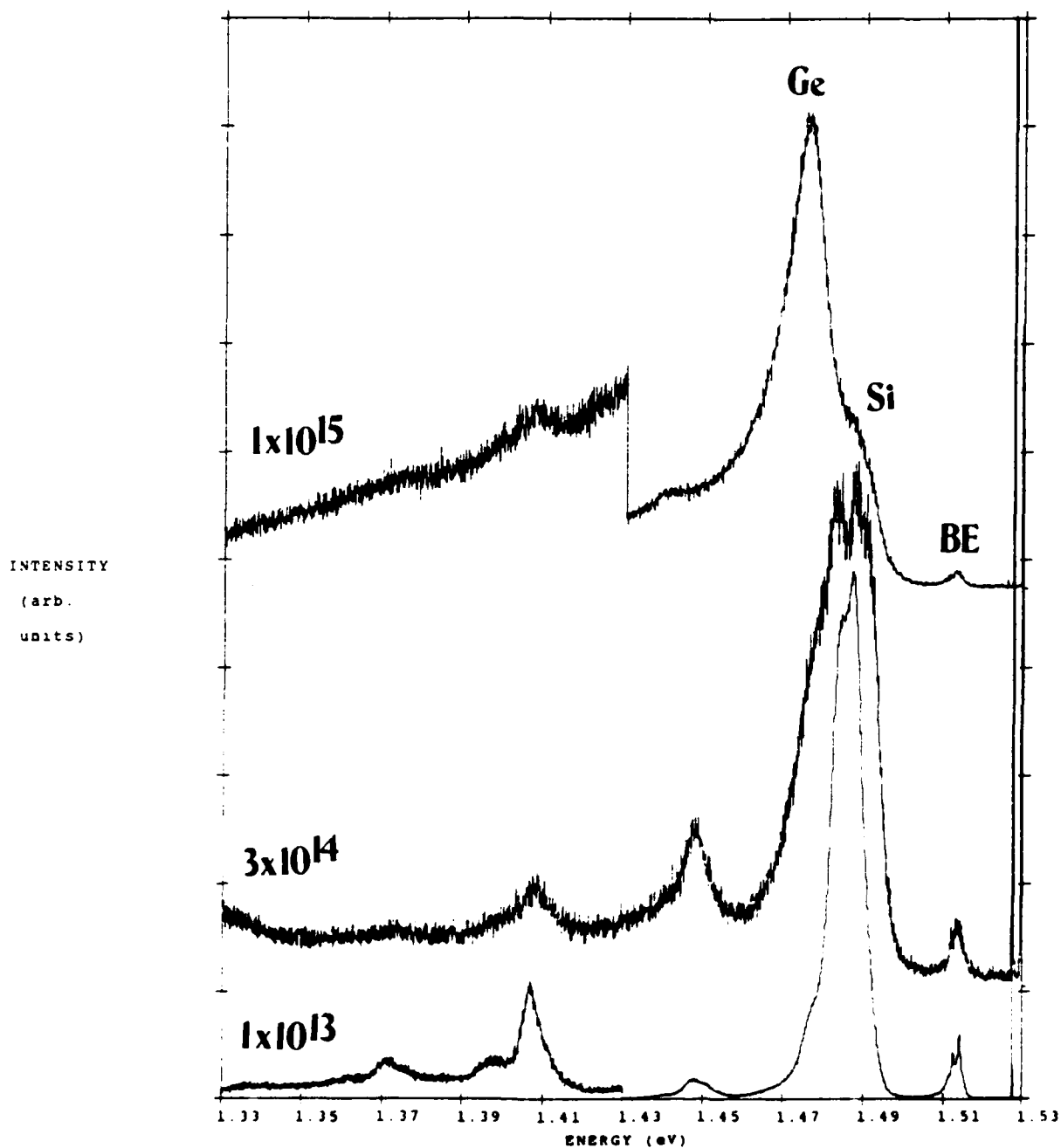
Fig. 35 PL dose dependence comparative spectra of
GaAs:Ge+Ga at about 5°K using 6471 Å line. Source
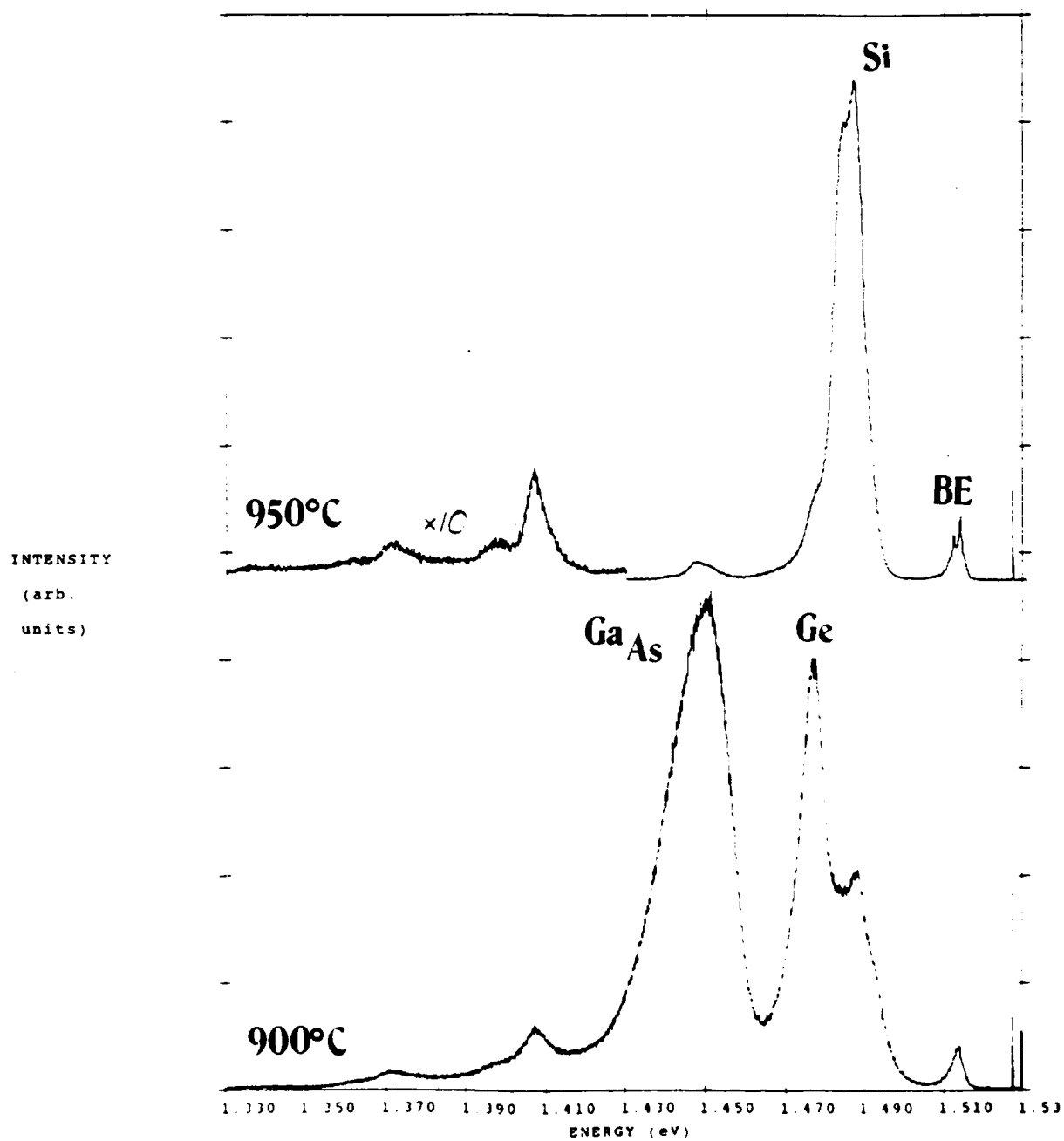intensity: 0.27 W/cm². Anneal temperature T_A=950°C for
15 min.

75
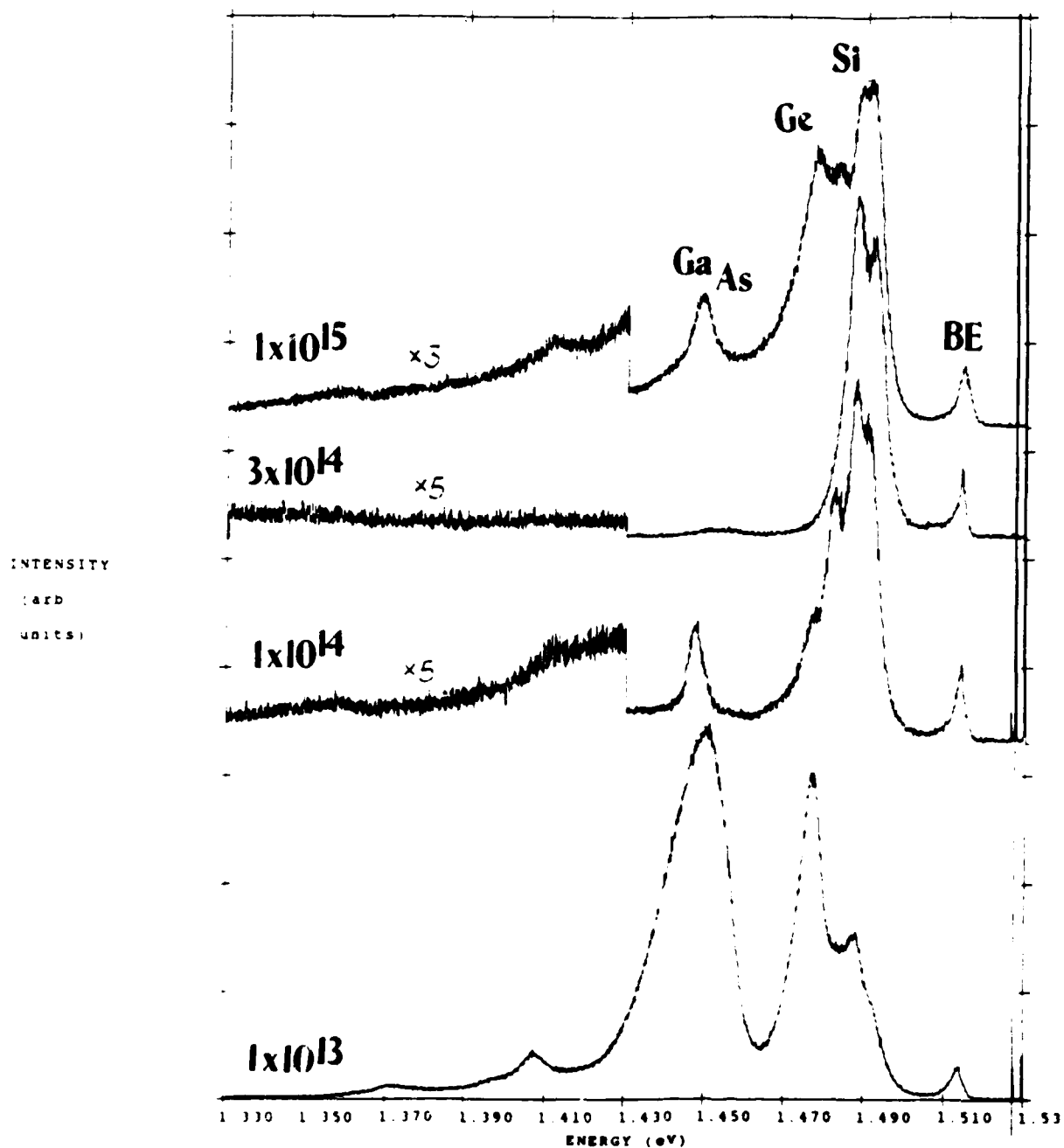
Fig. 36 PL dose dependence comparative spectra of
GaAs:Ge+Ga at about 5°K using 6471 A line. Source
intensity: 0.27 W/cm². Anneal temperature $T_A=900°C$ for
15 min.

76
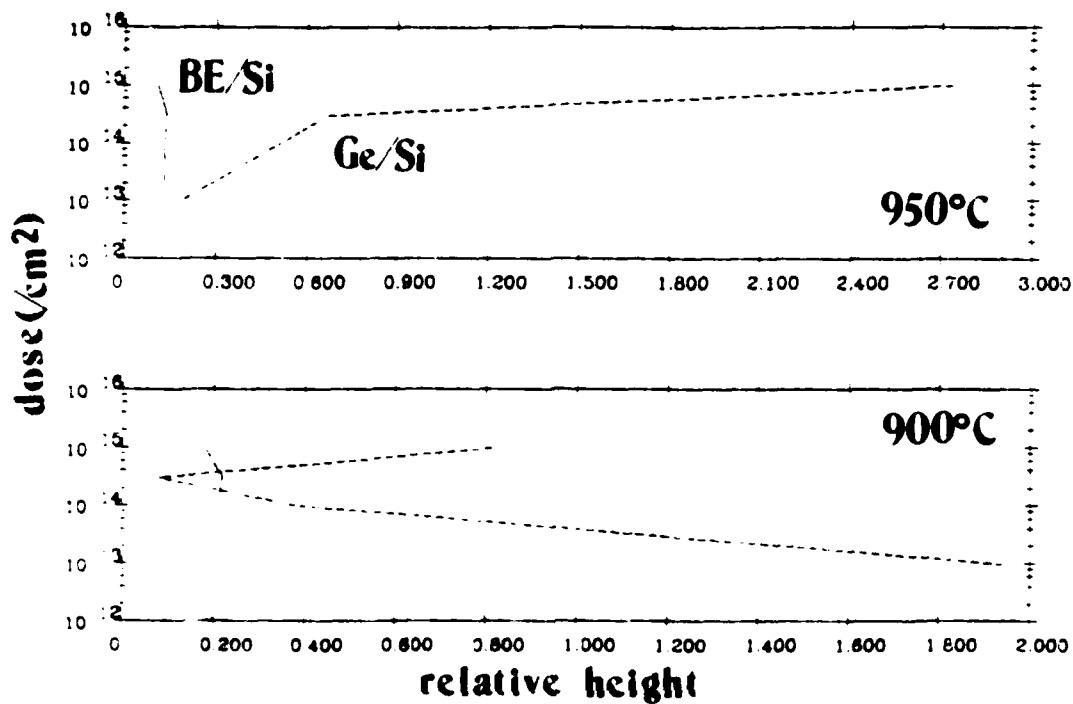
Fig. 37 Relative intensity ratios for different anneal
temperatures from PL spectra of GaAs:Ge+Ga. Dashed line
represents Ge$_{As}$/Si$_{As}$ relative peak height. Solid line
represents exciton/Si$_{AL}$ relative peak height. The X-axis
shows ratio value, the Y-axis shows dose concentration (/cm^2).

77

Fig. 38 Relative intensity ratios for three doses from PL
spectra of GaAs:Ge+Ga. Dashed line represents Ge_{AL}/Si_{AL}
relative peak height. Solid line represents $exciton/Si_{AS}$
relative peak height. The X axis shows ratio value, Y-axis
shows anneal temperature (In 100's °C).

78

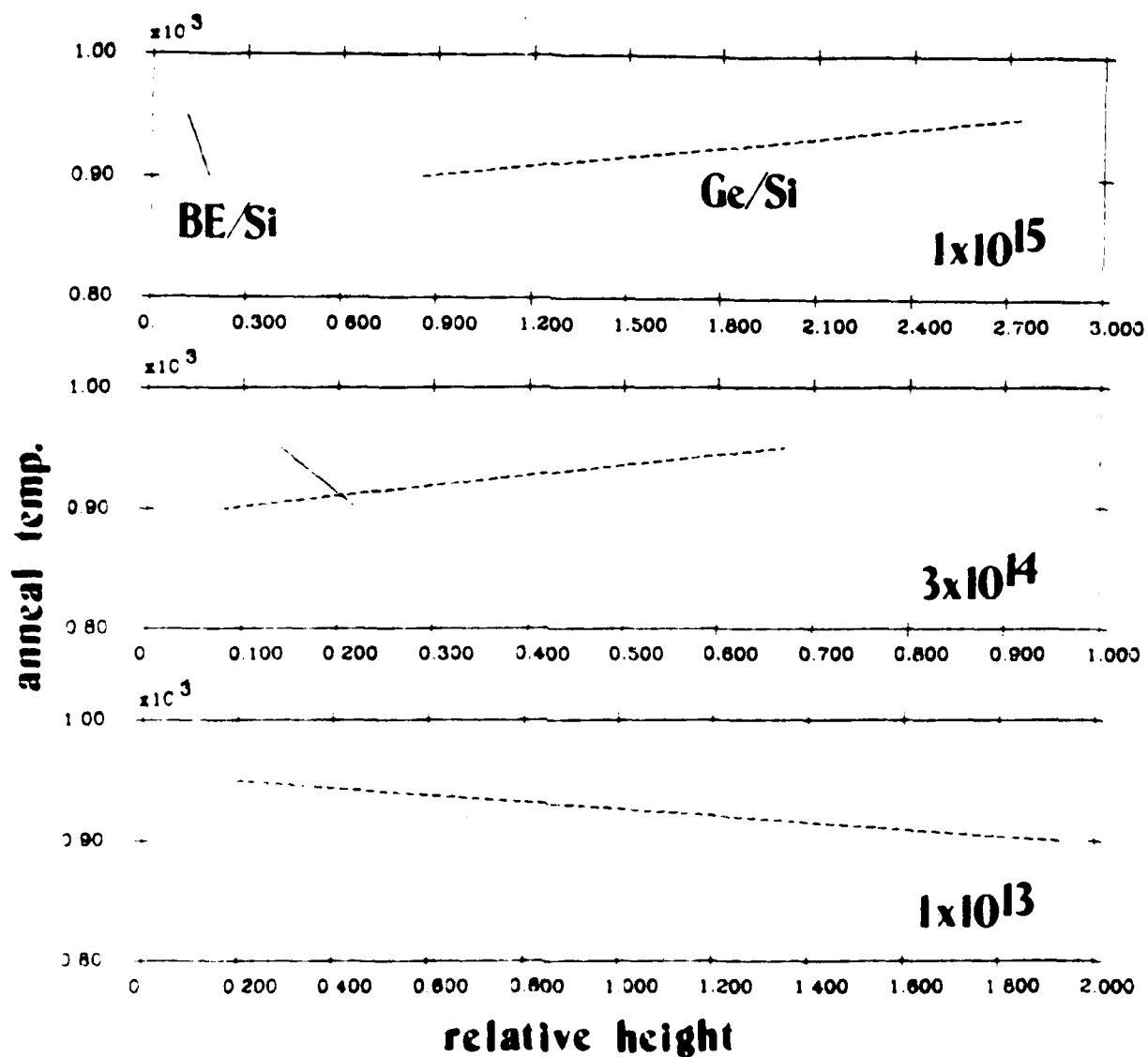attributed it to a donor-Ga_{As} double acceptor transition. The transition leaves the final state of the negatively charged double acceptor in an excited state (30).

The comparative spectra are presented in Figs. 32-36, and graphs of relative intensity ratios are presented in Figs. 37 and 38.   In observing the anneal temperature dependence (Figs. 32-34, and Fig. 38), a relative height increase occurs for the Ge_{As} peak and a decrease occurs for the exciton peak between 900 and 950°C for doses of 3×10^{14} and $1 \times 10^{15}/cm^2$. This suggests that Ge atoms are tending to locate more on As sites than on Ga sites from 900 to 950°C.   This is interesting because in the electrical data, GeAs:Ge+Ga showed a type conversion from p-type to n-type activity at these high anneal temperatures.   On the other hand, the PL data implies a shift to stronger p type electrical activity. At $1 \times 10^{13}/cm^2$, the relative height of both the Ge_{As} peak and the exciton peak decreases from 900 to 950°C. This behavior is not yet well understood.

The trends for dose dependence (Figs. 35-37) are also not well understood. At an anneal temperature of 900°C, the relative height of the Ge_{As} peak decreases with increasing dose up to $3 \times 10^{14}/cm^2$, at which point it mostly disappears. The peak returns at a dose of $1 \times 10^{15}/cm^2$. The relative height of the exciton peak shows a general decrease with increasing dose.   At an anneal temperature of 950°C, the trend shows a relative height increase for the Ge_{As} peak and a

79

decrease for the exciton peak with increasing dose, implying an increase in p-type electrical activity. This is just opposite of what one might expect, because in the electrical data there is a type conversion to n-type activity between doses of 3×10^{14} and $1\times10^{15}/cm^2$ at an anneal temperature of 950°C.

In the electrical data, for GaAs:Ge+Ga, the p-type activity was enhanced over that of GaAs:Ge for doses of $3\times10^{14}/cm^2$ or below, and the original n-type activity of GaAs:Ge changed to p-type except at 900°C or above.

The maximum activation efficiency occured at an anneal temperature of 950°C and a dose of $1\times10^{13}/cm^2$. From the PL data, it seems that the major contributor by far to the p-type activity for this sample is the Si_{As} peak, not the Ge_{As} peak, and this is not well understood at present.

At 900°C and $1\times10^{13}/cm^2$ an interesting phenomenon occurs. The Ga_{As} antisite defect peak at 1.450 eV shows up as the dominant peak in the spectrum. Other samples at 900°C anneal, 1×10^{14} and $1\times10^{15}/cm^2$ dose (Fig. 36), and one at 950°C anneal, $3\times10^{14}/cm^2$ dose (Fig. 35), show relatively large Ga_{As} peaks also. The implantation of Ga into the samples generally increases the probability of this defect occurring. This defect, which acts as a double acceptor, may contribute to the p-type electrical activity.

F. Ion Species Comparison

As a final comparison, several samples with identical anneal temperatures and dose concentrations but different ion

80

species combinations were measured optically and plotted together. The different combinations of ion species include Ge singly, Ge+As dually, Ge+Ga dually, Ga singly, and As singly implanted into GaAs. The data for Ga singly and As singly implanted at doses of $1x10^{13}$ and $1x10^{19}/cm^2$ and an anneal temperature of 900°C, was provided by Capt. K. Keefer. The comparative spectra are shown in Figs. 39-44.

Figs. 39-41 show how dually implanting Ge and Ga enhance the Ga_{As} antisite defect peak. In Fig. 42, implanting As enhances the 1.357 eV Ga vacancy related transition. Any trends dealing with the ion species dependence of the Ge_{As} peak and the exciton peak are not apparent. In Figs. 43 and 44, dually implanting Ge+Ga and annealing at 950°C greatly enhance the Si_{As} peak relative to the Ge_{As} peak, whereas Ge+As dual implantion seems to only slightly reduce the Ge_{As} peak relative to the Si_{As} peak. However, for a dose of $1x10^{19}/cm^2$ and an anneal temperature of 900°C (Fig. 39), dually implanting Ge+As greatly reduces the relative height of the Ge_{As} peak.

Fig. 39 PL ion species dependence comparative spectra of GaAs at about 5⁰K using 6471 Å line. Source intensity: 0.27 W/cm². Dose: 1x10¹³/cm², T$_A$-900⁰C.

Fig 40 PL Ion species dependence comparative spectra of
GaAs at about 50K using 6471 A line. Source intensity:
0.27 W cm⁻. Dose. 1x10¹³/cm², Tₐ 900°C.

GaAs
implants

Ge

Ge

Si

BE

INTENSITY
(arb
units)

Ga

Ge + Ga

Ga

Fig. 41 P:
GaAs et al
0.27 W/cm

1.0
4.5 **2.8** **2.5**
5.0
4.5 **3.2** **2.2**
3.6
4.0 **2.0**
1.1
1.8
1.25 **1.4** **1.**
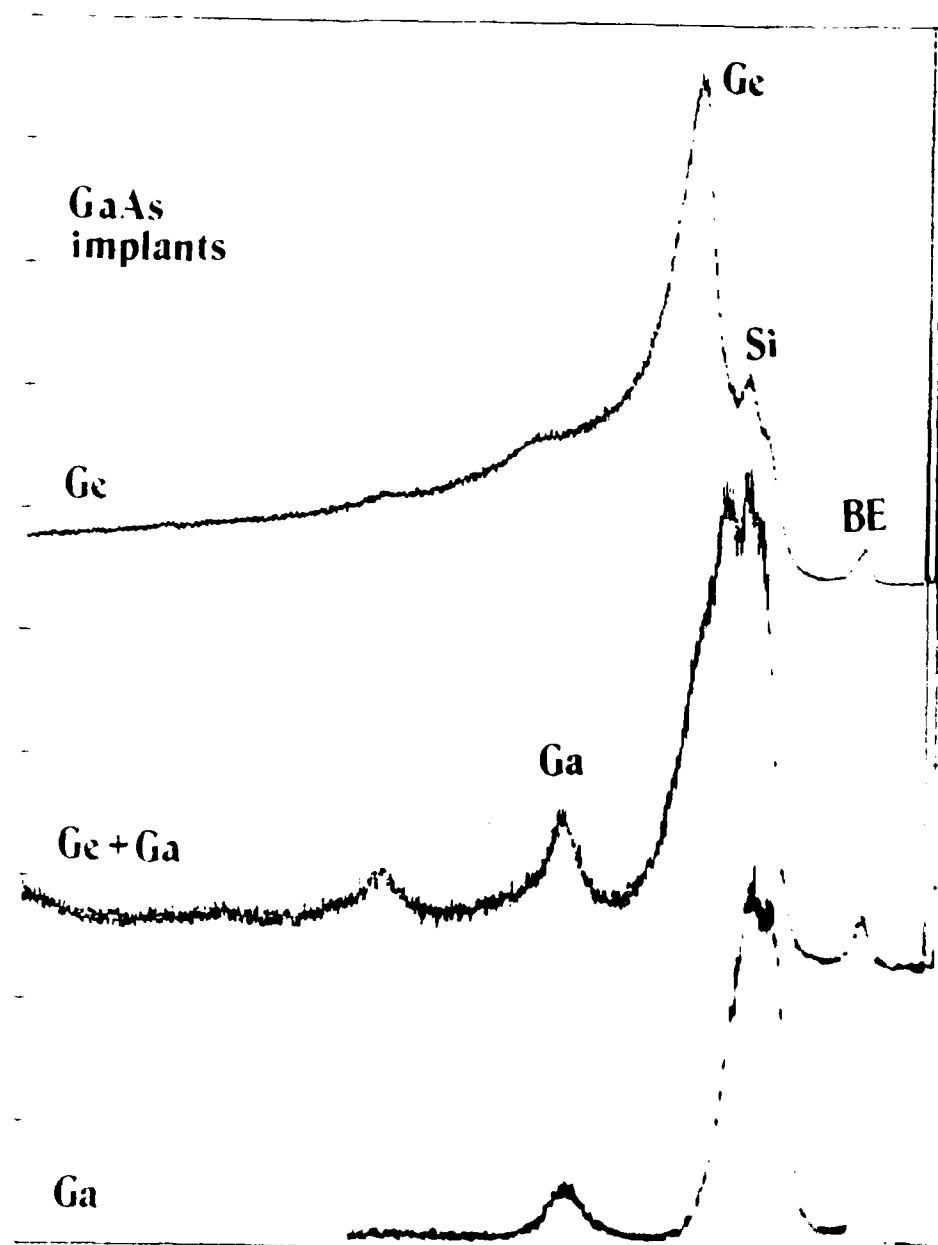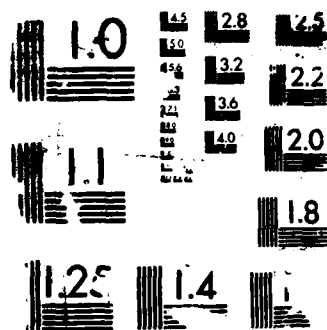
MICROCOPY RESOLUTION TEST CHART

Fig. 42 PL ion species dependence comparative spectra of
GaAs at about 5°K using 6471 Å line. Source intensity:
0.27 W/cm². Dose: 3x10¹⁴/cm², T$_A$=800°C.
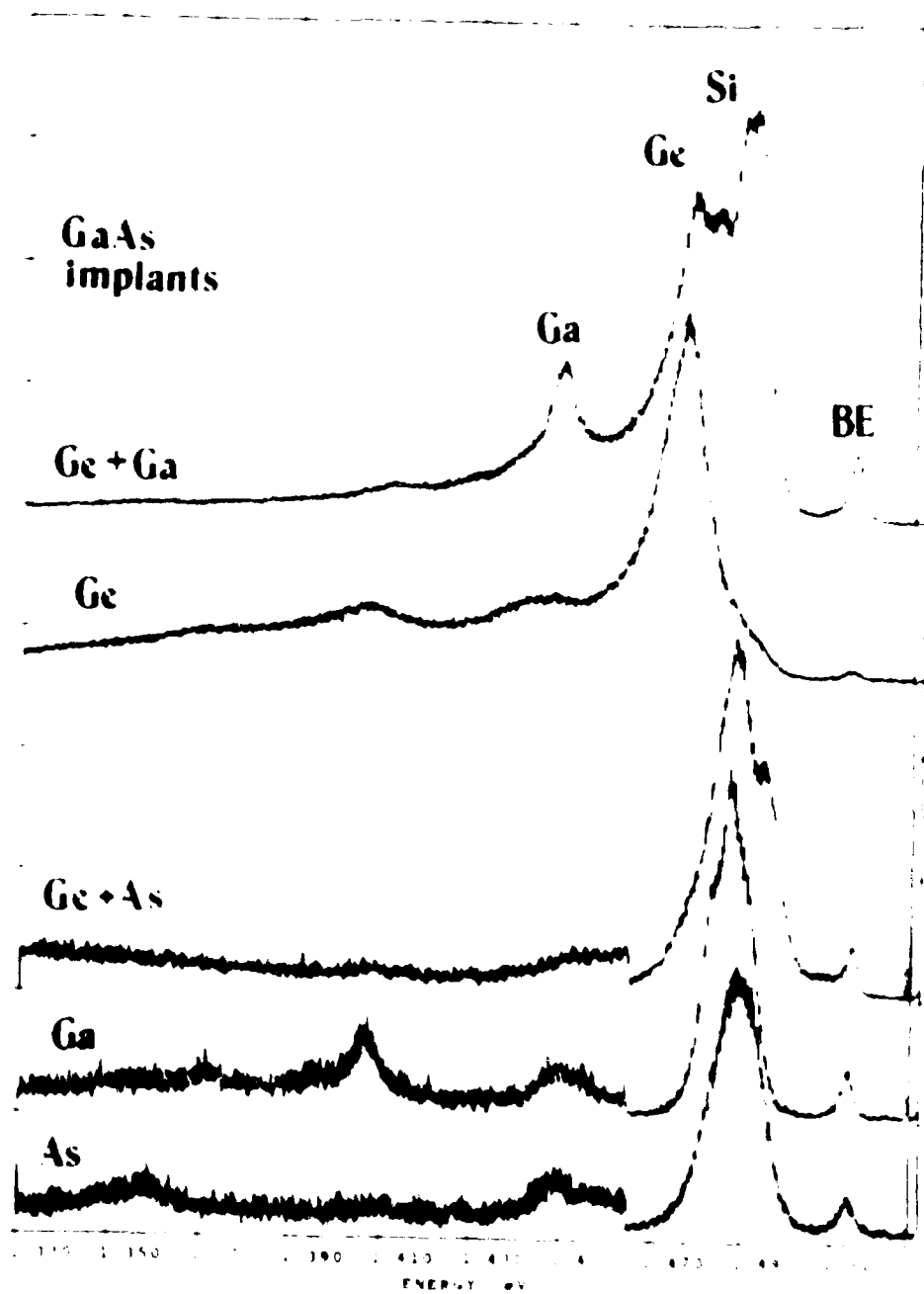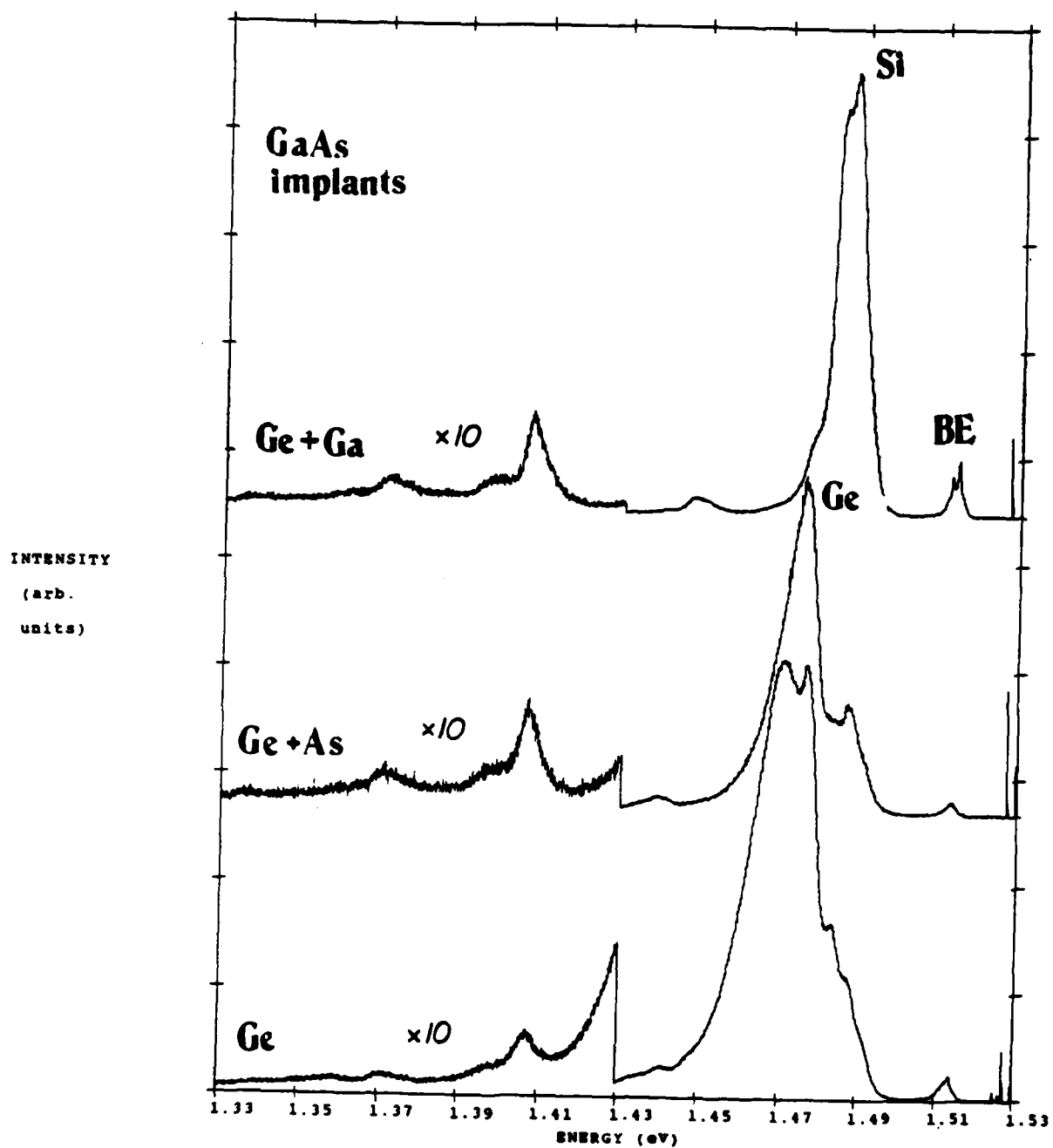
Fig. 43 PL ion species dependence comparative spectra of GaAs at about 5°K using 6471 Å line. Source intensity: 0.27 W/cm². Dose: 1x10¹³/cm², Tₐ=950°C.
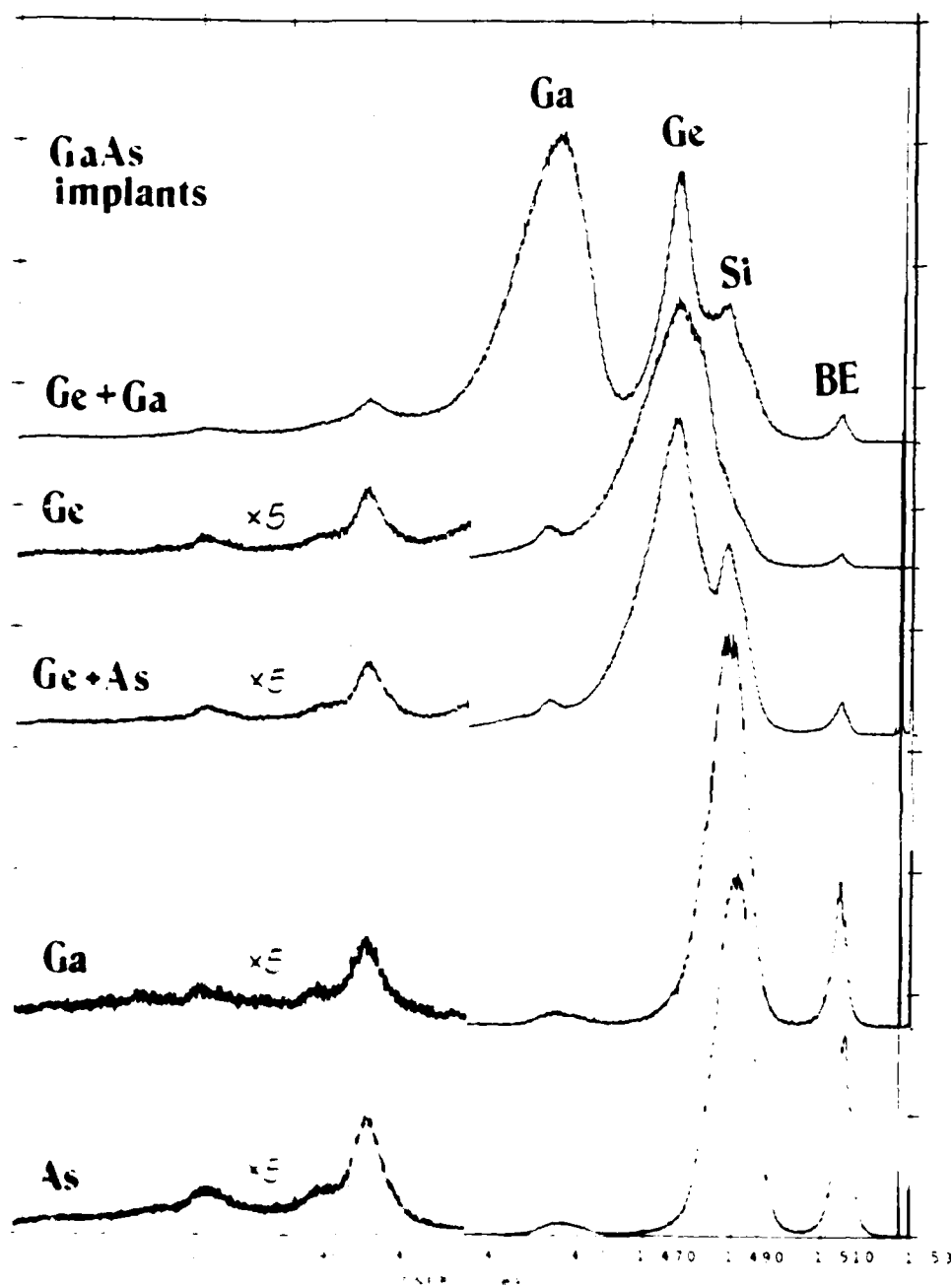
86
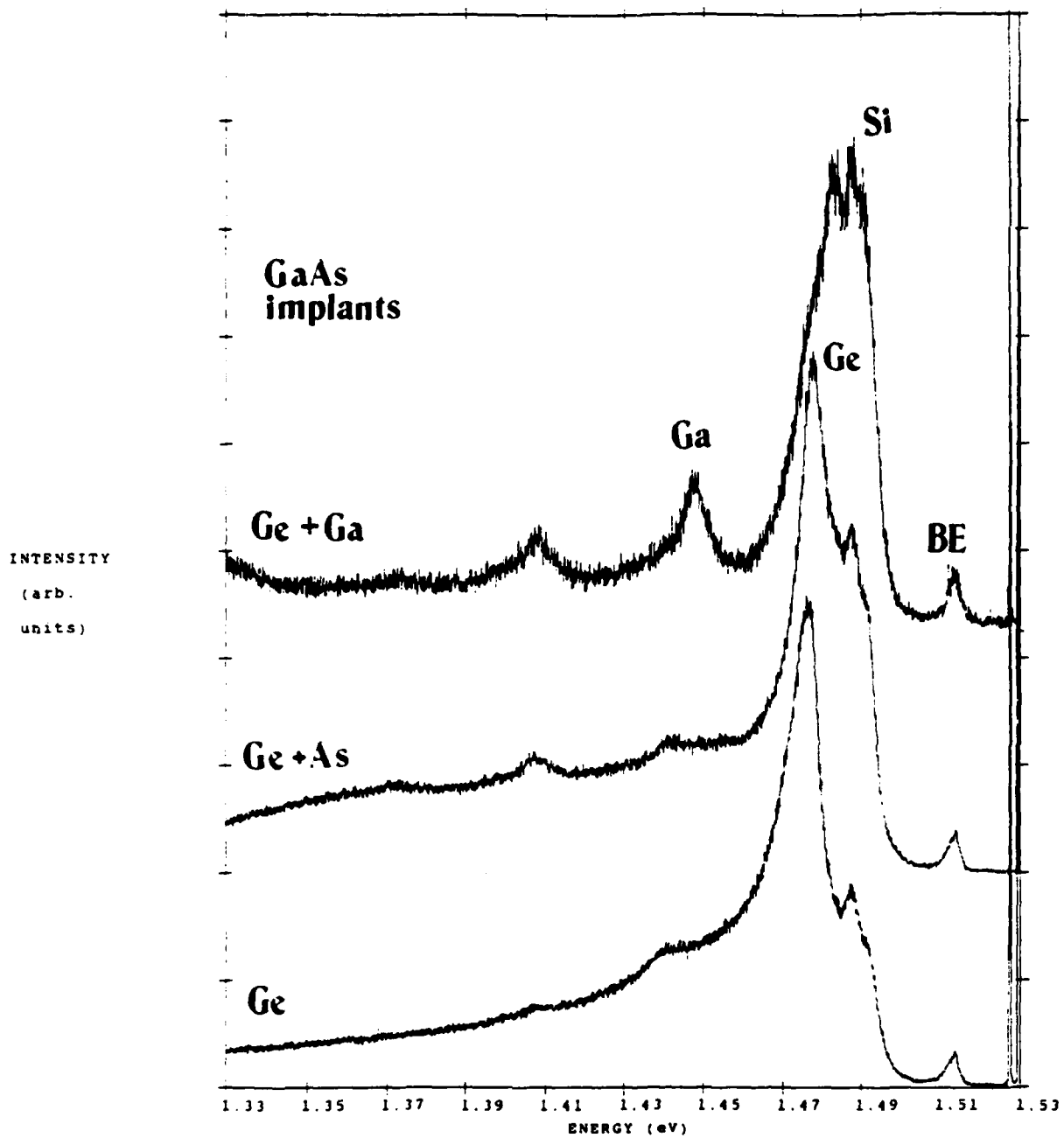
Fig. 44 PL ion species dependence comparative spectra of
GaAs at about 5ºK using a 6471 Å line. Source intensity:
0.27 W/cm². Dose: 3×10^{14}/cm², $T_A = 950$ºC.

V. Conclusions and Recommendations

A. Conclusions

In the past chapter, the comparative PL spectra was reviewed for Ge, Ge+As, and Ge+Ga implanted GaAs, some of which was compared to electrical data from previous studies as discussed in chapter III. Much of the PL data does not directly correlate with the electrical data. An effort was made to use the height of the Ge_{As} acceptor peak relative to the (e, Si_{As}) peak as an indicator of p-type activation and to use the height of the donor bound exciton peak as an indicator of n-type activation.

It seems that when the n-type electrical activity is the greatest in a group of samples, the PL trend becomes more apparant, and when th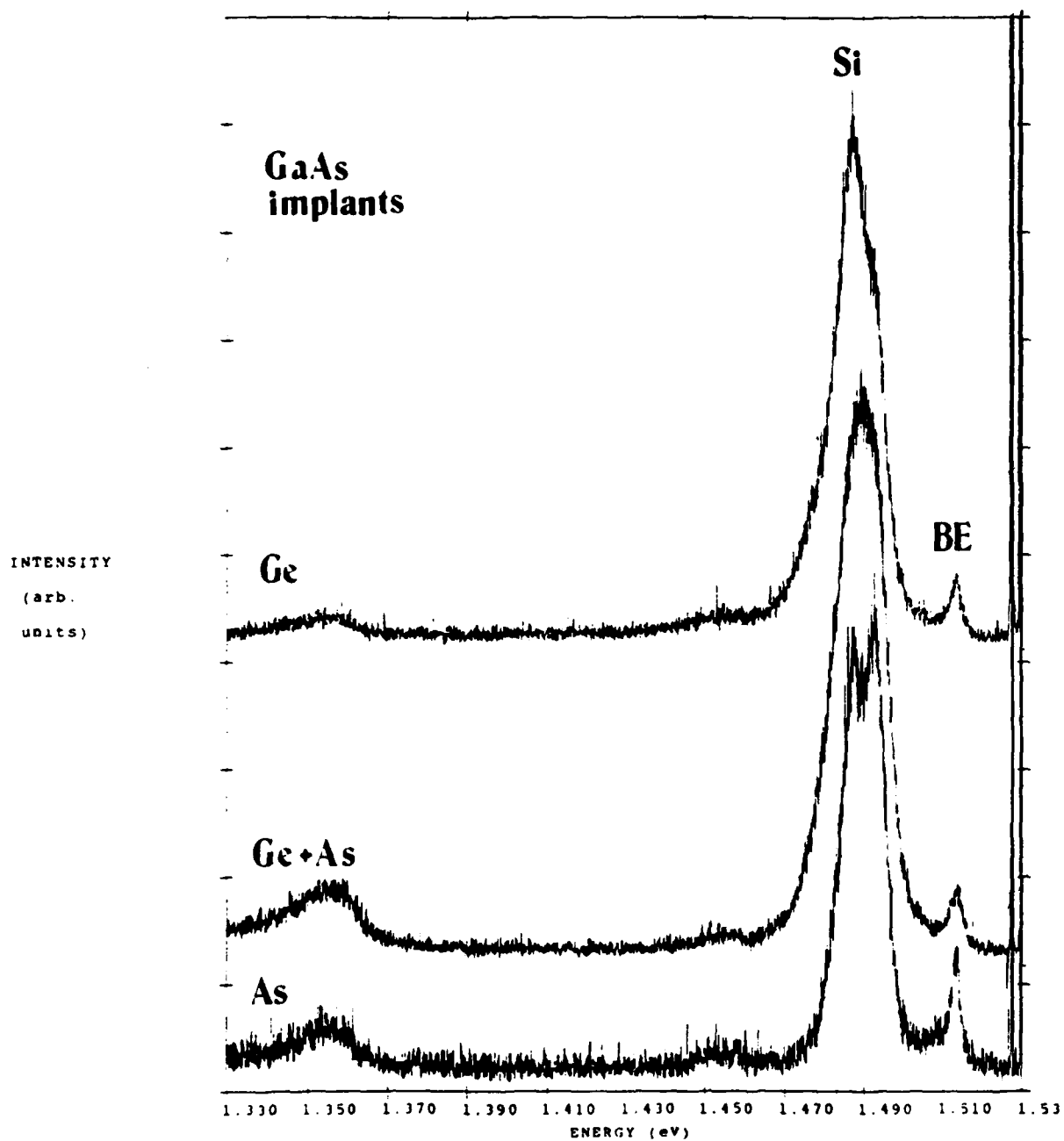e n-type activity is reduced, the PL trend is more obscure. This is substantiated by the fact that dual implantation of Ge and As showed trends that more closely matched the results of the electrical data, while the dual implantation of Ge and Ga showed the least clear trends.

The PL data for Ge+As dually implanted GaAs showed an overall dose dependent trend of a decreasing percentage of Ge atoms locating on As sites with increasing dose. It also showed an increasing number of Ge atoms locating on Ga sites, which is more apparent at higher doses. An anneal temperature dependent trend at a dose of $1 \times 10^{13}/cm^2$ indicated an overall tendency towards more n-type activation with increasing anneal temperature. However, other doses were less clear.

88

For Ge singly implanted GaAs, a clear trend in dose dependence, matching the electrical data, occurs at an anneal temperature of 950°C. The relative height of the Ge_{As} peak decreases while the exciton peak increases, indicating a tendency towards greater n-type behavior. The anneal temperature dependence for doses of $1x10^{15}$ and $1x10^{13}/cm^2$ showed a general tendency of increasing relative exciton peak height with increasing anneal temperature, while the other dose studied showed an increase in relative exciton peak height between 900 and 950°C. Although the indicator of p-type activity, the Ge_{As} peak, didn't show corresponding behavior, the exciton peak trend suggests an increase in donor activity with increasing anneal temperature at high ion dose concentration.

For Ge and Ga dually implanted GaAs, no definite trend is observed with the limited number of samples studied. However, adding Ga does generally enhance the Ga_{As} antisite defect transition that functions as a double acceptor.

B. Recommendations

The PL measurements in this study were all done using a 647.1 nm laser line. This line penetrates about 3000 Å, well past the Ge projected range of 464 Å, or most of the implanted region that extends to about 2400 Å. Therefore, it is possible that the Si and C transitions intrinsic to the substrate are masking the trends in the transitions occuring in the implanted layer. The use of a laser line less than

89

647.1 nm that does not penetrate the sample as far might have given clearer results by showing more of what goes on in the implanted layer only.

I would therefore recommend conducting a study similar to this one at a lower laser wavelength. The silicon acceptor peak may or may not still be a dominant transition.

A study could also be conducted as a function of depth into the sample by either etching samples themselves or varying the laser wavelength.

I would also recommend "filling in the gaps" in this study by especially measuring more GaAs:Ge+Ga samples annealed at lower temperatures than 900ºC. It might be useful to study more dose concentrations such as $3x10^{13}$ or $1x10^{14}/cm^2$ for all species of samples.

Bibliography

1. Frensley, William R. "Gallium Arsenide Transistors,"
    Sci. Am., 257(1980),80-87.

2. Chan, S. S., G. T. Marcyk, B. C. Streetman. "Electrical
    Properties and Photoluminescence Studies of Ge-
    Implanted GaAs," _J. Electron. Mat._, 10(1981), 213-238.

3. Ploog, K., A. Fischer, H. Kunzel. "Improved P/N
    Junctions in Ge doped GaAs Grown by Molecular Beam
    Epitaxy," _Appl. Phys._, 18(1979), 353-356.

4. Yoder, M. N. "Ohmic Contacts in GaAs," _Solid St.
    Electron._, 23(1980),117-119.

5. Yeo, Y. K., J. E. Ehret, F. L. Pedrotti, Y. S. Park,
    W. M. Theis. "Amphoteric Behavior of Ge Implants in
    GaAs," _Appl. Phys. Lett._, 35(1979), 197-199.

6. Yeo, Y. K., F. L. Pedrotti, Y. S. Park. "Modification
    of the Amphoteric Activity of Ge Implants in GaAs by
    Dual Implantation of Ge and As," _J. Appl. Phys._, 51
    (1980), 5785-5788.

7. Pedrotti, F. L., Y. K. Yeo, J. E. Ehret, Y. S. Park.
    "Dual Implantation of Ga and Ge into GaAs," _J. Appl.
    Phys._, 51(1980), 5781-5784.

8. Yu, P. W. "Deep Emission Centers in Ge-Implanted GaAs,"
    J. Appl. Phys., 50(1979), 7165-7167.

9. Thoma, Capt Barry P. _Photoluminescence Study of Ge
    Implanted GaAs_. MS thesis, AFIT/GEP/ENP/86D-11.
    School of Engineering, Air Force Institute of
    Technology (AU), Wright-Patterson AFB OH, Dec. 1986.

10. McKelvey, J. P. _Solid State and Semiconductor Physics_.
    New York: Harper Row Publishers, 1966.

11. Williams, E. W., H. Barry Bebb. "Photoluminescence II:
    Gallium Arsenide," _Semiconductors and Semi-metals, Vol.
    8_, edited by R. K. Willardson and A. C. Beer, New York:
    Academic Press, 1969.

12. Morgan, D. V. et. al. "Prospects for Ion Bombardment
    and Ion Implantation in GaAs and InP Device
    Fabrication," _IEE Proceedings_, 128(1981), 109-130.

13. Ambridge, T., and R. Heckingbottom. "Ion Implantation in Compound Semiconductors--An Approach Based on Solid State Theory," Radiat. Eff., 17(1973), 31-36

14. Smith, Kevin K. "Photoluminescence of Semiconductor Materials," Thin Solid Films, 84(1981), 171-182.

15. Heim, U., and P. Hiesinger. "Luminescence and Excitation Spectra of Exciton Emission in GaAs," Phys. Stat. Sol. (b), 66(1974), 461-464.

16. Pankove, J. I. Optical Processes in Semiconductors, Englewood Cliffs: Prentice-Hall Inc., 1971.

17. Dean, P. J. "Photoluminescence as a Diagnostic of Semiconductors," Progress in Crystal Growth Characterization, Vol. 5, Great Britain: Pergamon Press Ltd., 1982.

18. Park, Y. S., Y. K. Yeo, F. L. Pedrotti. "Dual Implantation and Amphoteric Behavior of Ge Implants in GaAs," Nuclear Instruments and Methods, 182/183(1981), 617-624.

19. "SPEX 1702 3/4 Meter Czerny-Turner Spectrometer Operating, Maintenance, and Instruction Manual," AFIT, WPAFB OH, 13 Oct. 1970.

20. Swaminathan, V. et. al. "Photoluminescence of Themally Treated n^+ Si-doped and Semi-insulating Cr-doped GaAs Substrates," Journal of Luminescence, 22(1981), 153-170.

21. Keefer, Capt Kevin. Photoluminescence Study of Silicon and Oxygen Implanted Gallium Arsenide. MS thesis, AFIT/ GEP/85D-8. School of Engineering, Air Force Institute of Technology (AU), Wright-Patterson AFB OH, Dec 1985.

22. Yu, P. W. "Excitation-Dependent Emission in Mg-, Be-, Cd-, and Zn-implanted GaAs," J. Appl. Phys., 48(1977), 5043-5051.

23. Adegboya, G. A. and B. Tuck. "Photoluminescence from Chromium Diffused GaAs," Solid State Communications, 40(1981), 487-489.

24. Chatterjee et. al. "Photoluminescence Study of Native Defects in Annealed GaAs," Solid State Communications, 17(1975), 1421-1424.

25. Tajima, M. "Correlation Between Photoluminescence Spectra and Impurity Concentrations in Silicon," Japan. J. Appl. Phys., 16(1977), 2265-2266.

26. Ashen, D. J. et. al. "The Incorporation and
     Characterization of Acceptors in GaAs," *J. of Phys. Chem
     and Sol.*, 36(1975), 1041-1053.

27. Bishop, S. G. et. al. "Photoluminescence and Infrared
     Spectroscopy of Acceptors in GaAs," *J. Appl. Phys.*,
     56(1984), 1785-1790.

28. Hallais, J. et. al. *Gallium Arsenide and Related
     Compounds*(Inst. Phys. Conf. Ser. No. 33b, 1976), 220.

29. Zucca, R. *Gallium Arsenide and Related Compounds*(Inst.
     Phys. Conf. Ser. No. 33b, 1976), 220.

30. Shanabrook, B. V. "Model for the 1.28 eV Double
     Acceptor Luminescence in GaAs," *J. Appl. Phys.*
     59(1986), 2535-2537.

VITA

First Lieutenant Thomas G. Alley was born 21 June 1960 in Salt Lake City, Utah. He graduated in 1978 from Bountiful High School in Bountiful, Utah and then attended the University of Utah. He graduated cum laude in 1984 with a Bachelor of Arts degree in Physics and a minor in Mathematics. Upon graduation, he received a commission in the USAF through the ROTC program. He then married Valerie K. Adamson before moving to Ohio to begin his first USAF assignment. His Air Force career began with an assignment as a program manager for the AN/ALQ-131 Electronic Countermeasures Set Receiver-Processor at the Deputate for Recon/Strike and Electronic Warfare Systems, Aeronautical Systems Division, Wright-Patterson Air Force Base, Ohio (1984-1986). In June 1986, he entered the School of Engineering, Air Force Institute of Technology to pursue a Master of Science degree in Engineering Physics.

Permanent Address: 1600 S. Orchard Dr.
                    Bountiful, Utah 84010

REPORT DOCUMENTATION PAGE

Form Approved
OMB No. 0704-0188

1a. REPORT SECURITY CLASSIFICATION	1b. RESTRICTIVE MARKINGS
Unclassified	None

2a. SECURITY CLASSIFICATION AUTHORITY	3. DISTRIBUTION / AVAILABILITY OF REPORT
2b. DECLASSIFICATION / DOWNGRADING SCHEDULE	Approved for public release; distribution unlimited.

4. PERFORMING ORGANIZATION REPORT NUMBER(S)	5. MONITORING ORGANIZATION REPORT NUMBER(S)
AFIT/GEP/ENP/87D-1	

6a. NAME OF PERFORMING ORGANIZATION	6b. OFFICE SYMBOL (If applicable)	7a. NAME OF MONITORING ORGANIZATION
School of Engineering Air Force Institue of Tech.	AFIT/EN	

6c. ADDRESS (City, State, and ZIP Code)	7b. ADDRESS (City, State, and ZIP Code)
Wright-Patterson AFB, OH 45433	

8a. NAME OF FUNDING / SPONSORING ORGANIZATION	8b. OFFICE SYMBOL (If applicable)	9. PROCUREMENT INSTRUMENT IDENTIFICATION NUMBER

8c. ADDRESS (City, State, and ZIP Code)	10. SOURCE OF FUNDING NUMBERS			
	PROGRAM ELEMENT NO.	PROJECT NO.	TASK NO	WORK UNIT ACCESSION NO.

11. TITLE (Include Security Classification)

See Box 19

12. PERSONAL AUTHOR(S)
Thomas G. Alley, 1st Lt., USAF

13a. TYPE OF REPORT	13b. TIME COVERED	14. DATE OF REPORT (Year, Month, Day)	15. PAGE COUNT
MS Thesis	FROM _____ TO _____	87 Dec	107

16. SUPPLEMENTARY NOTATION

17.	COSATI CODES		18. SUBJECT TERMS (Continue on reverse if necessary and identify by block number)
FIELD	GROUP	SUB-GROUP	Germanium Implanted Gallium Arsenide,
20	12		Photoluminescence, Ion Implantation, Gallium Arsenide

19. ABSTRACT (Continue on reverse if necessary and identify by block number)

TITLE: Optical Study of Germanium, Germanium plus Arsenic, and Germanium plus Gallium Implants in Gallium Arsenide

Thesis Advisors: Dr. R. L. Hengehold; Dr. Y. K. Yeo

Approved for public release: IAW AFR 190-1.

LYNN E. WOLAVER
Dean for Research and Professional Development
AFIT ...
W...

continued on reverse

20 DISTRIBUTION / AVAILABILITY OF ABSTRACT	21. ABSTRACT SECURITY CLASSIFICATION
☐ UNCLASSIFIED/UNLIMITED ☒ SAME AS RPT ☐ DTIC USERS	Unclassified

22a. NAME OF RESPONSIBLE INDIVIDUAL	22b. TELEPHONE (Include Area Code)	22c. OFFICE SYMBOL
Dr. R. L. Hengehold; Dr. Y. K. Yeo	513-255-2012	AFIT/ENP

DD Form 1473, JUN 86 — Previous editions are obsolete. — SECURITY CLASSIFICATION OF THIS PAGE

Block 19 cont.

The low temperature photoluminescence (PL) properties of single implants of Ge and dual implants of Ge+As or Ge+Ga into semi-insulating Cr-doped GaAs have been analyzed. Room temperature implantation was performed at 120 keV. When dual implantation was used, samples were implanted at the same dose and energy. Ion doses ranged from 1×10^{13} to $1\times10^{15}/cm^2$. Samples were encapsulated with Si_3N_4 and then annealed at temperatures ranging from 700 to 950°C. Si_3N_4 was removed prior to PL measurements.

A PL peak due to Ge-acceptors was identified. A bound exciton peak related to Ge-donors was also observed. An acceptor peak due to residual Si was found in all samples. The heights of the Ge-acceptor peak and exciton peak were compared to the height of the intrinsic Si-acceptor peak. The height comparison was used in an effort to find trends of Ge-acceptor and Ge-donor transitions as a function of anneal temperature and ion dose.

The PL data for GaAs:Ge+As showed a relative decrease of the Ge-acceptor related peak and an increase in the exciton peak with increasing dose. This is generally consistent with electrical measurements in previous work.

The PL data for GaAs:Ge at an anneal temperature of 950°C also showed a relative decrease in the Ge-acceptor related peak and an increase in the exciton peak with increasing dose. This is also consistent with electrical data. However, trends of dose dependence at other anneal temperatures were more complicated.

The anneal temperature dependence of the Ge related peaks for both GaAs:Ge and GaAs:Ge+As showed complicated behavior. At an anneal temperature of 800°C, the Ge-acceptor related peak becomes obscured in a large Si-acceptor related peak.

For GaAs:Ge+Ga, the addition of Ga to the implantation process generally enhances an observed Ga in As vacancy antisite defect transition.

END

DATE
3 - 88
DTIC